ACKNOWLEDGEMENTS

First and foremost, I would like to express my sincere appreciation and gratitude to my advisor, Dr. Ming Hu, for his guidance, scientic training and mentorship during the pursuit of my Ph.D. degree. Dr. Hu not only offers the scientific guidance and expertise to direct my reaserch work, but also sets up a perfect example as a caring educator and dedicated scientist, which will be an inspiration to me during my life.

I am deeply indebted to all my committee members, Drs. Diana Chow, Vincent Tam, Romi Ghose and Rong Yu for their continuous support and valuable advice. I would like to specially thank Dr. Zhi-Hong Jiang, Dr. Jing-Rong Wang and Dr. Jijun Chen for providing ginsenoside compounds, which enabled the completion of my QSAR study.

I would like to acknowledge Dr. Shuxing Zhang and John K. Morrow of University of Texas M.D. Anderson Cancer Center, and Dr. Gyorgy M. Keseru and Akos Tarcsay of University of Technology and Economics (Hungary) for providing molecular docking assistance and validated P-gp human homology model on P-glycoprotein binding work. My special thanks go to Dr. John Scott Daniels and Dr. Kaustubh Kulkarni of Vandebilt Universtiy for their help on confirmation study of ginsenosides in MDCKII cells.

I have the pleasure to express my deepest appreciation to my wife, Yang (Angela) Teng for her continued support, love and understanding during the long journey. I am especially grateful to my parents, Huijian Yang and Shengqin Wang, for their encouragement and support of my pursuit for the highest education.

Finally, I would like to thank all the members of Dr. Ming Hu's lab for their help of my study, especially to Dr. Song Gao, Dr. Haiyan Xu, Taijun Yin and Baojian Wu. I must also thank all the members of PPS department at the University of Houston for providing me with the opportunity and environment to pursue my studies.

ABSTRACT

Objective: The overall goal is to determine the major factors limiting oral bioavailability of ginsenosides and utilizing the knowledge gained to increase the oral bioavailability of ginsenosides via a machenism-based biopharmaceutical approach. The objectives of this project were 1) to determine the major reasons responsible for low oral bioavailability of ginsenosides using various ADME assays including presystemic stability, solubility, permeability and metabolism; 2) to delineate the absorption mechanism of various ginsenosides including the identification of responsible transporters; 3) to enhance oral bioavailability of ginsenosides based on the knowledge obtained in the first two aims.

Method: For objective 1), saturated solubility measurement in different aqueous matrics, permeability in Caco-2 cells were determined along with stability in GI tract and in vitro metabolism in pooled intestinal/liver s9 fractions prepared from A/J mice. For objective 2), in vitro transcellular transport experiments employing Caco-2 and MDCK II cell monolayers were performed, together with in situ intestinal perfusion and in vivo pharmacokinetic experiments utilizing wild-type and MDR1 knockout mice. For objective 3), in vitro transcellular transport model using Caco-2 cell monolayers were used as a screening tool for identifing effective inhibitors or inhibitor combo using fourth generation P-glycoprotein inhibitors that are considered to be safe, and the most effective inhibitor combo was then used for the enhancement of bioavailability of ginsenosides in A/J mice.

Results: 1) Poor solubility and permeability were identified to be the major reasons for low oral bioavailability of ginsenosides. Although CYP metabolism occurred at in vitro system, the phase I metabolite was not found in vivo. 2) Rh2 and C-K were found to be good substrates of P-gp and inhibition/knockout of P-gp can significantly enhance their oral bioavailability. A structure-transport mechanism study utilizing twenty-two ginsenosides demonstrated that P-glycoprotein-mediated efflux mechanism was responsible for the efflux of ginsenosides with one glucose attached to one or both OH groups of the aglycone. 3) A combination of fourth generation P-gp inhibitors (i.e., biochanin A, wogonin and piperine @ 50 μM each) decreased efflux of ginsenosides Rh2s and C-K in Caco-2 cells. The effective and efficient inhibition of P-gp by the same inhibitor combo led to an increased oral bioavailability of Rh2s and C-K in A/J mice, primarily through increased volume of distribution.

Conclusion: The poor solubility and slow permeation were the major reasons causing low oral bioavailability of ginsenosides. Systematic studies showed that P-gp is the exclusive efflux transporter for ginsenosides Rh2 and C-K and that structure-dependent P-gp-mediated ginsenoside efflux is mainly due to difference in the number of sugar moieties. In vitro and in vivo study demonstrated that inhibition of P-gp can significantly increase oral bioavailability of ginsenosides. A triple combination of biochanin A, wogonin and piperine led to an increased oral bioavailability of Rh2s and C-K in vivo.

LIST OF FIGURES

LIST OF TABLES

TABLE OF CONTENTS

LITERATURE REVIEW AND INTRODUCTION TO PROJECT

Panax ginseng has been used as an herbal supplement to improve life and physical condition in Asian countries for thousands of years [1]. In the last two decades, American ginseng has also begun to gain great interest in the west. Ginsenosides are the major active components in ginseng [2-4]. More than 150 ginsenosides has been identified so far, and Rb1, Rb2, Rc, Re and Rg1 are the main naturally occurring constituents, representing 80% of ginsenosides [5-7]. But many activity and clinical studies showed that the minor ginsenosides present in plants, such as Rh2, compound K, Rg5, Rg3 and their aglycons, protopanaxadiol and protopanaxatriol have stronger anticancer activity than primary ginsenosides [8-11]. It is worth noting that chemical or medicinal processing (e.g., steaming) of ginseng plants or ginseng extract could significantly increase the amounts of minor ginsenosides, thereby potentially enhancing its anticancer activities.

The chemoprevention and anticancer mechanism of ginsenosides include mitigation of DNA damage, induction of apoptosis, and inhibition of proliferation as well as positive immunomodulation [12]. Considering oral route of administration may be the most compliant and reasonable approach for chemoprevention, the biggest challenge to expand the clinical usefulness of ginsenosides is their low oral bioavailability, usually less than 5% in rodents [3,

13, 14]. The low oral bioavailability is the major factor causing ambiguous results in clinical trials, and represents a major obstacle for these compounds to be developed as effective chemopreventive and/or chemotherapeutic agents.

There are many factors responsible for the low bioavailability of ginsenosides, including low aqueous solubility, poor permeability, good substrate for efflux transporters, instability in gastrointestinal fluid, enzymatic degradations by glucosidases, extensive metabolism and etc [3, 13, 15-17]. However, the leading cause for low oral bioavailability of ginsenosdies has not been revealed clearly. We systemically investigated various factors affecting oral bioavailability of three most active ginsenosides and identified the leading cause in chapter 4.

Furthermore, poor oral absorption was considered as one of major factors contributing to low bioavailability of ginsenosides [3, 18], but the transport mechanisms for ginsenosides were unknown in literature. In chapter 5 & 6, gisnenosides Rh2 and C-K were chosen as lead compounds to test our hypothesis that oral bioavailability of ginsenosides could be increased via a mechanism-based biopharmaceutical approach.

Ginsenosides could be mainly divided into four groups including protopanaxadiols (PPT), protopanaxatriols (PPD), type C and type D (derivatives of PPT and PPD) (Fig.1). In order to fully investigate the absorption mechanism

of various ginsenosides, we chose twenty-two ginsenosides which are either highly abundant in ginseng or have potent anticancer/chemoprevention activity covering these four groups. Permeability measurement and various methods on identifying transporters were performed in chapter 7 to reveal structure-absorption mechanism of ginsenosides.

Finally, we continue our efforts to enhance oral bioavailability of ginsenosides with less pharmacologically active compound suitable for long-term clinical use. The results showed that it is possible to increase oral bioavailability of Rh2s by using combination of natural compounds via inhibition of P-gp in vivo (chapter 8).

In this chapter (Chapter 1), the first section (1.1) gives a detailed introduction of ginsenosides with regards to their proposed beneficial effects, mechanisms of action, structures and their problems with regards to the drug development. Section (1.2) introduces the basic concept of oral bioavailabilty and various factors affecting low oral bioavailability including absorption and metabolism, the basic concept of each parameter were introduced. The last section (1.3) discusses the strategy to improve oral bioavailablity, majorly focuses on reversing efflux transporters.

1.1.1. Introduction of ginsenosides

Ginseng has been used as an herbal supplement to improve life and physical conditioning in Asian countries for thousands of years [1]. Ginseng is top ten most consumed tonic herbs in US which has rejuvenating and invigorating properties. In the last two decades, both panax ginseng (Asian ginseng) and panax quinquefolius L.(American ginseng) attacted many scientists and physicans' interest due to its potent pharmacological effects [19]. The major active components of ginseng are considered as ginsenosides, which are mainly triterpenoid saponin derivatives [2-4]. Ginsenosides are mainly extracted from the flower, root and leaves of ginseng. Due to various structures, ginsenosides possess a wide range of therapeutic and pharmacological effects. Researchers are now focused on purified individual ginsenosides to reveal their pharmacological effects. There are more than 150 ginsenosides identified so far, and Rb1, Rb2, Rc, Re and Rg1 are the main constituents which consisted 80% of ginsenosides [5-7].But many activity and clinical studies showed the minor ginsenosides present in plants, such as Rh2, compound K, Rg5, Rg3 and their aglycon protopanaxadiol and protopanaxatriol have stronger anticancer activity than primary ginsenosides [8-11]. It is worth noting that chemical or medicinal processing (e.g., steaming) of ginseng plants or ginseng extract could significantly increase the amounts of minor ginsenosides, thereby potentially enhancing its anticancer activities.

1.1.2. Proposed benefits of ginsenosides

Potential benefits of gisnenosides include antioxidation, chemoprevention, anticarcinogenation, antihypertension, as well as antidiabetic effects and improved cognition on the central nervous system [7]. Previous epidemiological results have shown that in a case-controlled study including 1987 pairs of Korean subjects, the long-term consumption of ginseng was shown to be associated with a significant reduction in many different types of malignancies including lung cancer [1]. Ginsenosides Rg3 and Rg5 showed statistically significant reduction of lung tumor incidence and Rh2 had a tendency to decrease the incidence [1]. A 9-week animal study also showed Rh2s had a tendency to decrease lung tumor incidence in mice after its oral consumption [1].

1.1.3. Clinical indication

ShenYi® capsule, which contains 95% of Rg3, has been used in China as an anticancer drug treating non-small-cell lung cancer and esophageal cancer since 2006 [20, 21]. The combination of ShenYi capsule with chemotherapy showed significantly better therapeutic effects than chemotherapy alone in terms of one-year survival time and qualifies of life. The mechanism might be correlated with improved immune function and anti-tumor angiogenesis [21]. “SHENMAI” injection composed of red ginseng and ophiopogon has beed used to treat cardiomyopathy, myocardial infarction and hypertention in China [22-24]. Its

major components are ginsenosides Rb1, Rb2, Rb3, Re, Rc, Rh1, Rg1 and Rg2 [24].

So far 42 clinical trials on ginseng or ginsenosides have been completed or are ongoing to prevent and treat various disorders from cancer-related fatigue, blood pressure regulation, metabolic syndrome, diabetes, schizophrenia to alzheimer disease and etc. (www.clinicaltrials.org). They have demonstrated certain therapeutic benefits of ginseng or ginsenosides in treating hypertension, improving glycemic control, treating erectile dysfunction and attenuating atherosclerotic symptom [25-28]. The detailed clinical applications have been succinctly summarized in several reviews [29-31]. In this thesis, we are focusing on their chemoprevention and anticancer activities.

1.1.4. Mechanism of action

The chemoprevention and anticancer mechanism of ginsenosides include mitigation of DNA damage, induction of apoptosis, anti-angiogenesis and inhibition of proliferation as well as positive immunomodulation [12]. Ginsenosides Rh2 has been shown to induce G1 phase arrest, followed by progression to apoptosis in many human cancer cell lines [32-34]. Rg3 can induce apoptosis by interfering with several signaling pathways, including modulating the AMPK (AMP-activated protein kinase) and Transient Receptor Potential Melastatin 7 Channels [34, 35]. Ginsenoside 20(S)-protopanaxadiol

inhibits the proliferation and invasion of human fibrosarcoma HT1080 cells through apoptosis [36]. The chemoprevention of Rb1 and Re showed protective effects on DNA damage or inducing DNA repair [37, 38].

1.1.5. Structure of ginsenosides

Ginsenosides are mainly triterpenoid saponin derivatives [2-4] and they could be mainly divided into four groups including protopanaxadiols (PPT), protopanaxatriols (PPD), type C and type D [7] (Fig.1). Some minor ginsenosides, like F0, F11, 25-OH-PPT and 25-OH-PPT do not belong to any of these four groups and be considered as other ginsenosides. With more ginsenosides discovered, the classification of structure will be updated accordingly. Based on the current knowledge, the PPD series has sugar moieties attached to the β-OH at C-3 and/or C-20; the PPT series has sugar moieties attached to the α-OH at C-6 and/or β-OH at C-20; Type C and Type D series were the derivatives of PPT and PPD, with double bond in aliphatic side [29] (Fig.1).

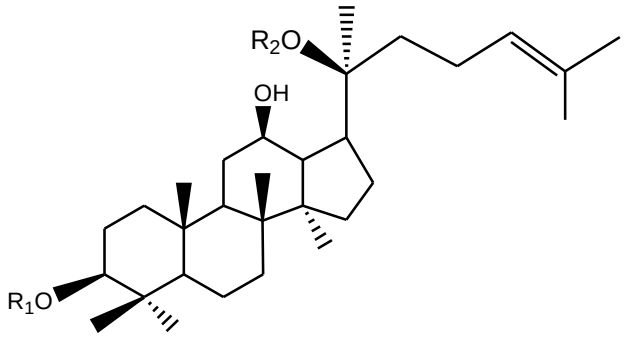

PPD series

PPD series	R1	R2
Rb1	Glu^{2}-Glu	Glu^{6}-Glu
Rb2	Glu^{2}-Glu	Glu^{2}- Arap
Rb3	Glu^{2}-Glu	Glu^{2}- Xyl
Rc	Glu^{2}-Glu	Glu^{6}- Araf
Rd	Glu^{2}-Glu	Glu
Rg3	Glu^{2}-Glu	H
Rh2	Glu	H
F2	Glu	Glu
CK	H	Glu
PPD	H	H

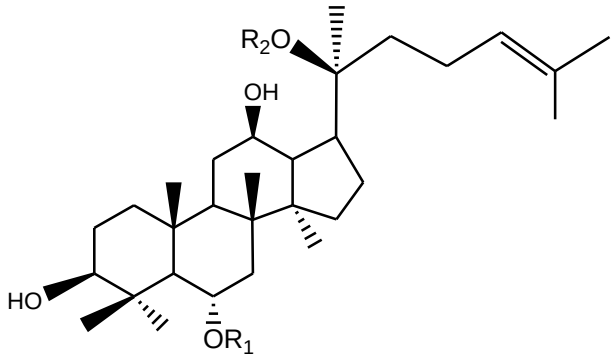

PPT series

PPT series	R1	R2
Rh1	Glu	H
Rg1	Glu	Glu
Re	Glu^{2}-Rha	Glu
F1	H	Glu
R1	Glu^{2}- Xyl	Glu
Rg2	Glu^{2}-Rha	H
R2	H	Glu^{2}- Xyl
PPT	H	H

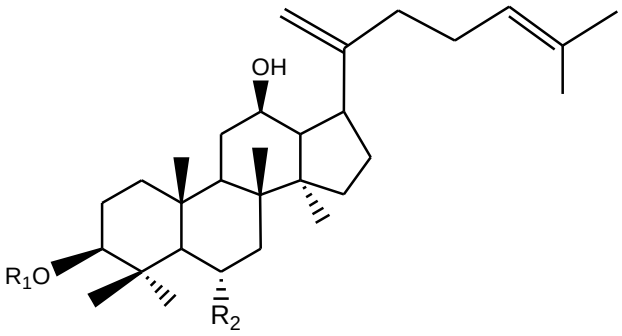

Type C

Type C	R1	R2
Rg5	Glc^{2}-Glc	H
Rh3	Glc	H

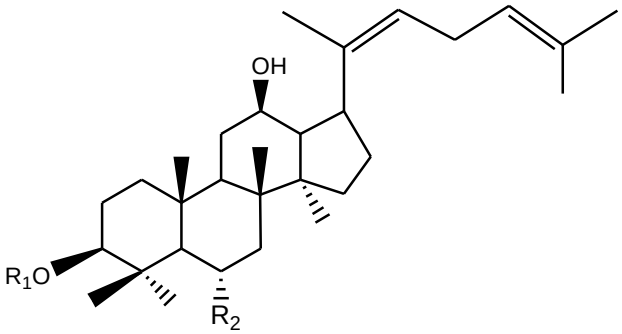

Type D

Type D	R1	R2
Rk1	Glc^{2}-Glc	H
Rk2	Glc	H

Figure 1. Chemical structures of ginsenosides including PPD series, PPT series, Type C and Type D.
Glu=β-D-glucose; Arap=α-L-arabinose (pyranose); Araf=α-L-arabinose (furanose); Xyl=β-D-xylose; Rha=α-L-rhamnose.

1.1.6. Challenges for clinical usage

Although ginsenosides showed promising chemoprevention and anticancer effect in epidemiological study and various animal/cell models [1, 29], only a few of them showed significant efficacy in strictly double-blind clinical trials and most of them showed weak or no significant difference, which resulted in unimproved therapeutical effects [39, 40]. One of the major reasons may derive from well-reported low oral bioavailability, which causes large variations in clinical trials and its low exposure in vivo may eventually decrease its efficacy. Even for the approved ginsenoside drug (i.e. Rg3), the plasma level is below quantification limit (2.5 ng/ml) at 0.8 mg/kg and C_{max} is only 15.6 ng/ml at 3.2 mg/kg in human [41, 42]. The oral bioavailabilities of various ginsenosides obtained from rats were summarized in Table 1. As we can see from the data, oral bioavailability of most ginsenosides are less than 5%, some of them are even not detectable in rat plasma. PPD is the only ginsenoside reported to show relatively high oral bioavailability (20~40%) at different doses from two different labs.

Table 1. The oral bioavailability of various ginsenosides in rats after oral administration at different doses.

In Rat	Oral bioavailability (%)	Dose (mg/kg)	reference
Rh2	4.7	1 ,3,9	[3]
Rh2	N/A (< LOQ)	100	[43]
Rg3(r)	N/A (< LOQ)	100	[13]
Rg3	2.63	10	[44]
CK	3.52-6.57	30	[45]
	1.8	5	
	4.3	10	
	35.0	20	
			[46]
Re	0.16-0.28	1	[47]
Rb1	4.35	10	[48]
Rd	2.36	10	[49]
Rg1	1.33	100	[50]
PPD	36.8	2	[51]
	20.7	25	
	22.4	25	[52]

1.2.1. Introduction to oral bioavailability

Bioavailability represents the extent and rate at which the active moiety enters systemic circulation to cause desired response at the site of action. Given that the therapeutic effect is usually associated with the drug concentration in a patient's blood, bioavailability is essentially important to identify the response to a drug dose [53]. Bioavailability can be applied to various administration routes (e.g. oral, intraperitoneal, inhalation, topical and etc), and oral administration is the most convenient route due to lower development cost and improved patient's compliance, and it is the common route especially for chemoprevention purpose. Oral bioavailabilty may vary largely due to numerous barriers and biotransformation in vivo and it can be greatly influenced by these factors. From industry interest, it is well established that poor oral bioavailability is one of the leading causes of compound failure in drug development. Poor oral bioavailability not only causes low therapeutic effects but also generates large variations in clinical trials which can result in ambiguous and insignificant conclusion.

Generally, there are two types of calculations on the oral bioavailability in previous publications. One refers to the absolute bioavailability which is calculated by comparing the plasma/urine AUC_{oral} to AUC_{iv} after dose correction (classic pharmacokinetics definition). It is the most accurate measurement and commonly used in animal studies when AUC is available following intravenous

administration [54, 55]. The other definition is to calculate plasma/urine AUC_{oral} or obtain the % recovery based on the administrated dose. It is usually applied in clinical pharmacokinetics or nutrition studies as the intravenous administration is not available due to practical or ethical issues [56, 57]. In this thesis, bioavailablility of gisnenosdies was calculated as absolutely bioavailability.

1.2.2. Factors affecting oral bioavailability

Absorption and metabolism are the two main features determining the oral bioavailability of drug. Absorption is regarded as drug transfer from the site of administration, across the intestinal epithelium and into portal vein. From physicological perspective, oral absorption takes place when drug molecules enter the mucosal membrane of the gastrointestinal (GI) tract. Once drug molecules enter intestinal membrane, it is considered as absorbed from GI lumen [58]. However, it is noted that drug may go through metabolism in epithelia cells and the parent compound may stay in epithelia cells due to protein binding or binding to receptors for various time before moving to mesenteric vein. Therefore, Caco-2 cell and intestinal perfusion may be the proper tools to directly measure and predict durg's oral absorption in human. As indicated in BCS (biopharmaceutics classification system) that solubility and permeability are two fundamental parameters controlling the rate and extend of oral absorption [59].

Metabolism includes presystemic stability in GI tract (e.g. reduction and hydrolysis reaction by gut microbial) and systemic metabolism majorly occurred

in enterocytes and hepatocytes. Presystemic stability determines how much of dose is available for intestinal absorption after oral administration. It is particularly important for ginsenosides absorption since most of them are glycosides and abundant glycosidase existed in lumen may hydrolyze them efficiently [60]. Drug-metabolizing enzymes, i.e. CYP and UGTs/SULTs are the causes for first-pass effect in intestine and liver, which represent a major obstacle for oral bioavailability. Based on the parameters described in BDDCS (biopharmaceutical drug disposition classification system), solubility and metabolism are the two major factors determining drug disposition [61]. Here the metabolism refers to systemic metabolism and it takes consideration of permeability since drug need to be absorbed first before metabolism reactions occur.

1.2.3. Absorption

Drug absorption is usually determined by drug's physicochemical properties after oral administration. Passive diffusion and carrier-mediated absorption are the two major absorption pathways.

1.2.4. Passive diffusion

Most of drugs are absorbed across the intestinal membrane by passive diffusion, and it can be further divided into two categories: paracellular and transcellular pathway [62]. In paracellular pathway, many hydrophilic (usually Log P<0) and small molecules (usually Mw<200) can diffuse through the aqueous pores at the

tight junctions between intestinal enterocytes [63] whereas lipophilic molecules traverse the cell membrance of intestinal enterocytes in transcellular pathway. However, it has to be noted that paracellular absorption is the minor pathway due to tight junctions of enterocytes and much small surface areas compared to transcellular pathway [64]. The rate of passive diffusion is mainly determined by the physicochemical properties of the drugs. In general, the absorbed compounds are unionized, with balanced lipophilicity and hydrophilicity, and suitable molecular weight. Lipinski's 'rules of five' is a well known criterion to evaluate whether the compound has good oral absorption. It states as following: 1) molecular weight less than 500 daltons; 2) an octanol-water partition coefficient (Log P) less than 5; 3) number of hydrogen bond donors (OH and NH group) less than 5; 4) number of hydrogen bond acceptors less than 10. If any compound violates any two of the above rules, it is likely to be poorly absorbed [65].

1.2.5. Carrier-mediated absorption

For carrier-mediated absorption, it can be divided into facilitated and active transport based on energy requirement during the transport. Facilitated transport does not require energy, but follows the concentration gradient whereas active transport needs energy (usually from ATP hydrolysis) and transport against concentration gradient during absorption. For example, GLUT (glucose transporter) is the facilitated transporter while SGLT (sodium-dependent glucose

transporters) is the active transporter for glucose transport. Transporters are the gatekeepers for all cells and organelles, controlling uptake and efflux of endobiotics and xenobiotics. Membrane transporters can be further divided into two main classes: solute carrier family (SLC) and ATP-binding cassette (ABC) transporters.

1.2.6. Solute carrier transporter

The solute carrier transporters (SLC) contains more than 300 members with 47 families [66] and they are responsible for the uptake of amino acids, peptides, ions, xenobiotics, endobiotics, sugars and other biologically active compounds [67]. Solute carrier transporters are widely expressed in most tissues, including intestine, liver, kidney, lung and etc. They are located on the cell membrane as well as on the intracellular membrane of organelles. There is compelling evidence that these uptake transporters are involved in drug absorption, disposition and drug-drug interactionin in clinical studies [68]. The most important SLC transporters include 1) expressed in the apical side of intestinal epithelia: organic anion transporting polypeptide (OATP) family, peptide transporter 1 (PEPT1), and apical sodium/bile acid co-transporter (ASBT); 2) expressed in the basolateral side of human hepatocytes: sodium/taurocholate co-transporting peptide (NTCP), OATP1B1, 1B3 and 2B1, organic anion transporter 2 (OAT2), OAT7 and OCT1; 3) expressed in the kidney proximal tubules: OAT4, PEPT1, PEPT2, urate transporter 1 (URAT1), organic cation/ergothioneine

transporter (OCTN1, OCTN2) and OAT1, OAT2 and OAT3; 4) expressed in brain capillary endothelial cells contributing to the functions of the blood-brain barrier: OATP1A2 and OATP2B1 [68]. FDA issued guidelines for assessing transporter mediated drug interaction for five SLC transporters with demonstrated clinical significance: OCT2, OAT1, OAT3, OATP1B1 and OATP1B3 [68].

1.2.7. ATP-binding cassette (ABC) efflux transporters

ABC transporters transport a wide range of substrates mainly to the outside of a cell membrane. Their substrates include: lipids and sterols, ions, small molecules, drugs and large polypeptides. The human genome contains 49 ABC genes, which are further classified into seven distinct subfamilies from ABCA to ABCG based on sequence and organization of their ATP-binding cassette domains [69]. The common feature of all ABC transporters is that they all consist of the transmembrane domain (TMD) and the nucleotide-binding domain (NBD). The TMD, embedded in the membrane bilayer, recognizes a variety of substrates and undergoes conformational changes to transport the substrate across the membrane whereas the NBD is the ATP binding site located in the cytosol side. ABC transporters play a critical role in the development of multi-drug resistance in cancer cells and it is well accepted that their roles are to facilitate efflux of their substrates and to serve as rate-limiting step for oral absorption of therapeutical drugs [70-72]. The important ABC transporters in human include P-gp (ABCB1), MRP (ABCC), BCRP (ABCG2), cholesterol transporter (ABCG5/8) and bile salt

efflux pump transporter (BSEP). P-gp and BCRP are two ABC transporters that FDA requires routine drug interaction assessment [68].

1.2.8. P-glycoprotein (ABCB1)

P-glycoprotein (P-gp) was first identified in 1976 as a surface phosphoglycoprotein using Chinese hamster ovary cells when a cross-resistance to anticancer agents was observed [73-75]. P-gp consists of 1280 amino acids with molecular weight (Mw) of 170 kDa, and its gene name is MDR1, also called ABCB1. Humans have two genes from MDR family (MDR1 and MDR3) whereas rodents have three Mdr genes (Mdr1a, Mdr1b, and Mdr2). The P-gp encoded by human MDR1 and mouse Mdr1a/1b are responsible for drug efflux, whereas human MDR3 and mouse Mdr2 encoded P-glycoprotein are functional in phospholipid transport [69]. Some results also suggest MDR3 P-glycoprotein is able to transport drugs, like digoxin, paclitaxel and vinbalstine in addition to phospholipids [76].

P-gp consists of 12 transmembrane domains and 2 nucleotide binding domain. A recently published mouse P-gp crystal structure revealed an inward facing conformation that is believed to be important for binding substrate along the inner leaflet of the membrane. Additional structures binding with two different cyclic peptides revealed poly-specific drug binding site and the promiscuous binding pocket of P-gp is lined with aromatic amino acid side chains [77]. There are

several proposed molecular mechanism of transport, including hydrophobic vacuum cleaner model, flippase model and phospholipid flip-flop within the lipid bilayer, but the deep understanding of its mechanism remains to be revealed [69]. P-gp is one of the most prevalent efflux transporters expressed in multidrug resistance cancer cells and in several organs such as intestine, liver, kidney and the blood-brain barrier [78]. P-gp plays an important role in limiting the intestinal absorption of its substrates in vivo [79] and inhibition of P-gp leads to the improvement of bioavailability of several orally administrated anticancer drugs [80-82].

1.2.9. Localization and expression of P-gp

P-gp is expressed in many cancer cell lines such as Caco-2 cells [83], and tumor tissues such as hepatocellular carcinoma, breast cancer and primary testicular tumors [84-86], which may be one of the major reasons responsible for the failure of treatment of patients with metastatic cancer. In addition to the expression in tumor cells, it is highly expressed in normal tissues, like intestine, liver, kidney and brain. In human intestine, P-gp is expressed in apical membrane of enterocytes and its mRNA level is highest in jejunum, followed by ileum and colon [87]. In contrast, protein level of P-gp in mice is highest in colon, followed by ileum and jejunum [88]. In liver, P-gp is highly expressed on the canalicular membrane of hepatocytes to facilitate the biliary excretion of many P-gp substrates, like daunomycin and doxorubicin [89, 90].

1.2.10. Substrates of P-gp

P-gp has broad substrate specificity, recognizing hundreds of compounds including lipids, steroids, xenobiotics, chemotherapeutics, peptides, glycosides, biliruin and etc. The molecular weight ranges from 250 daltons (cimetidine) up to several thousand daltons (cyclosporine A). Although most of the drugs transported by P-gp are basic or uncharged compounds, there are many exceptions [91]. One common feature is that most P-gp substrates are hydrophobic and partition into the lipid bilayer [91, 92]. Didziapetris et al raised the concept that substrates of P-gp could be predicted by a “rule of four” that compounds with (N + O) $\geqslant$ 8, MW > 400 and acid pKa > 4 are likely to be Pgp substrates, whereas compounds with (N + O) $\leqslant$ 4, MW < 400 and base pKa < 8 are likely to be non-substrates [93]. Other studies have shown that both the lipophilicity and number of hydrogen bonds of compounds are the most important parameters to be recognized as substrates of P-gp [94].

1.2.11. Multidrug-resistance associated proteins (MRPs/ABCC)

So far 12 members have been identified in human ABCC subfamily which consists of ABCC1 through ABCC12, and nine of them are MRP transporters [69]. ABCC1 (MRP1), ABCC2 (MRP2/cMOAT), ABCC3 (MRP3), ABCC6 (MRP6), and ABCC7 (CFTR) are the larger MRPs containing three transmembrane domains (TMDs) whereas ABCC4 (MRP4), ABCC5 (MRP5), ABCC8 (SUR1), and ABCC9

(SUR2) contain two TMDs. MRP2 is one of the most studied transporter among MRP family due to well reported clinical significance. It is the largest MRP with a MW of 190 kDa and 1545 amino acids. MRP2 is expressed in many cancer cell lines [83], and tumor tissues [84-86] resulting in multidrug resistance in cancer chemotherapy [95]. It is also highly expressed in various normal tissues, such as the apical side of enterocytes, the canalicular membrane of the liver and the brush-border membrane of proximal tubule epithelial cells [96-98]. The substrate of MRP2 includes a variety of drugs such as doxorubicin, mitomycin C, cisplatin, 5-fluorouracil, etoposide as well as endogenous compounds and metabolites [71, 99-104]. Unlike P-gp, MRP2 substrates have been shown to include many hydrophilic compounds, i.e. phase II metabolites of endogenous and exogenous compounds such as bilirubin glucuronides and flavonoids glucuronides [105, 106]. Highly expressed MRP2 in intestine and liver may decrease drug absorption and facilitate its excretion, consequently cause low oral bioavailability. Other MRP members, like MRP3 and MRP4 are located on the basolateral side of enterocytes and hepatocytes, and apical side of renal tubular cells. Knockout of MRP3 and MRP4 was reported to lead low plasma level of glucuronides of morphine and bilirubin indicating they are responsible for excreting metabolites into blood [107, 108]. MK571 is the commonly used chemical inhibitors for MRP members and so far there are no specific inhibitors for individual MRP transporters.

1.2.12. Breast Cancer Resistance Protein (BCRP, ABCG2)

Unlike P-gp and MRP2, BCRP is a half-size ABC transporter as it has one NBD at the N-terminus and one TMD containing 6 transmembrane regions at the C-terminus. There are reports showed that BCRP possibly functions as a homodimer [109]. BCRP is not only expressed in many cancer cell lines and solid tumor tissues for its multidrug resistance function [110], but also expressed in various normal tissues, such as the apical membrane of trophoblast cells in placenta, the brush-border membrane of intestinal epithelial cells, canalicular membrane of hepatocytes and the luminal surface of endothelium in brain microvessels [110-112]. BCRP has been reported to confer a variety of drugs for multidrug resistance function such as mitoxantrone, daunorubicin, doxorubicin, cisplatin, SN-38, topotecan and dipyridamole[110, 113-115]. BCRP substrates have also been reported to include many phase II metabolites, especially for sulfation conjugates [116]. KO143, FTC and LTC4 are commonly used as chemical inhibitors for BCRP and KO143 is the most potent one with IC_{50}=33 nM [117].

1.2.13. Cholesterol transporter (ABCG5/G8)

ABCG5 and G8 functions as a sterol efflux heterodimer pump for mediating the secretion of sterols from the liver and efflux of dietary sterols from the gut [118, 119]. As the member of G subfamily of ABC transporters, G5 and G8 are also half-transporter and oligomerize to form the functional transporter. They are

highly expressed on the apical membrane of hepatocytes and expressed at low levels in the apical membrane of enterocytes in small intestine and colon. It has been reported that net cholesterol absorption correlates with the expression levels of ABCG5/8 in intestine in mice [120]. Biliary cholesterol concentrations were extremely low in Abcg5 Abcg8 (−/−) knockout mice when compared with wild-type mice [121]. Similarly, plasma level of dietary plant sterols are many fold higher in Abcg8 (−/−) knockout mice than wild-type mice [121]. So far there are no specific inhibitors for Abcg5 and Abcg8, and sterols are commonly used as competitive inhibitors. Expression of Abcg5 and Abcg8 were regulated by liver X receptor (LXR), and the inducer of LXR, like TO901317 could increase their expression level [122].

1.2.14. Bile salt export pump (BSEP/ABCB11)

Bile salt export pump (BSEP), formerly called sister of p-glycoprotein, belongs to ATP binding cassette B subfamiliy. It is responsible for active transport of bile acids across the hepatocyte canalicular membrane into bile, and recently studies showed that it can also transport non bile acid substrate, like statin-type drugs [123]. In human, BSEP is highly expressed in liver, and also expressed in intestine and kidney in a relatively low level [124]. BSEP inhibitors include natural bile salts and xenobiotics such as rifampicin and troglitazone [125].

1.2.15. Metabolism

Metabolism is the major elimination route for drugs. Drug is chemically modified into polar metabolites that can be easily excreted through urine or bile. However, extensive metabolism in intestine and liver is one of the major reasons causing low oral bioavailability. From industry perspective, drug candidates should have good metabolism stability to allow for decent bioavailability and long dose internal, and further decrease the uncertainty related to metabolites.

Metabolism can be generally divided into two processes, phase I and phase II metabolism.

1.2.16. Phase I metabolism

Phase I enzymes can catalyze a variety of chemical reactions including oxidation, reduction, hydrolysis and the final products of phase I metabolism are usually modified to contain a functional group (i.e., hydroxyl, amine, sulfa and carboxylic acid) that are chemically and pharmacologically active [126]. Most often, this simply modification could be sufficient to increase the hydrophilicity of drug or xenobiotics, facilitating their elimination through kidney. The majority of research in Phase I metabolism has focused on cytochrome P450 enzymes [121].

1.2.17. The Cytochrome P450s (CYPs)

CYPs are membrane bound proteins and located in the endoplasmic reticulum. It has an approximate molecular mass of 50 kD and contain a heme moiety. CYPs are responsible for primary metabolism of various of xenobiotics [127] and the overall main catalytic functions are to transfer one oxygen atom from NADPH to a substrate. The nomenclature for CYPs is essentially based on gene sequence similarity. There are about 30 human cytochrome P450 enzymes and six of them, CYP1A2, CYP2C9, CYP2C19, CYP2D6, CYP2E1 and CYP3A4 are the major drug metabolizing enzymes. The profound understanding of CYPs metabolism is greatly moved forward by many crystal strucutures of CYP isoforms and well defined substrates and inhibitors. FDA requires CYP metabolism data including identifying CYP isoform and CYP inhibition/induction in IND (Investigational New Drug) and NDA (New Drug Application).

1.2.18. Phase II metabolism

Phase II metabolism includes glucuronidation, sulfation, amino acid conjugation, acetylation, methylation and glutathione conjugation. It may be directly biotransformed from parent compound or derived from Phase I metabolites for further increasing hydrophilicity. Generally, phase II metabolites are detoxifying products and have much less efficacy than phase I metabolites. Glucuronidation and sulfation are the most two important metabolism pathways in phase II

metabolism. The substrates of phase II metabolism include many phenols and endobiotics, like steroids, bilirubin, serotonin, carbohydrates and etc.

1.3. 1. Strategy for improving oral bioavailability

According to the literature, many newly discovered leads based on various pharmacological model tend to have high molecular weight with low solubility, resulting in BCS III and IV compounds that are usually associated with poor oral bioavailability [65]. For low soluble compounds, micronization, surfactants, co-solvents, cyclodextrin, liquid--based formulation and suspensions are commonly used to improve solubility. In general, aqueous formulations were preferred over lipophilic preparations. In formulations containing organic co-solvents, the aqueous phase was 70% or greater. The final preparation was maintained between pH 4–8 [128, 129]. From industry perspective, various high throughput ADME assays could be screened during the early phase of drug discovery to identify the limiting factors causing low oral bioavailability of drug candidates. Based on the characterization of compounds, strategies are usually targeted on solubility, permeability and metabolism correspondingly. Empirical and SAR (structure-activity relationship) guided chemical synthesis are involved during the whole process of drug discovery and development to resolve those individual issues without losing its potency [62]. For example, if solubility is the limiting step, chemical modification of crystal lattice energy and lipophilicity should be performed. If permeability and metabolism are the limiting factors, Caco-2 SAR,

P-gp SAR and metabolism SAR should be utilized, respectively [62]. Other approaches include prodrug, targenting on uptake transporters and etc. will be also considered during the early stage of drug discovery and development [130-132].

When drug developments come into in clinical phase or developing certain potent natural compounds, chemical strucutures of the molecures cannot be easily modified, therefore, formulation and biopharmaceutical approaches are usually used to overcome the obstacles of low oral bioavailability. Optimization of formulation and taking consideration of the biopharmacokinetic property of compounds (through drug-drug combination) are proved to be successful in improving oral bioavailability [133, 134]. In this chapter, overcoming efflux transporters effects will be mainly focused.

1.3.2. Reversing efflux transport

Efflux transporters play a major role in limiting the intestinal absorption of various xenobiotics. P-gp is the most studied efflux transporter and many clinical studies showed that P-gp is the major reason causing drug resistance and low oral bioavailability [135]. Four generations of P-gp modulators has emerged to overcome this phenotype. The first generation of P-gp inhibitors include verapamil and cyclosporine A, but their clinical studies indicated significant toxicity and low potency after coadministration with other drugs [136, 137], which

lead to chemical systhesis of the second generations of P-gp inhibitors, like PSC-833. PSC-833 is the derivative from cyclosporine A and showed high potency with lower but not negligible toxicity. The third generation of P-gp inhibitors such as GF120918 and LY335979, showed even better potency (Ki=~50nM) with minimal pharmacokinetic interactions. Some of them showed promising results in clinical study and more conclusive conclusions are waiting for further clinical study. Development of natural compounds as P-gp inhibitors has emergied in the recent ten years and it was considered as fourth generation of reversing agent [138]. Natural products caught many researchers' attention because of well known herb or food-drug interaction in term of transporter perspective. Natural products such as curcumin and some flavonoids showed significant P-gp inhibition effect in human cell lines. Most importantly, natual products which have been used for long history have much lower toxicity compared to synthesized reversing agents [138-140].

OBJECTIVES AND HYPOTHESIS

Preclinical pharmacokinetics showed the bioavailability of ginsenosides after oral administration is generally less than 5% [3]. Several clinical pharmacokinetic studies showed that the exposure level of ginsenosides are extremely low in plasma (several nanomolar range), even below the quantification limit at the low dose [41]. However, the reasons for low oral bioavailability of ginsenosides have not been clearly revealed. Previous studies indicated that oral absorption of ginsenosides is poor but the underlying mechanism is not well understood. Some studies even have contradictory conclusions with respect to the resposible efflux transporter, especially p-glycoprotein [141, 142], understanding of which may hold the key to overcome the absorption barrier. The current approaches to increase oral bioavailability of ginsenosides are mainly focused on formulation optimization and the improvement is marginal and not clinical significant.

2.1. Objectives

The overall goal is to increase the oral bioavailability of ginsenosides via mechanism-based biopharmaceutical approaches. In order to achieve the goal, we will 1) determine the limiting factors causing low oral bioavailability of ginsenoisdes using various ADME assays; 2) delineate absorption mechanisms of ginsenosides and its structure-absorption relationship; and 3) improve the oral

bioavailability of ginsenosides based on the knowledge obtained in the first two aimes.

2.2. Hypothesis

The hypotheses for this thesis are as follows:

H1. Low oral absorption is the leading causes limiting oral bioavailablity of ginsenosides.

H2. Ambiguous and even contradictory understandings of transport mechanism of ginsenosides can be resolved clearly via a biopharmaceutics-based systematic approach.

H3. Disruption of efflux transporter will enhance oral bioavailability of ginsenosides via increased absorption and/or decreased clearance.

GENERAL METHODOLOGY

3.1. Aqueous solubility study

Compound's aqueous solubility could be measured by various approaches. In general, solubility can be divided into thermodynamic and kinetic solubility [65]. Thermodynamic solubility refers to equilibrium concentration of a compound in an oversaturated solution. On the other hand, kinetic solubility is measured when the compound precipitates out in an aqueous solution using a titrating method [143]. Thermodynamic method is more accurate due to consideration of compound crystal lattice, temperature and pressure [144]. Therefore, we measure thermodynamic solubility of ginsenosides in HBSS buffer, pure water and simulated intestinal fluid at different physiological environment pH values. Detailed method for aqueous solubility measurement will be discussed in later chapters.

3.2. Caco-2 cell transport model

Caco-2 cell TC-7 clone was used for the permeability measurement and transport mechanism study. TC-7 is one of the subclones isolated from Caco-2 cells. It was reported to have very similar cell morphology as in Caco-2 cells, such as the polarity of membrane and the formation of tight junctions. The permeability values of passively absorbed drugs in TC-7 clone correlated well as in parental Caco-2 cells to the extent of absorption in humans. The protocol

performing Caco-2 transport of genistein is the same as those described previously [105]. Detailed method for the Caco-2 model will be discussed in later chapters.

3.3. Presystemic stability in GI tract

Due to the glycoside bond in ginsenosides' structure, abundant β-glucosidase existed in GI tract may hydrolyze parent compounds to its aglycone causing great pre-systemic loss during the absorption. Therefore, the stability of ginsenosides in GI environment will be investigated by incubating them in the simulated gastric and intestinal fluid. The intestinal fluid is obtained by perfusing A/J mice intestine with blank HBSS. Detailed method for presystemic stability study will be discussed in later chapters.

3.4. Phase II metabolism experiments

3.4.1. Mouse S9 fractions preparation

S9 fraction contains a wide range of enzymes located in endoplasmic reticulum (ER) and cytosol including P450 enzymes, flavin-monooxygenases, carboxyl-esterases, epoxide hydrolase, UDP-glucuronosyltransferases, sulfotransferases, methyltransferases, acetyltransferases, glutathione S-transferases and other drug-metabolizing enzymes. It is the ideal enzyme system used to measure metabolism stability of compounds and identify the potential metabolites in vivo.

The preparation of mouse S9 fractions were modified from a previously published method to prepare microsomes [145]. Detailed method for Mouse S9 fractions preparation will be discussed in later chapters.

3.4.2. CYP reaction in intestinal or hepatic S9 fractions

The incubation procedures for CYP reaction using liver/intestine S9 fractions were the same as those published previous by our laboratory [146, 147]. Detailed method for CYP reaction will be discussed in later chapters. EMS (enhanced full scan) and MS2 (fragmental ion) mode was used to search for possible CYP metabolites of ginsenosides. Positive control experiment was done by determining the concentrations of 6β-hydroxytestosterone and testosterone after 10 μM testosterone was incubated in the same conditions.

3.4.3. Glucuronidation in S9 fractions

The incubation procedures for UGT reaction were the same as those published previous by our laboratory [147]. Detailed method for UGT reaction will be discussed in later chapters. EMS (enhanced full scan) and MS2 (fragmental ion) mode was used to search for possible glucuronidation metabolites of ginsenosides. Positive control experiment was done by determining the concentrations of genistein glucuronides after 10 μM genistein was incubated in the same conditions.

3.4.4. Sulfation in S9 fractions

The incubation procedures for SULT reaction were the same as those published previous by our laboratory [116]. Detailed method for SULT reaction will be discussed in later chapters. EMS (enhanced full scan) and MS2 (fragmental ion) mode was used to search for possible sulfation metabolites of ginsenosides. Positive control experiment was done by determining the concentrations of genistein sulfates after 10 μM genistein was incubated in the same conditions.

3.5. Mouse intestinal perfusion models

The mouse intestinal surgical procedures were approved by University of Houston Institutional Animal Care and Use Committee and are the same as those described previously [145]. We perfused two segments (upper small intestine and colon, 5-10 cm each) of the mouse intestine (a two-site intestinal perfusion model). Detailed method for mouse perfusion model will be discussed in later chapters.

3.6. Pharmacokinetic studies

Pharmacokinetics of ginsenosides were performed to determine the oral bioavailability of gisnenosides. A/J mice were used as lung cancer prevention animal model. Wild-type and MDR1a/b knockout mice were used to determine the role of P-gp on the oral bioavailability of ginsenoisdes. Cyclosporine A and

other natural productes were coadministrated with ginsenosdies to investigate their effects on bioavailability of ginsenosides. Detailed method for mouse pharmacokinetic studies will be discussed in later chapters.

3.7. Pharmacokinetic analysis

WinNonlin 3.3 (Pharsight Corporation, Mountain View, California) was used for Rh2s pharmacokinetic analysis. Both compartmental and non-compartmental model were applied for pharmacokinetic analysis. Pharmacokinetic parameters, including C_{max}, T_{max}, k_e, half-life and AUC were directly derived from WinNonlin. The absolute oral bioavailability (F) was calculated by the following equation (1):

$$F\% = \frac{Dose_{i.v.}AUC_{p.o.}}{Dose_{p.o.}AUC_{i.v.}} \times 100\% \quad (1)$$

The clearance and apparent volume of distribution at steady state after oral administration were corrected from the original CL (CL_o) and V_{ss} (V_{sso}) obtained from WinNonlin using the F values, as shown in equations (2 & 3).

$$\mathrm{CL} = F \times \mathrm{CL_o}/100 \quad (2)$$

$$V_{ss} = F \times \mathrm{V_{ss_o}}/100 \quad (3)$$

3.8. Statistical analysis

The data in this thesis were presented as means ± S.D., if not specified otherwise. We use triplicates for in vitro studies including solubility, permeability in Caco-2 cell, stability in GI tract and metabolism in S9 fraction. We use quadruplicates for in situ intestinal perfusion studies and n=5 for pharmacokinetic studies. Significance differences were assessed by using Student's t-test or one-way ANOVA. A p value of less than 0.05 was considered as statistically significant.

Biopharmaceutical characterizations of ginsenosides reveal poor oral absorption is the major reason for low bioavailability

4.1. Abstract

Ginsenosides are reported to have chemopreventive and anticancer activities [1, 148]. but their low oral bioavailability (generally <5%) is the major factor causing ambiguous results in clinical trials and further represents a major obstacle when used as chemopreventive or chemotherapeutic agents. We determined the main factors causing low oral bioavailability of ginsenosides using various ADME assays. Three ginsenosides, Rg3, Rh2 and PPD were chosen as lead compounds. Saturated aqueous solubility tests revealed that ginsenosides Rg3s, Rh2s and PPD have poor solubility, less than 10 μM in various biological media including HBSS buffer, water and simulated intestinal fluid. Caco-2 cell permeability study showed that Rg3s and Rh2s have poor permeability (< 10^{-6} cm/s) whereas PPD has moderate permeability. Presystemic stability in GI tract indicated that these ginsenosides were chemically and enzymatically stable during oral absorption. In vitro metabolism showed that Rh2s and PPD could be extensively metabolized in liver S9 fraction, but we did not observe obvious metabolites in vivo after oral administration. In conclusion, the results indicated that poor solubility and permeability may be the major reasons responsible for low oral bioavailability of ginsenosides. Although CYP metabolism occurred at in vitro system, it may not present as the main obstacle in vivo.

Key words: ginsenosides, solubility, permeability, metabolism, stability, CYP (Cytochrom P450).

4.2. Introduction

Ginsenosides are reported to have chemopreventive and anticancer activities [1, 148]. but their low oral bioavailability (generally <5%) is the major factor causing ambiguous results in clinical trials and further represents a major obstacle for these compounds to be used effectively as chemopreventive or chemotherapeutic agents. Gu et al reported that oral bioavailability of ginsenoside Rh2 was 5% in rat after administratin at 1, 3 and 9 mg/kg [3]. The oral bioavailability of Rg3 was 0.5% in dog after 2 mg/kg [14] and it was not detectable in rat plasma after oral administration at 100 mg/kg [13]. Ginsenoside Re showed very low oral bioavailability ranging from 0.19-0.28% after oral administration of 50 mg/kg in mice [47]. Ginsenoside aglycone, protopanaxadiol has relatively high oral bioavailability at 20-22% after using oil and emulsion formulation at 25 mg/kg [52]. Oral bioavailability of compounds is usually influenced by many factors, including solubility, permeability, presystemic stability in GI tract, metabolism and etc [130]. Solubility and permeability are two major parameters used to describe drug's bioavailability as suggested in BCS (biopharmaceutical classification system). Evaluation of presystemic stability of ginsenoside in GI tract is important as some reports indicated that ginsenosides in vivo can be deglycosylated by intestinal bacteria via stepwise cleavage of the sugar moieties [2, 149, 150]. In vivo metabolism of ginsenosides should be considered since some of ginsenosides, especially the potent ginsenosides with less sugar moieties are very hydrophobic and may be metabolized to facilitate its

elimination in vivo [17]. Because of variable structures among ginsenosides, we chose three highly active ginsenosides with different numbers of sugar moieties, Rg3, Rh2 and protopanaxdiol as lead compounds. Systematic research to biopharmaceutically characterize these ginsenosides has not been conducted. Therefore the underlying mechanisms for their low oral bioavailability have not been revealed clearly. In this study, we will perform four biopharmaceutical experiments, saturated aqueous solubility, intestine membrane permeability study, stability in acid stomach fluid and intestine fluid and metabolism in S9 fraction to reveal the causes for low oral bioavailability of these ginsenosides.

4.3. Materials and methods

4.3.1. Materials

Ginsenosides was prepared by Dr. Zhi-Hong Jiang's laboratories at Hong Kong Baptist University. Simulated gastric fluid was purchased from VWR. 3'-phosphoadenosine 5'-phosphosulfat was purchased from Cayman Chemicals (Ann Arbor, MI). Pepsin, uridine diphosphoglucuronic acid (UDPGA), alamethicin, D-saccharic-1,4-lactone monohydrate, magnesium chloride, phenylmethylsulfonyl fluoride (PMSF) nicotinamide adenine dinucleotide phosphate (NADP), glucose-6-phosphate sodium (6-DP), glucose-6-phosphate dehydrogenase (6-DPD), saccharolactone, alamethicin, magnesium chloride, phosphoricacid and Hanks' balanced salt solution (HBSS, powder form) were

purchased from Sigma-Aldrich (St. Louis, MO). All other materials were analytical grade or better.

4.3.2. Animals

Male A/J mice (6-8 weeks old) weighing between 20 and 25 g were purchased from Harlan Laboratories (Madison, WI). They were acclimated in an environmentally controlled room (temperature: 25 ± 2°C, humidity: 50 ± 5%, 12 h dark-light cycle) for at least 1 week prior to experiments.

4.3.3. Aqueous solubility measurement

The saturated aqueous solubility of Rg3s, Rh2s and PPD were measured in HBSS buffer, pure water and simulated intestinal fluid at different physiological environment pH values. The HBSS buffer is composed of HBSS powder (9.8 g/L), $NaHCO_3$ (3.502 g/L), HEPES (5.963 g/L) and D-glucose (3.502 g/L). Simulated intestinal fluid (SIF) was prepared by adding 3.2 g pepsin into 1 L commercially simulated intestinal fluid (VWR) and adjusted pH value at 6.8. Stock solutions of ginsenoside were prepared in alcohol at 10 mM. 10 µl of ginsenosides stock solution were spiked into 1 ml HBSS/water/SIF in triplicate and shaked overnight at 37ºC to make saturated solution. The glass vials were centrifuged at 15,000 g for 20 minutes, 400 µl of supernatant would be carefully taken, added with 100 µl formononetin (I.S.) and dried it under air. The residue were reconstituted with

200 µl methanol and centrifuged at 15,000 g for 10 minutes. 10 µl supernatant were injected to LC/MS/MS for analysis.

4.3.4. Permeability in the Caco-2 monolayer cells

The transcellular transport study was performed as described previously [147]. Briefly, 2.5 ml of ginsenosides solution was loaded onto one side of the cell monolayer, and 2.5 ml of blank HBSS onto the other side. Five sequential samples (0.5 ml) were taken at different times (0, 1, 2, 3 and 4 hrs) from both sides of the cell monolayer. The same volume of ginsenosides solution and receiver medium (fresh HBSS) was added immediately to replace the volume lost because of sampling. The pH values of HBSS in both apical and basolateral side were 7.4. The apparent unidirectional permeability was obtained according to the following equation (Eq.4):

$$\mathrm{P_{app}} = \frac{dC}{dt} \times \frac{V}{\mathrm{SC_0}} \qquad (4)$$

where $\frac{dC}{dt}$ is the rate of concentration change in the receiver chamber (equals to the slope of the regression line derived for the amount transported vs. time profile), V is the chamber volume (2.5 ml), S is the surface area of the monolayer (4.65 cm^2), and C_0 is the starting concentration in the donor side.

4.3.5. Presystemic stability of ginsenosides in GI tract

Due to the glycoside bond in Rg3 and Rh2 molecular structure, abundant β-glucosidase existed in GI tract may hydrolyses parent compounds to its aglycone causing great pre-systemic loss during the absorption. Therefore, the stability of Rg3s, Rh2s and PPD in GI environment will be investigated by incubating them in the simulated gastric and intestinal fluid. The intestinal fluid is obtained by perfusing A/J mice intestine with blank HBSS. The fluid were spiked with Rg3s, Rh2s and PPD at 2, 2 and 0.5 μM and immediately put into a rotating (40 rpm) water bath kept at 37ºC. The study will be performed based on triplicate samples. After 0, 1, 2, 4 and 8 h, 0.5 ml of the incubated fluids were collected and followed the same procedure mentioned above to analysis by LC/MS/MS.

4.3.6. Metabolism of ginsenosides

4.3.6.1. Mouse intestinal and hepatic S9 fraction preparation

This method was adapted from a previously published microsome preparation method [145, 151]. Briefly, A/J mice that were fasted overnight with access to water only were euthanized with anesthesia cocktail. The cocktail was composed of ketamine (50 mg/ml), xylazine (3.3 mg/ml) and acepromazine (3.3 mg/ml). Mouse intestines were cut out into two segments, small intestine and colon. After the same segments were pooled from ten mice, each segment was flushed with ice-cold saline containing 1 mM dithiothreitol (wash solution). Intestinal segments

were washed twice with the ice-cold solution containing 8 mM KH_2PO_4, 5.6 mM Na_2HPO_4, 1.5 mM KCl, 96 mM NaCl, 27 mM sodium citrate, and 0.04 mg/ml phenylmethylsulfonyl fluoride (PMSF) (solution A). The intestinal strips were then blot dried with paper and cut open lengthwise, and mucosal cells were scraped off in a 4°C cold room. The scraped mucosal cells were put into an ice-cold solution containing 8 mM KH_2PO_4, 5.6 mM Na_2HPO_4, 1.5 mM EDTA, and 0.5 mM dithiothreitol and 0.04 mg/ml PMSF (solution B). Cells were collected by centrifugation at 900×*g* for 5 min and washed twice in 12 ml of homogenization buffer, which consists of 10 mM KH_2PO_4, 250 mM sucrose, 1 mM EDTA, and 0.04 mg/ml PMSF (pH 7.4). The cells were resuspended in 2 ml of homogenization buffer, and homogenized with a motorized Teflon/glass homogenizer (four strokes). After 15-min centrifugation in 10,000×*g* at 4°C, the fat layer and pellet were discarded and the supernatant was removed with a Pasteur pipette, aliquoted and stored at -80°C until use. In the mean time, the livers of ten mice were collected in ice-cold solution B in the 4°C cold room. The livers were cut into tiny pieces and suspended into 100 mL homogenization buffer, and homogenized with a motorized Teflon/glass homogenizer. After 15-min centrifugation in 9,000×*g* at 4°C, the fat layer and pellet were discarded and the supernatant was removed with a Pasteur pipette, aliquoted and stored at -80°C until use.

4.3.6.2. Protein concentration measurement

Protein concentrations of S9 fractions were determined using a protein assay kit (Bio-Rad, Hercules, CA), with bovine serum albumin serving as a standard.

4.3.6.3. CYP reaction of ginsenosides in intestinal or hepatic S9 fractions

The incubation procedures for CYP reaction using liver/intestine S9 fractions were the same as those published previous by our laboratory [146, 147]. The conditions were as follows: (1) mix S9 fractions (final concentration $\approx$ 1mg protein/ml), NADP (2.61 mM), Glucose-6-phosphate (6.6 mM), $MgCl_2$ (6.6 mM), 2 μM ginsenoside (2.5 μM for Rh2s and Rg3s, 1 μM for PPD) in a 50 mM potassium phosphate buffer (pH 7.4), and Glucose-6-phosphate dehydrogenase in 5 mM sodium citrate solution (40 U/ml, add last); (2) incubate the mixture (final volume= 200 μl) at 37 °C for 1 h; (3) end the reaction with the addition of 50 μl formononetin (0.5 μM as the internal standard) solution in acetonitrile. The samples were vortexed for 30 s, centrifuged at 15,000 rpm for 10 min, and 10 μl of supernatant was injected into UPLC–MS/MS system for analysis. EMS (enhanced full scan) and MS2 (fragmental ion) mode was used to search for possible CYP metabolites of ginsenosides. Positive control experiment was done by determining the concentrations of 6β-hydroxytestosterone and testosterone after 10 μM testosterone was incubated in the same conditions.

4.3.6.4. Glucuronidation of ginsenosides in intestinal or hepatic S9 fractions

Glucuronidation of ginsenosides by S9 fractions was measured using procedures described previously [145, 147, 152]. The conditions were as follows: (1) mix S9 fraction (final concentration≈1 mg protein/ml), magnesium chloride (0.88 mM), saccharolactone (4.4 mM), alamethicin (0.022 mg/ml), ginsenosides (2.5 μM for Rh2s and Rg3s, 1 μM for PPD) in a 50mM potassium phosphate buffer (pH 7.4), and UDPGA (3.5mM, add last); (2) incubate the mixture (final volume = 200 μl) at 37 °C for 1 h; (3) end the reaction with the addition of 50 μl formononetin (as the internal standard) solution in acetonitrile. The samples were vortexed for 30 s, centrifuged at 15,000 rpm for 10 min, and 10 μl of supernatant was injected into UPLC–MS/MS system for analysis. Genistein glucuronidation reaction was conducted as the positive control and the same experiment but added water instead of UDPGA as the negative control.

4.3.6.5. Sulfation reaction of ginsenosides in intestinal S9 fractions

Sulfation of ginsenosides by S9 fractions was measured using procedures described previously with minor modifications [153]. Briefly, S9 fractions (1 mg/ml) were mixed with ginsenosides (2.5 μM for Rh2s and Rg3s, 1 μM for PPD) in 50 mM potassium phosphate buffer (pH 7.4), and 0.1 mM 3'-phosphoadenosine 5'-phosphosulfate (PAPS) solution was added last to the

reaction mixture (total volume 200 µl). The mixture was incubated in a 37°C reciprocal shaking (50 rpm) water bath for 60min. The reaction was stopped with the addition of 50 µl formononetin (as the internal standard) solution in acetonitrile. Genistein sulfation reaction was conducted as the positive control and the same experiment but added water instead of PAPS as the negative control.

4.3.6.6. Phase I Metabolism of Rh2s and PPD after Oral Administration

Since Rh2s and PPD showed extensive oxidative metabolism in vitro especially in mouse liver S9 fraction, their oxygenated metabolites in plasma were detected after oral administration of 20 mg/kg of Rh2s and 5 mg/kg PPD, respectively. Blood samples (20-25 µl) were collected at 15, 30, 60, 120, 180, 240, 360, 480, 720 and 1440 min by snipping its tail after mice were anesthetized with isoflurane gas. The blood samples were collected in heparin treated tubes and stored at -20°C until analysis. The quantification was performed using multiple reactions monitoring mode (MRM) with ion pair transitions to monitor metabolites of Rh2s and PPD (Internal standard).

4.3.7. Data analysis

4.3.7.1. UPLC-MS/MS analysis of ginsenosides

An API 3200 QTrap triple quadrupole mass spectrometer (Applied Biosystem/MDS SCIEX, Foster City, CA, USA) equipped with a TurboIonSpray^{TM} source was operated in negative ion mode to perform the analysis. The main working parameters for the mass spectrometers were set as follows: ion spray voltage, -4.5 kV; ion source temperature, 650°C; the nebulizer gas (gas1), nitrogen, 50 psi; turbo gas (gas2), nitrogen, 50 psi; curtain gas, nitrogen, 20 psi.

Ginsenosides metabolites were identified by MS full scan and MS2 full scan modes. The quantification was performed using multiple reactions monitoring mode (MRM) with ion pair transitions to monitor ginsenosides and formononetin (Internal standard). The compound dependent parameters for LC/MS/MS determination were showed in Table 2.

UPLC conditions for the analysis of these three ginsenosides were: system, Waters Acquity™ (Milford, MA, USA) with DAD detector; column, Acquity UPLC BEH C18 column (50×2.1mm I.D., 1.7μm, Waters); mobile phase A, double distilled water; mobile phase B, 100%, methanol; gradient, 0-0.5 min, 0% B, 0.5-1 min, 0-80% B, 1-2.3 min, 80-95% B, 2.3-2.9 min, 95% B, 2.9-3.2 min, 95-0% B, 3.2-3.7 min, 0% B. Flow rate, 0.45 ml/min, column temperature, 60 degree;

injection volume, 10 µl. The chromatograph of Rg3s, Rh2s, PPD and I.S. is shown in Figure 2. Typical precision and accuracy were within 15%, and linear response range was 19.5 nM - 10 µM.

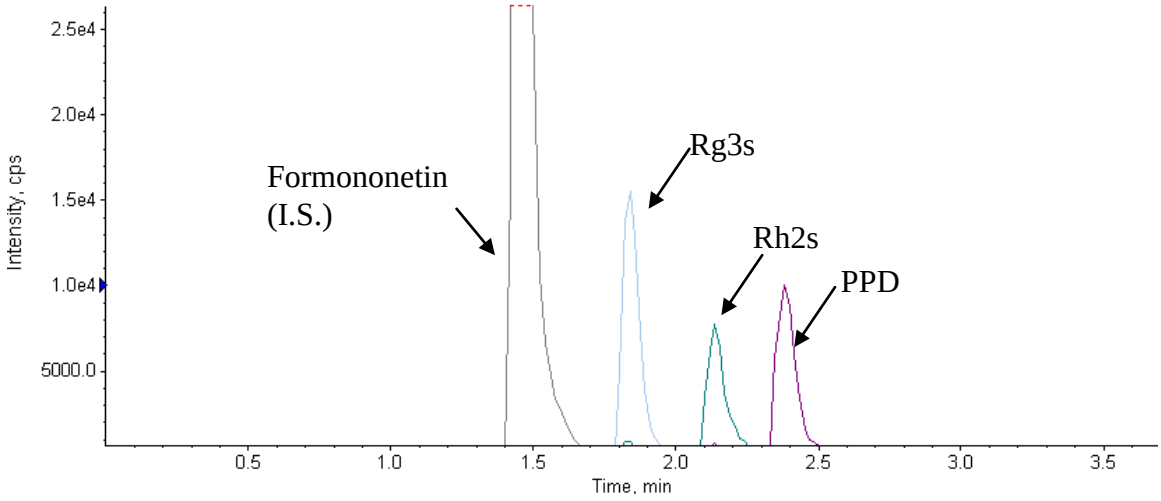

Figure 2. LC/MS/MS Chromatograms of ginsenosides Rg3s, Rh2s and PPD in HBSS buffer.

4.3.7.2. Data analysis in the permeability of ginsenosides in Caco-2 cell model

The transcellular transport study was performed as described previously [147]. Briefly, 2.5 ml of individual ginsenoside solution was loaded onto one side of the cell monolayer, and 2.5 ml of blank HBSS onto the other side. Five sequential samples (0.5 ml) were taken at different times (0, 1, 2, 3 and 4 hrs) from both sides of the cell monolayer. The same volume of individual ginsenoside solution and receiver medium (fresh HBSS) was added immediately to replace the volume lost because of sampling. The pH values of HBSS in both apical and basolateral side were 7.4. The apparent unidirectional permeability was obtained according to the equation 4.

4.3.7.3. Statistical analysis

Independent Student's *t* test and one-way ANOVA followed by Tukey post hoc test were used to analyze the data. The level of significance was set at $P < 0.05$.

4.4. Results

4.4.1. Saturated aqueous solubility of ginsenosides Rh2s, Rg3s and PPD

We measured the saturated aqueous solubility of three ginsenosides in HBSS at different pHs (Figure 3). The results showed that Rg3s has the highest solubility (8.93 μM), followed by Rh2s (4.64 μM), and PPD has the worst solubility (0.57

μM) (Figure 3A). There was no significant difference in solubility at different pH values according to a one-way ANOVA analysis. The solubility of Rg3s, Rh2s and PPD were significantly higher in water than in HBSS buffer, indicating the possible salting-out effects on their solubility (Figure 3B). In simulated intestinal fluid at pH 6.8, Rg3s, Rh2s showed similar solubility at 4.7 and 5.5 μM, respectively, and PPD showed higher solubility (2.8 μM) than in HBSS buffer (Figure 3C). Overall, the aqueous solubility of ginsenoside Rg3s, Rh2s and PPD were low in three different matrixes and it may represent as a major obstacle for low oral bioavailability.

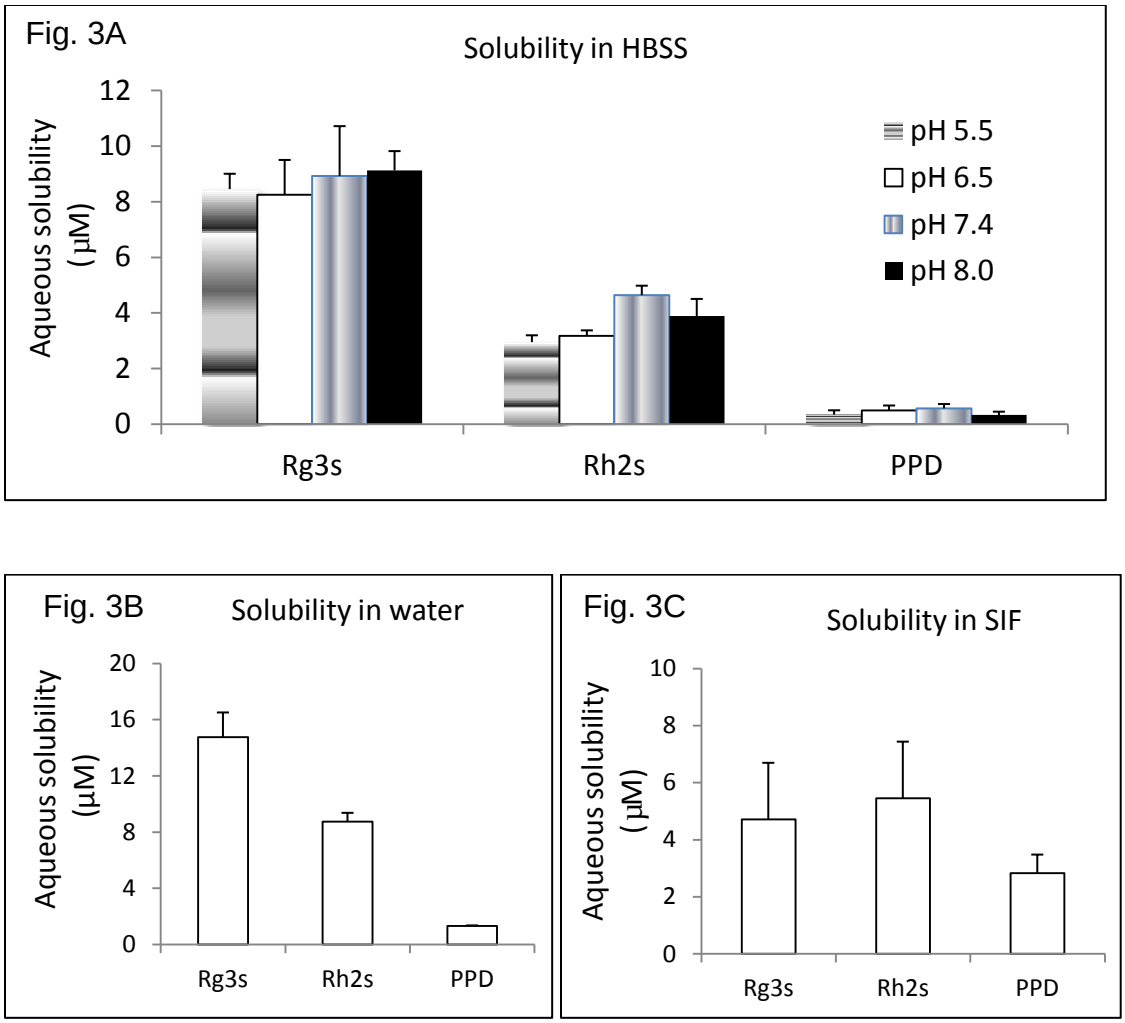

Figure 3. Saturated aqueous solubility of Rg3s, Rh2s and PPD in HBSS buffer at 37°C at different pHs (A). Saturated aqueous solubility of Rg3s, Rh2s and PPD in water at 37°C at pH 6.8 (B). Saturated aqueous solubility of Rg3s, Rh2 and PPD in simulated intestinal fluid at 37°C at pH 6.8 (C).

4.4.2. Permeability of ginsenosides in Caco-2 cells

Due to limited solubility of ginsenosides in HBSS, 2 μM for Rg3s and Rh2s, and 0.125 μM for PPD were used as donor side concentration in transport study. The permeabilities of Rg3s, Rh2s and PPD from apical to basolateral side were measured in Caco-2 cell transport model at pH 7.4 at 2 μM (Figure 4). The results showed all these ginsenosides have poor-moderate permeability (around 1×10^{-6} cm/s). According to the correlation between compound permeabilities in Caco-2 cell model and % absorption in humans, a permeability value of greater than 1×10^{-5} cm/s indicated good absorption (75% or more) in human and permeability less than 1×10^{-6} cm/s indicated poor absorption (15% or less) [154]. Therefore, the results implied poor absorption may be the main reason causing these three ginsenosides low oral bioavailability.

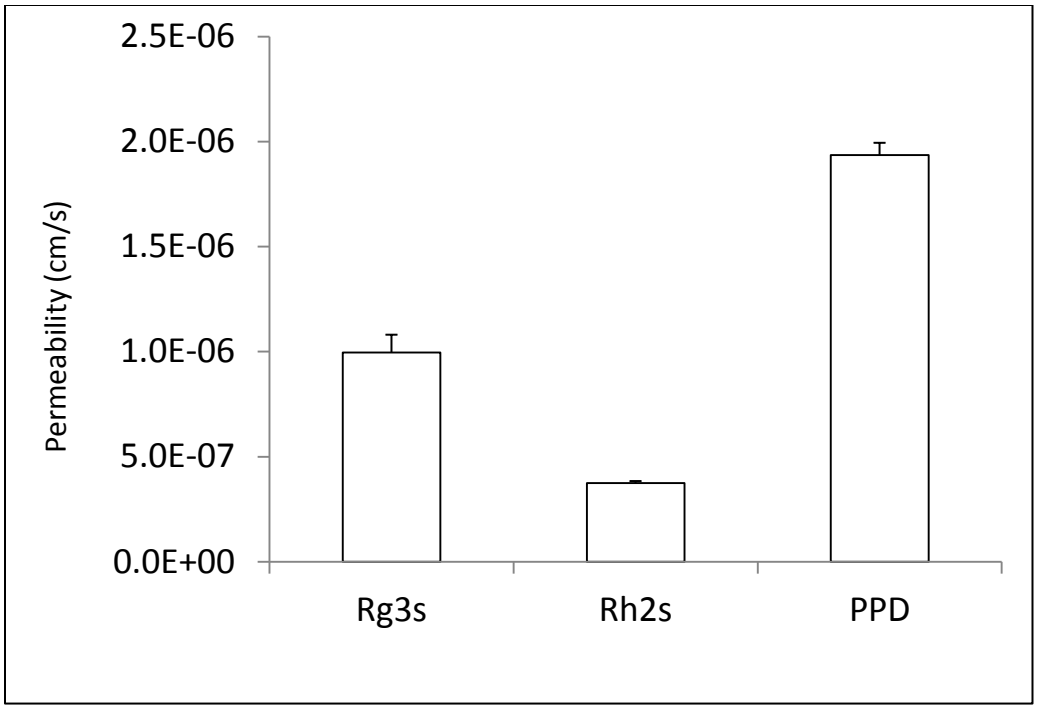

Figure 4. Permeability of Rg3s, Rh2s and PPD in Caco-2 cells at pH 7.4, respectively.

4.4.3. Presystemic stability of ginsenosides in GI tract

0.5 μM of Rg3s, Rh2s and PPD were tested for their stability in simulated gastric fluid, small intestine perfusate and colon perfusate. The results showed there were no significant disappearances of Rg3s, Rh2s and PPD after incubation for 8 hours (Figure 5) in various gastrointestinal fluids. It indicated that Rg3s, Rh2s and PPD were stable in the entire gastrointestinal tract. Only less than 2% of Rh2s was detected in Rg3s incubation within these three matrixes and no PPD was detected. Less than 2 % of PPD was detected in Rh2s incubation with these three matrixes (data not shown). The results indicated that pre-system loss is the not the main reason causing low oral bioavailability of Rg3s, Rh2s and PPD.

Fig. 5A

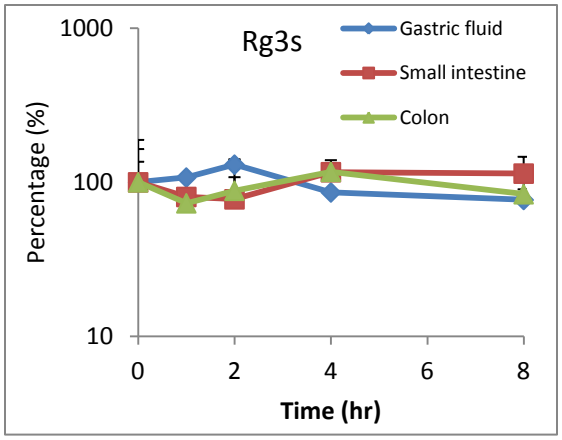

Fig. 5B

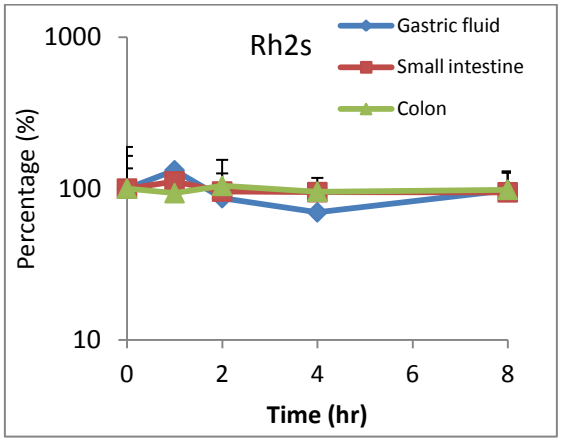

Fig. 5C

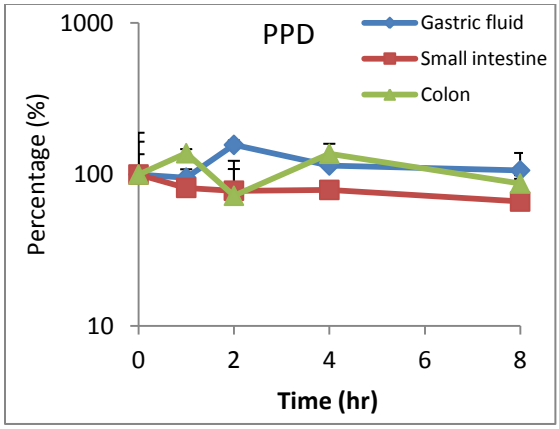

Figure 5. The stability of Rg3s in simulated gastric fluid (diamond), small intestine perfusate (square) and colon perfusate (triangle) up to 8 hrs incubation at 37°C (A); The stability of Rh2s in simulated gastric fluid (diamond), small intestine perfusate (square) and colon perfusate (triangle) up to 8 hrs incubation at 37°C (B); The stability of PPD in simulated gastric fluid (Diamond), small intestine perfusate (square) and colon perfusate (triangle) up to 8 hrs incubation at 37°C (C) (n=4).

4.4.4. Ginsenosdies metabolism in mouse S9 fractions

1ml of ginsenosides (5 µM Rg3s, 2.5 µM Rh2s and 1 µM of PPD, respectively) were incubated with liver, small intestine and colon S9 fraction obtained from A/J mice, respectivley for 1 hours at 37ºC.

4.4.4.1. Metabolism of Rg3s

Based on the metabolism stability in mouse S9 fraction, Rg3s was stable in both Phase I and Phase II metabolism system. Rg3s could not be metabolized by CYP450 as more than 90% Rg3s remained after incubation with mouse S9 fraction prepared from liver, small intestine and colon compared to negative control. Similarly, no glucruronidation/sulfattion of Rg3s nor hydrolytic metabolites (Rh2s and PPD) were found by LC/MS/MS analysis. It indicated that Rg3s was enzymaticaly stable in vitro.

4.4.4.2. Metabolism of Rh2s

The results of Rh2s metabolism in mouse liver, small intestine and colon S9 fraction studies showed that Rh2s was extensively metabolized by CYP450. Liver S9 fraction completely converted Rh2s (2.5 µM) in 1 hour and small intestine S9 fraction converted 10% of Rh2s while no metabolism occurred in colon S9 fraction (below detection limit). 50 µM ketaconazol (CYP3A inhibitor) inhibit Rh2s (2.5 µM) metabolism by 95% in liver S9 fraction after incubation for

1 hours, which indicated that Rh2s may be metabolized by CYP3A. No hydrolytic metabolites such as PPD were found in the reaction mixture. No glucruronidation/sulfattion reaction metabolites were found.

The major metabolites, monooxygenated (molecular ion, M+16, m/z 637.6) and di-oxygenated (molecular ion, M+32, m/z 653.6) of Rh2s were identified and confirmed by full scan mass spectrum and MS2 spectrum shown in Fig. 6. There are at least two monooxygenation and dioxygenation metabolites in S9 fraction and the the chromatographs were shown in Figure 6.

4.4.4.3. Metabolism of PPD

PPD can be extensively metabolized by CYP450. Two main metabolites, monooxygenated (molecular ion, M+16) and di-oxygenated (molecular ion, M+32) of PPD were identified in liver microsome based on fragment ions in Mass spectrometer. Liver S9 fraction completely converted PPD (1 μM) in 1 hour and small intestine S9 fraction converted 15% of PPD, while no metabolites were found in colonic S9 fraction (below detection limit). 50μM ketaconazol (CYP3A inhibitor) inhibit PPD (1 μM) metabolism by 95%in liver S9 fraction after incubation for 1 hours, which indicated that PPD may be metabolized by CYP3A. No glucruronidation/sulfattion reaction metabolites were found. The major metabolites, monooxygenated (molecular ion, M+16, m/z 475.6) and di-

oxygenated (molecular ion, M+32, m/z 491.6) of PPD were identified (Figure 7). The MS2 spectrum is not available due to detection limit.

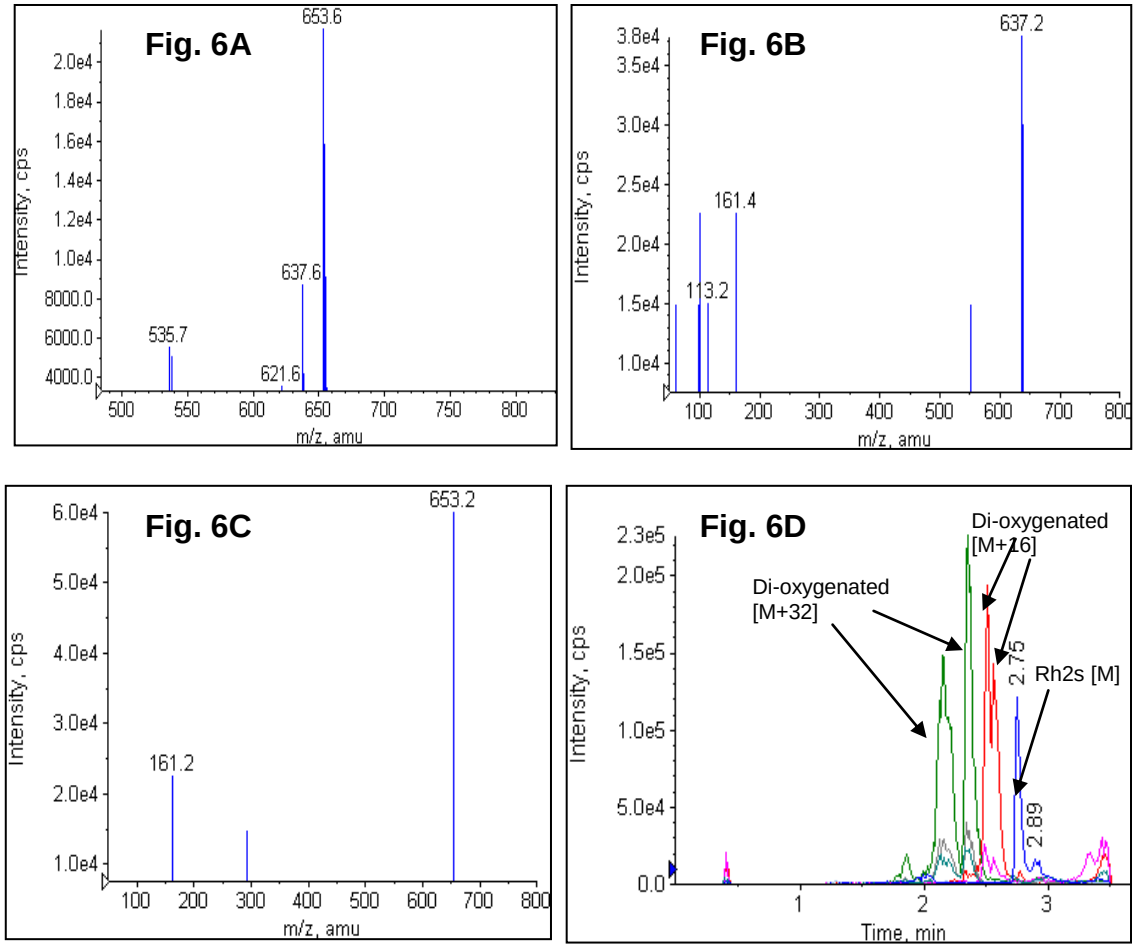

Figure 6. Full-scan mass spectrum of monooxygenated and dioxygenated Rh2s (A); MS2 spectrums of monooxygenated Rh2s (B) and dioxygenated Rh2s (C); and the chromatograph of Rh2s and its oxygenated metabolites in liver S9 fractions (D). The molecular ion of Rh2s was m/z 621.6. The molecular ion of monooxygenated Rh2s was m/z 637.2 (M+16) whereas the molecular ion of dioxygenated Rh2s was m/z 653.2 (M+32). Both monooxygenated and deoxygenated Rh2s were confirmed by their MS2 spectrums (m/z 161, glucose molecular ion).

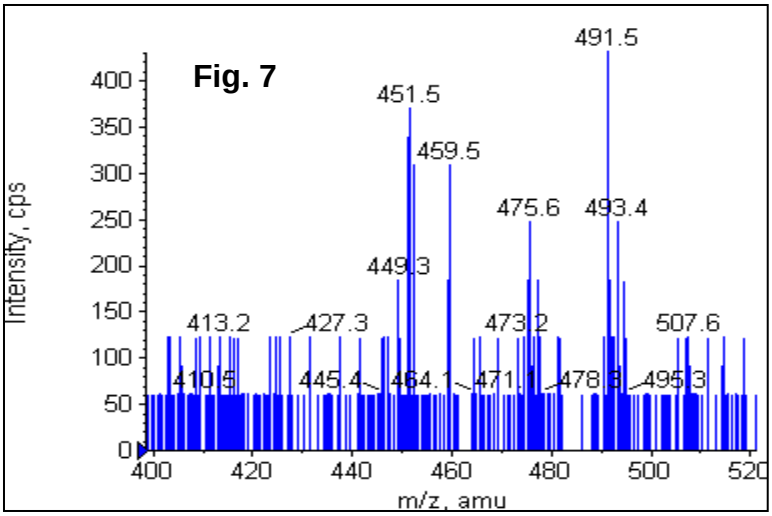

Figure 7. Full-scan mass spectrum of monooxygenated and dioxygenated PPD. The molecular ion of PPD is m/z 459.5. The molecular ion of monooxygenated Rh2s was m/z 475.6 (M+16) whereas the molecular ion of dioxygenated Rh2s was m/z 491.5 (M+32).

4.4.4.4. Phase I Metabolism of Rh2s and PPD after Oral Administration

Although Rh2s and PPD showed extensive oxidative metabolism in vitro especially in mouse liver S9 fraction, the oxygenated metabolites in plasma were surprisingly below quantification limit (19.5 nM for Rh2s and 9.8 nM for PPD) after oral administration of 20 mg/kg of Rh2s and 5 mg/kg PPD, respectively. The quantification limit was estimated assuming similar signal response of parent compound and metabolites in mass spectrometer. It indicated that in vivo metabolites of Rh2s and PPD are negligible and may not be the major reason causing low oral bioavailability of ginsenosides in vivo.

Table 2. Compound dependent parameters for monooxygenated and deoxygenated metabolites of Rh2s and PPD and I.S. in MRM mode for UPLC–MS/MS analysis.

Analyte	Q1 mass	Q3 mass	DP (V)	CEP (V)	CE (V)	CXP (V)
Monooxygenated Rh2s	637.6	160.9	-68	-34	-28	-3
Dioxygenated Rh2s	653.6	160.9	-81	-36	-36	-4
Monooxygenated PPD	475.5	375.4	-81	-36	-36	-4
Dioxygenated PPD	491.5	375.5	-50	-30	-30	-3
Formononetin (I.S.)	267.1	252.1	-47	-23	-30	-1

4.5. Discussion

Ginsenosides have similar backbone structures (triterpenoid) with different numbers of sugar moieties ranging from 0-5 [29]. From literature report, ginsenosides with less sugar moieties showed potent cytotoxicity against tumor cell lines and better anticancer and chemoprevention effect in animal models [8-11]. Ginsenosides Rg3s (2 glucose), Rh2s (1 glucose) and PPD (aglycone) were tested in our lab for their proliferation activity in LM1 lung cancer cell lines, and showed very potent anticancer activity (IC_{50}=3-30 μM). Therefore, they were chosen as the lead ginsenosides to study their ADME properties.

This is the first report to measure aqueous solubility of ginsenosides Rg3s, Rh2s and PPD in various biological matrixes. Although low solubility of ginsenosides (one or two sugar moiety) is generally mentioned, the accurate values were never reported based on our best knowledge. Our results showed low solubility of these ginsenosides in three different aqueous matrixes and simulated intestinal fluid is the most relevant media to mimic in vivo enviroment. The solubility results not only showed that low aqueous solubility of ginsenosides is the major reason causing low oral bioavailability of ginsenosides, but also indicated the maximum donor side concentration should be used in the following ADME studies.

Permeability of ginsenosides in Caco-2 cells has been reported before, but most of donor concentrations were used at 10 μM or even higher concentrations [3, 18] due to the possible analytical challenges. Gu et al reported that permeability of Rh2 was 0.2×10^{-7} cm/s when 10 μM Rh2 were used and Liu et al showed that permeability of Rg3s was 0.8×10^{-7} cm/s [18]. All of these measurements were significantly lower than our results (9.95×10^{-7} cm/s for Rg3s and 3.74×10^{-7} cm/s for Rh2s) and the possible reason is that high concentration of ginsenosides they used were not soluble in donor side which resulted in underestimation of permeability since the solubility is much less than 10 μM in HBSS buffer.

Presystemic degradation of ginsenosides was reported by many previous publications since ginsenosides could be stepwisely hydrolyzed by glucosidase, which is largely presented in gut microbial and fecal flora [60, 155, 156]. Tawab et al and Han et al showed that ginsenoside Rh1 and F1 were the hydrolysis products of protopanaxatriol ginsenosides [60, 155]. Protopanaxadiol ginsenosides, like Rb1 and Rb2, are mainly converted to compound K via ginsenosides Rd and F2 by intestinal bacterial flora [157] . Rg3, Rh2 and PPD could be transformed by treatment with mild acid such as stomach acid and steaming [158]. Some study also suggested that ginsenoside Rg3 may convert to ginsenoside Rh2 and protopanaxadiol when anaerobically incubated with human

fecal microflora [8]. However, our study did not show significant hydrolysis product after incubation in intestinal perfusate up to 8 hours. The possible reasons is that certain fecal microflora presented in human, like Bacteroides sp., Eubacterium sp., and Bifidobacterium sp. which metabolize ginsenoside Rg3 to protopanaxadiol via ginsenoside Rh2, may not presented in A/J mice intesinte [8]

The metabolism study of ginsenosides was only revealed recently. Hao et al showed that protopanaxatriol ginsenosides could be extensively metabolized by P450 in human and rat hepatic microsomes, and CYP 3A may be the major isoforms responsible for biotransformation [17]. Metabolism of protopanaxadiol ginsenosides were not reported except its aglycone, PPD. Li et al identified 24 metabolits of PPD in human hepatocytes [16] and our results were consistent with their report showing monooxygenated and deoxygenated metabolites were the major metabolites of PPD in A/J S9 liver fraction.

Although extensive metabolism of Rh2 and PPD were observed at in vitro system, their in vivo importance is unknown. We are the first one to establish quantification method to measure metabolites of Rg3s, Rh2s and PPD. Our results showed that metabolites of Rh2s and PPD were not the major obstacle for low oral bioavailability (below detection limit). Low exposure level of metabolites may due to poor oral absorption or low uptake in hepatocytes.

In summary, low aqueous solubility and permeability were the major reasons causing low oral bioavailability of ginsenosides Rg3s, Rh2s and PPD. Presystemic stability of Rg3s, Rh2s and PPD is good in GI tract of A/J mice. Rh2 and PPD could be extensively metabolized in vitro, but in vivo metabolites were not quantifiable indicating metabolism is not the major limiting step for their low oral bioavailability.

Enhancement of oral bioavailability of ginsenoside 20(s)-Rh2 through improved understanding of its absorption and efflux mechanisms

5.1. Abstract

The development of ginsenoside 20(s)-Rh2 (Rh2s) as a chemoprevention agent is limited by its low oral bioavailability. The goals of this study were to determine the mechanisms responsible for its poor oral absorption and to improve its bioavailability by overcoming the barrier to its absorption. Comprehensive studies were conducted using the following models: 1) monolayers of Caco-2, parental and MDR1 overexpressing MDCKII cells; 2) pharmacokinetics in wild-type (WT) FVB, MDR1a/b knockout (MDR1a/b $^{-/-}$) FVB and A/J mice; and 3) intestinal perfusion in WT, MDR1a/b $^{-/-}$ FVB and A/J mice. Two P-gp inhibitors verapamil and cyclosporine A substantially decreased efflux ratio of Rh2s from 28.5 to 1.0 and 1.2, respectively in Caco-2 cells. The intracellular concentrations of Rh2s were also significantly increased (2.3 and 3.9 fold) in the presence of inhibitors. Similar results were obtained when transcellular transport of Rh2s were determined using MDR1-overexpressing MDCKII cells in the absence or presence of cyclosporine A. Compared to WT mice, the plasma C_{max} and $AUC_{0-\infty}$ of Rh2s were substantially increased by 17 and 23 fold in MDR1a/b $^{-/-}$ FVB mice, respectively. In the A/J mice, the oral bioavailability of Rh2s (0.94% at 5 mg/kg and 0.52% at 20 mg/kg) was substantially increased by P-gp inhibitor to 33.18%

and 27.14%, respectively. As expected, deletion or inhibition of P-gp significantly increased absorption and steady-state plasma concentration of Rh2s in a mouse intestinal perfusion model. In conclusion, Rh2s is a good substrate of P-gp and inhibition of P-gp can significantly enhance its oral bioavailability.

Key words: ginsenoside Rh2s, P-glycoprotein, Caco-2, absorption, efflux, bioavailability.

5.2. Introduction

Ginseng is a promising candidate for cancer chemoprevention based on preclinical and epidemiological studies [12, 159, 160]. In a case-controlled study including 1987 pairs of Korean subjects, the long-term consumption of ginseng was shown to be associated with a significant reduction in many different types of malignancies including lung cancer [1]. Ginsenosides are the main active components of ginseng and there are more than 150 ginsenosides identified so far [7]. The chemoprevention and anticancer mechanism of ginsenosides include mitigation of DNA damage, induction of apoptosis, and inhibition of proliferation as well as positive immunomodulation [12].

However, extensive pharmacokinetic studies indicated that many active ginsenosides have very poor oral bioavailability (much less than 5%), which had been attributed to poor oral absorption [3, 18]. Poor bioavailability of ginsenosides greatly impedes our ability to demonstrate the potency of ginsenosides in vivo, and our ability to overcome this impediment perhaps holds the key to advance these agents into clinical trials that will unequivocally demonstrate their clinical effectiveness [27, 161, 162].

In this study, ginsenoside 20(s)-Rh2 (Rh2s) was selected as a lead compound to demonstrate the absorption mechanisms of ginsenosides. Ginsenoside Rh2s is one of the most studied ginsenosides since it displayed potent anticancer activity,

especially in lung cancer cell lines [33, 163]. A 9-week animal study also showed Rh2s had a tendency to decrease lung tumor incidence in mice after its oral consumption [1]. Like many other ginsenosides, Rh2s was reported as having low oral absorption/bioavailability [3, 43]. However, current understanding of Rh2s absorption mechanism is ambiguous. Gu et al. reported that ABC efflux transporters may be involved in Rh2s absorption, but no actual transporter was identified [164]. The latest publication from the same group found that Rh2s was a non-competitive inhibitor but not a substrate of P-gp [165]. Therefore, identification of the predominant transporter for Rh2s and demonstration that the inhibition of relevant efflux transporters would increase oral bioavailability of Rh2s (and maybe other ginsenosides) would help us to further understand and delineate this class of compounds' pharmacological characteristics.

P-glycoprotein (P-gp), a member of the adenosine triphosphate (ATP)-binding cassette (ABC) superfamily, is one of the most prevalent efflux transporters expressed in multidrug resistance cancer cells and in several organs such as intestine, liver, kidney and the blood-brain barrier [78]. P-gp plays an important role in limiting the intestinal absorption of its substrates in vivo [79] and inhibition of P-gp leads to the improvement of bioavailability of several orally administrated anticancer drugs [80-82]. Most P-gp substrates are hydrophobic, and a recently published mouse P-gp crystal structure revealed that P-gp has distinct drug-

binding sites (in the large internal activity cavity) favoring hydrophobic and aromatic interactions [77].

Therefore, the aims of this study were 1) to systemically investigate mechanisms responsible for poor absorption of Rh2s by elucidate which efflux transporter was mainly involved in the transport of Rh2s using a complementary set of *in vitro*, *in situ* and *in vivo* models; 2) to demonstrate that it is possible to increase oral bioavailability of Rh2s via a mechanism-based approach (i.e., focus on inhibiting the elucidated efflux transporter derived from aim 1).

5.3. Materials and methods

5.3.1. Materials

Purified Rh2s (HPLC purity>95%, Fig. 1) were prepared by Dr. Zhi-Hong Jiang's laboratories at Hong Kong Baptist University. Cloned Caco-2 cells (TC7) cells were a kind gift from Dr. Monique Rousset of INSERM U178 (Villejuit, France). Parental MDCKII and MDR1-MDCKII cells were provided by the Netherland Cancer Institute (Amsterdam, Netherland). Digoxin, cyclosporine A, verapamil and Hanks' balanced salt solution (powder form) were purchased from Sigma-Aldrich (St. Louis, MO). MK571 and Ko143 were purchased from Tocris Bioscience (Ellisville, MO). Oral suspension vehicle was obtained from Professional Compounding Centers of America (Houston, TX). Simulated intestinal fluid was purchased from VWR (Houston, TX). BCA protein assay kit was purchased from Thermo Scientific (Rockford, IL). All other materials (typically analytical grade or better) were used as received.

5.3.2. Animals

Male A/J and FVB mice (6-10 weeks) were purchased from Harlan Laboratory (Indianapolis, IN). Male MDR1a/b knockout mice (6-10 weeks) were purchased from Taconic Farms (Germantown, NY). They were acclimated in an environmentally controlled room (temperature: 25 ± 2°C, humidity: 50 ± 5%, 12 h

dark-light cycle) for at least 1 week prior to experiments. The mice were fed with rodent diet (Labdiet® 5001), and fasted overnight before pharmacokinetic studies.

5.3.3. Cell culture

The Caco-2 cell culture is routinely maintained in this laboratory for the last 2 decades. The culture conditions for growing Caco-2 cells were the same as those described previously [147]. Porous polycarbonate cell culture inserts (3 μm) from Corning (Catalog No: 3414) were used to seed the cells at a seeding density of 100,000 cells/cm^2. Other conditions such as growth media (Dulbecco's modified Eagle's medium supplemented with 10% fetal bovine serum), and quality control criteria were all implemented according to a previous published report [147] . Caco-2 TC7 cells were fed every other day, and cell monolayers were ready for experiments from 19 to 22 days post-seeding.

Parental MDCKII and MDR1-MDCKII cells were cultured in Dulbecco's modified Eagle's medium supplemented with 10% fetal bovine serum, 1% nonessential amino acids, 100U/ml penicillin and gentamicin. Cell culture was maintained at 5% CO2 and 90% relative humidity at 37°C. They were seeded at 2.0×106 cells/well into the same cell culture inserts as those used for Caco-2 cells, and fed every day. The MDCKII or MDR1-MDCKII cell monolayers were ready for experiments from 4-5 days post-seeding. The expression levels of MDR1 in MDR1-MDCKII were monitored by western blotting analysis.

5.3.4. Saturated aqueous solubility measurement

Ginsenoside Rh2s is a strong lipophilic (log P=4.0, predicted by Molecular Operating Environment and Discovery Studios) compound and its solubilities in various media had not been reported. HBSS buffer was commonly used in absorption models including the Caco-2 cells and in situ rodent intestinal perfusion study [54]. The saturated aqueous solubility was measured in HBSS using pH values ranging from pH 5.5 to pH 8.0. The solubility of Rh2s was also determined in pure water at pH 7.4 and in simulated intestinal fluid (SIF) at pH 6.8 to mimic the in vivo environment. Stock solution of ginsenoside Rh2s was prepared in alcohol at 10 mM. 10 µl of Rh2s was spiked into glass vials in triplicate and dried under air. A volume of 1 ml HBSS/water/SIF at appropriate pH values was then added into a glass vial and the mixture was shaken overnight at 37°C. After the mixture was centrifuged at 15,000 rpm for 20 minutes, 400 µl of supernatant was then carefully transferred into a new vial. The vial was then added with 100 µl formononetin (10 M) as the internal standard (I.S.) and dried under air. The residue was reconstituted with 200 µl methanol and centrifuged at 15,000 rpm for 10 minutes. A volume of 10 µl supernatant was injected to UPLC-MS/MS for analysis.

5.3.5. Transcellular transport study

The transcellular transport study was performed as described previously [147]. Briefly, 2.5 ml of Rh2s solution was loaded onto one side of the cell monolayer, and 2.5 ml of blank HBSS onto the other side. Five sequential samples (0.5 ml) were taken at different times (0, 1, 2, 3 and 4 hrs) from both sides of the cell monolayer. The same volume of Rh2s solution and receiver medium (fresh HBSS) was added immediately to replace the volume lost because of sampling. The pH values of HBSS in both apical and basolateral side were 7.4. The apparent unidirectional permeability was obtained according to equation 4 as described in chapter 4.

Both permeability from apical to basolateral side (P_{a-b}) and basolateral to apical side (P_{b-a}) were calculated according to the above equation. Digoxin, a substrate of P-gp, was used as the positive control for the transport study in Caco-2 and MDR1-MDCKII cell monolayers. The efflux ratio was calculated as P_{b-a}/P_{a-b}, which represented the degrees of efflux transporter involvement. In the present study, inhibitors of efflux transporters were only added to the apical side of cell monolayers, regardless of where Rh2s was loaded.

Intracellular concentrations of Rh2s were determined at the end of a transport study. The protocol for determining Rh2s intracellular amounts in cells was the same as those described previously [151]. Briefly, after 4 hours of a transcellular

transport study, the cell membranes were rinsed three times with ice-cold HBSS buffer, and cells attached to the polycarbonate membranes were cut off from the inserts with a sharp blade. The latter was immersed into 1 ml HBSS, and sonicated for half an hour at 4°C to break up the cells. The mixture was centrifuged at 15,000 rpm for 15 minutes and 500 µl of the supernatant were recovered and air-dried. The residue were reconstituted with 200 µl methanol and analyzed by UPLC-MS/MS. The protein concentration of cell lysate was measured to normalize the accumulation of Rh2s inside the cells using the BCA protein assay kit.

5.3.6. In situ two-site mouse intestinal perfusion study

The animal protocols used in this study were approved by the University of Houston's Institutional Animal Care and Uses Committee. The intestinal surgical procedures were described in our previous publications [151]. Two segments of intestine, upper small intestine and colon (8-12cm each) were simultaneously cannulated. The perfusion studies were performed at a flow rate of 0.191 ml/min with 2 µM Rh2s in HBSS iso-osmotic solution (pH 7.4) using A/J, WT and MDR1a/b $^{-/-}$ FVB mice. Cyclosporine A solution (10 µM) was mixed with 2 µM Rh2s in A/J mice to test the effects of P-gp inhibitors on Rh2s transport. To keep the temperature of the perfusate constant, the inlet cannulate was insulated and kept warm by a 37°C circulating water bath.

After a 30 min washout period with perfusate, perfusate samples were collected every 30 min (60, 90, 120, 150 min). At the end of the perfusion experiment, the length of the each segment of intestine was measured and each tube containing sample was weighted after perfusion. 50 µl of blood was collected from tail vein at the end of perfusion experiment (2.5 hr after the start). Loss of water during perfusion was monitored by measuring the net weight of perfusate sample and the absorption data was discarded if the water flux is more than 5% per 10 cm for the small intestine and 10% per 10 cm for the colon. The perfusate samples were immediately processed the same way as the cellular transport samples, and analyzed by UPLC-MS/MS. The plasma concentrations of Rh2s were measured following the same protocol in pharmacokinetic study.

5.3.7. Pharmacokinetic studies of Rh2s in wild-type and MDR1a/b $^{-/-}$ FVB Mice

Pharmacokinetic studies of Rh2s were performed in wild-type and MDR1a/b $^{-/-}$ FVB mice to confirm the role of MDR1/P-gp in determining Rh2s bioavailability in vivo. Rh2s dispersed in the oral suspending vehicle (Supplemental Table 1) was given by gavage to each group at 20 mg/kg. Each pharmacokinetic study was performed on five mice and 10 timed blood samples (20-25 µl) were taken by snipping its tail, after mice were anesthetized with isoflurane gas. The blood samples were collected in heparin treated tubes and stored at -20°C until analysis.

5.3.8. Pharmacokinetic studies of Rh2s alone or with cyclosporine A in A/J mice

Pharmacokinetic studies of Rh2s were performed in A/J mice for both i.v. and oral administrations. Rh2s (1 mg/ml) was prepared in 20% alcohol and 20% propylene alcohol in normal saline and was intravenously injected through lateral tail vein at the dose of 5 mg/kg. In oral dosing groups without cyclosporine A (control group), 4 mg/ml Rh2s was dispersed in oral suspending vehicle and the content of Rh2s in oral suspending vehicle was measured before administration to make sure it was evenly suspended. The ingredients of oral suspending vehicle are shown in Table S1. In the group with co-administration of P-gp inhibitors, 50 mg/kg solid cyclosporine A dispersed in the same oral suspending vehicle was orally administrated to A/J mice 30 minutes before Rh2s administration while the same volume of blank vehicle was given to the control group. The blood sample collection and processing procedures used for A/J mouse samples were the same as those described for the FVB mouse pharmacokinetic study.

5.3.9. Sample Processing and Quantitative Determination of Rh2s

An API 3200 Qtrap® triple quadrupole mass spectrometer (Applied Biosystems/MDS SCIEX, Foster City, CA, USA) equipped with a TurboIonspray™ source, operated in a negative ion mode, was used to perform the analysis of the eluent from the UPLC. The flow dependent parameters for

introduction of the samples to the mass spectrometers ionization source were set as follows: ion spray voltage, -4.5 kV; ion source temperature, 650°C; the nebulizer gas (gas1), nitrogen, 50 psi; turbo gas (gas2), nitrogen, 50 psi; curtain gas, nitrogen, 10 psi. The quantification was performed using multiple reactions monitoring mode (MRM) with ion pair transitions to monitor Rh2s and formononetin (Internal standard). The fragments for each compound detected were 621.4/160.9 (m/z) for Rh2s and 267.1/252.1 (m/z) for formononetin. UPLC conditions for Rh2s analysis were: system, Waters Acquity™ (Milford, MA, USA) with DAD detector; column, Acquity UPLC BEH C18 column (50×2.1mm I.D., 1.7μm, Waters); mobile phase A, double distilled water; mobile phase B, 100%, methanol; gradient, 0-0.5 min, 0% B, 0.5-1 min, 0-80% B, 1-2.3 min, 80-95% B, 2.3-2.9 min, 95% B, 2.9-3.2 min, 95-0% B, 3.2-3.7 min, 0% B. Flow rate, 0.45 ml/min, column temperature, 60 degree; injection volume, 10 μl.

The standard curves of Rh2s were linear in the concentration range of 0.0195-10 μM and the LLOQ was 0.00975 μM in blood. The intra-day and inter-day precision were within 15% for all QC samples at three concentration levels (2.5, 0.3125 and 0.039 μM). The mean extraction recoveries determined using three replicates of QC samples at three concentrations in mouse blood were from 55.8 to 67.0%. The stability of Rh2s in mouse blood were evaluated by analyzing three replicates of quality control samples after short-term (25°C, 4h), post processing (20°C, 8h), long-term cold storage (-20°C, 7days) and within three

freeze-thaw cycles (-20 to 25°C). All the samples displayed 85-115% recoveries after various stability tests.

Quantification of digoxin (positive control in Rh2s transport studies) was performed in UPLC-MS/MS with the same instrumental conditions used for analysis of Rh2s. Before samples could be introduced into the UPLC, they were processed to remove proteins and other related substances. A volume of 200 µl methanol (containing 1 µM formononetin) was added into 20 µl aliquot of mouse blood sample. The sample mixtures were vortexed for about 30 seconds and precipitates were removed by centrifugation at 15,000 rpm for 15 min. The supernatant was transferred into a clean glass vial and evaporated to dryness at 40°C under air. The dry residue was reconstituted in 100 µl of 100% methanol (v/v), and a 10 µl aliquot of the resulting solution was injected into the UPLC-MS/MS system for analysis.

5.3.10. Pharmacokinetic analysis

WinNonlin 3.3 (Pharsight Corporation, Mountain View, California) was used for Rh2s pharmacokinetic analysis. The non-compartmental model was applied for pharmacokinetic analysis of Rh2s profiles. Pharmacokinetic parameters, including C_{max}, T_{max}, k_e, half-life and AUC were directly derived from WinNonlin.

The absolute oral bioavailability (F) was calculated by equation (1) as mentioned in chapter 3.

×100% The clearance and apparent volume of distribution at steady state after oral administration were corrected from the original CL (CL_o) and V_{ss} (V_{sso}) obtained from WinNonlin using the F values, as shown in equations (2 & 3) in chapter 3.

5.3.11. Statistical analysis

The data in this paper were presented as means ± S.D., if not specified otherwise. Significance differences were assessed by using Student's t-test or one-way ANOVA. A p value of less than 0.05 was considered as statistically significant.

5.4. Results

5.4.1. Transcellular transport of Rh2s across Caco-2 cell monolayers

Before the transport study were performed, the transcellular transport of a prototypical substrate of p-glycoprotein (digoxin) was used as the positive control. The results showed that transcellular transport of digoxin displayed significant efflux ratio (21.1) and P_{a-b} was 0.74×10^{-6} cm/s, which was similar to the published results [166]. In the presence of 20 μM cyclosporine A, the efflux ratio of digoxin was decreased to 1.2.

As expected, transcellular transport of Rh2s (2 μM) across Caco-2 monolayer from basolateral (B) to apical (A) side was significantly higher than the transport from A to B side, and the efflux ratios (P_{b-a} /P_{a-b}) were 28.5 (Table 3). Use of two MDR1/P-gp inhibitors alone at the apical side, 50 μM verapamil or 20 μM cyclosporine A, was able to completely inhibit the efflux transport of Rh2s, and the efflux ratio was decreased to close to 1. As expected, the P_{a-b} was significantly increased by 9 and 4 fold; and the P_{b-a} was significantly decreased by 3 and 6 fold after verapamil and cyclosporine A treatment, respectively (Table 3). Consistent with the permeability results, two p-glycoprotein inhibitors also significantly increased the intracellular accumulation of Rh2s following treatment with 50 μM verapamil (from 0.14 to 0.31 nmol/mg) or 20 μM cyclosporine A (from 0.14 to 0.54 nmol/mg).

Because there are three main efflux transporters (P-gp, MRP2 and BCRP) present at the apical membrane of the Caco-2 cells, chemical inhibitors of MRP2 (20 μM MK571) and BCRP (5 μM Ko143) were also used in transport study to determine their possible involvements. The inhibitors and inhibitor concentrations were chosen based on the reported Ki (constant of inhibition) value of 5.6 μM for MK571 [167] and 0.6 μM for Ko143 [168] in the Caco-2 cells. Using the efflux ratio as the indicator of efflux transporter function, neither of these inhibitors was effective (Table 3). Similarly, the intracellular accumulations of Rh2s were not increased by either Ko143 or MK571, in line with the absence of the role of MRP2 or BCRP in limiting the uptake of Rh2s into Caco-2 cells.

Table 3. Transcellular transport of Rh2s across monolayers of Caco-2, MDCKII, and MDR1-MDCKII cells in the absence or presence of inhibitors. Data are presented as mean ± S.D; n=3.

Cell model	Substrate concentration (μM)	Inhibitor	Inhibitor concentration (μM)	P_{a-b} ($\times10^{-6}$ cm/s)	P_{b-a} ($\times10^{-6}$ cm/s)	Efflux ratio (P_{b-a}/P_{a-b})	Intracellular amounts (nmol/mg)
Caco-2	2	-	-	0.37±0.01	10.66±1.74	28.5±4.7	0.14±0.02
		Verapamil	50	3.21±0.35*	3.25±0.46*	1.0±0.1*	0.31±0.04**
		Cyclosporine A	20	1.42±0.18*	1.71±0.23*	1.2±0.2*	0.54±0.08**
		KO143	5	0.39±0.13	8.97±2.40	22.7±6.1	0.13±0.02
		MK571	20	0.39±0.34	16.01±1.46	41.1±4.0	0.33±0.20
MDCK II	2	-	-	4.97±0.69	11.97±2.40	2.4±0.5	0.25±0.09
MDR1-MDCKII	1	-	-	0.49±0.06	32.77±3.33	65.7±6.7	0.06±0
	2			0.68±0.21	19.16±4.92	28.0±7.2	0.03±0.02
	3.3			2.17±0.39	26.79±2.77	12.4±1.3	0.19±0.05
	5			3.51±0.73	23.50±1.93	6.7±0.6	0.67±0.14
	2	Cyclosporine A	20	0.84±0.14	1.19±0.21**	1.4±0.2*	0.61±0.09***

"P_{a-b}" refers to the permeability from apical to basolateral and "P_{b-a}" refers to the permeability from basolateral to apical side. Permeability, ER and intracellular amounts were compared to control group. Data are the means ± S.D. of three independent experiments.

– indicated no inhibitor; * indicated $p<0.05$; ** indicated $p<0.01$; *** indicated $p<0.001$.

5.4.2. Transcellular transport of Rh2s in MDR1- MDCKII cells

Human MDR1/P-gp over-expressing MDCKII cells were used to confirm the predominant role of P-gp in the transport of Rh2s. Prior to the transport studies of Rh2s, 2 μM digoxin was used as a positive control in MDR1-MDCKII cell transport study. The efflux ratio of digoxin was 64.0 in MDR1-MDCKII cell and the P_{a-b} is 2.98×10^{-7} cm/s, which was similar to the ratio reported in a previous publication [169].

The transport of Rh2s in parental MDCKII cells was used as a negative control since the cells have very low expression of P-gp [170]. As expected, the efflux ratio of Rh2s was much lower in parental MDCKII cells compared to MDR1-MDCKII cells at 2 μM (28.0 vs 2.4). Likewise, the P_{a-b} of Rh2s was more than 7 fold higher in the parental MDCKII cells (4.97×10^{-6} cm/s) than MDR1-MDCKII cells (0.68×10^{-6} cm/s).

Four different concentrations of Rh2s were used in bi-directional transport study in MDR1- MDCKII cells and the efflux ratio was 65.7, 28.0, 12.4 and 6.7 at 1, 2, 3.3 and 5 μM, respectively. The significantly decreased efflux ratios observed with increasing donor concentration of Rh2s ($p<0.05$) was due to an increased P_{a-b} value from 0.49×10^{-6} to 3.51×10^{-6} cm/s ($p<0.01$) and decreased P_{b-a} value

from 32.77×10^{-6} to 23.5×10^{-6} cm/s. Similar to the results of inhibition studies in Caco-2 cells, the presence of 20 μM cyclosporine A substantially decreased P_{b-a} (by 16 fold) and the efflux ratio (from 28.0 to 1.2) (Table 3).

The intracellular accumulations of Rh2s were also measured and the results showed that Rh2s accumulation was significantly higher (8.5 fold) in parental MDCKII cells (0.25 nmol/mg) than in MDR1-MDCKII cells (0.03 nmol/mg). Consistently, the intracellular accumulation of Rh2s was significantly increased by 20 fold ($p<0.001$), after co-incubation with CsA in MDR1- MDCKII cells (Table 3).

5.4.3. Effects of MDR1 on the oral bioavailabilities of Rh2s

In order to investigate whether MDR1/P-gp has major effects on Rh2s oral bioavailability, plasma profiles of Rh2s were compared between MDR1a/b $^{-/-}$ and wild-type FVB mice after oral administration (20 mg/kg). In MDR1a/b $^{-/-}$ mice, the plasma C_{max} was significantly increased by 17 fold ($p<0.01$) and $AUC_{0-\infty}$ was significantly increased by 23 fold ($p<0.001$) when compared to wild-type FVB mice (Fig 8, Table 5).

In MDR1a/b $^{-/-}$ mice, K_e was significantly decreased by 70% (from 0.50 ± 0.25 to 0.15 ± 0.02 hr^{-1}, $p<0.05$) compared to wild-type FVB mice. The $t_{1/2}$ of Rh2s was significantly increased by 2.5 fold (from 1.85 ± 1.27 to 4.60 ± 0.71 hr, $p<0.01$). The decreased K_e and increased $t_{1/2}$ could be attributed to the decreased elimination of Rh2s due to the knockout of the MDR1 gene (Table 5).

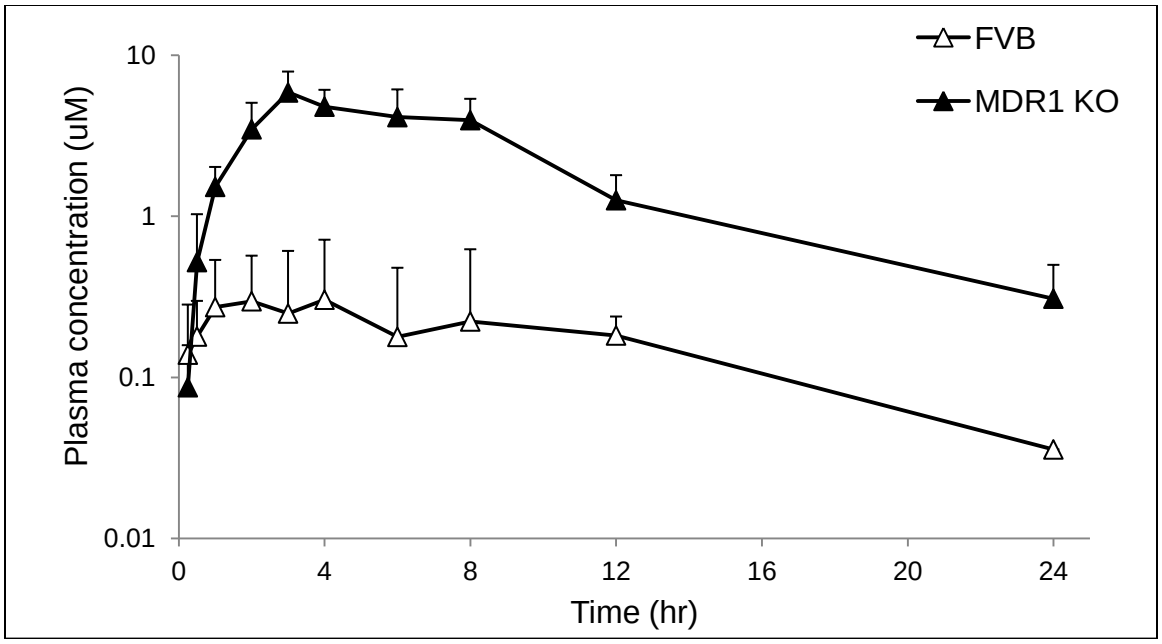

Figure 8. The plasma concentrations of Rh2s in wild-type and MDR1a/b -/- FVB mice after oral administration at 20 mg/kg. Data are presented as mean ± S.D.; n=5.

5.4.4. Effects of cyclosporine A on Rh2s oral bioavailabilities in A/J mice

Coadministration of the P-gp inhibitor, cyclosporine A (50 mg/kg), with Rh2s significantly increased the plasma C_{max} and $AUC_{0-\infty}$ of Rh2s at both 5 and 20 mg/kg (Figure 9). The plasma C_{max} was significantly increased ($p<0.01$) by 14 fold at 5 mg/kg, and by 38 fold at 20 mg/kg. The plasma $AUC_{0-\infty}$ was significantly increased ($p<0.001$) by 36 fold at 5 mg/kg and 52 fold at 20 mg/kg. Pharmacokinetic parameters of Rh2s after i.v. administration were shown in Table 2 and the plasma $AUC_{0-\infty}$ from i.v. administration was used to calculate the absolute oral bioavailability for Rh2s. The absolute oral bioavailability of Rh2s was substantialy increased by 36 fold (from 0.94% to 33.18%, $p<0.001$) and 52 fold (from 0.52% to 27.14%, $p<0.001$) at 5 and 20 mg/kg, respectively.

Coadministration of cyclosporine A also decreased K_e by 2.8 fold (from 0.48 ± 0.25 to 0.17 ± 0.04 hr^{-1}, $p<0.05$) and 2 fold (from 0.32 ± 0.30 to 0.16 ± 0.03 hr^{-1}) at 5 and 20 mg/kg, respectively. Consistently, the half-life of Rh2s increased 78% (from 1.78 ± 0.90 to 4.41 ± 1.05 hr, $p<0.05$) and 36% (from 3.37± 1.78 to 4.60 ± 1.32 hr) at 5 and 20 mg/kg, respectively. Co-administration of cyclosporine A also increased V_{ss} from 0.26 ± 0.24 to 0.49 ± 0.10 ($p<0.05$) L/Kg and 0.38 ±0.20 to 0.51 ± 0.12 ($p=0.2$) L/Kg at 5 and 20 mg/kg, although clearance of Rh2s was not changed after cyclosporine A treatment (Table 4).

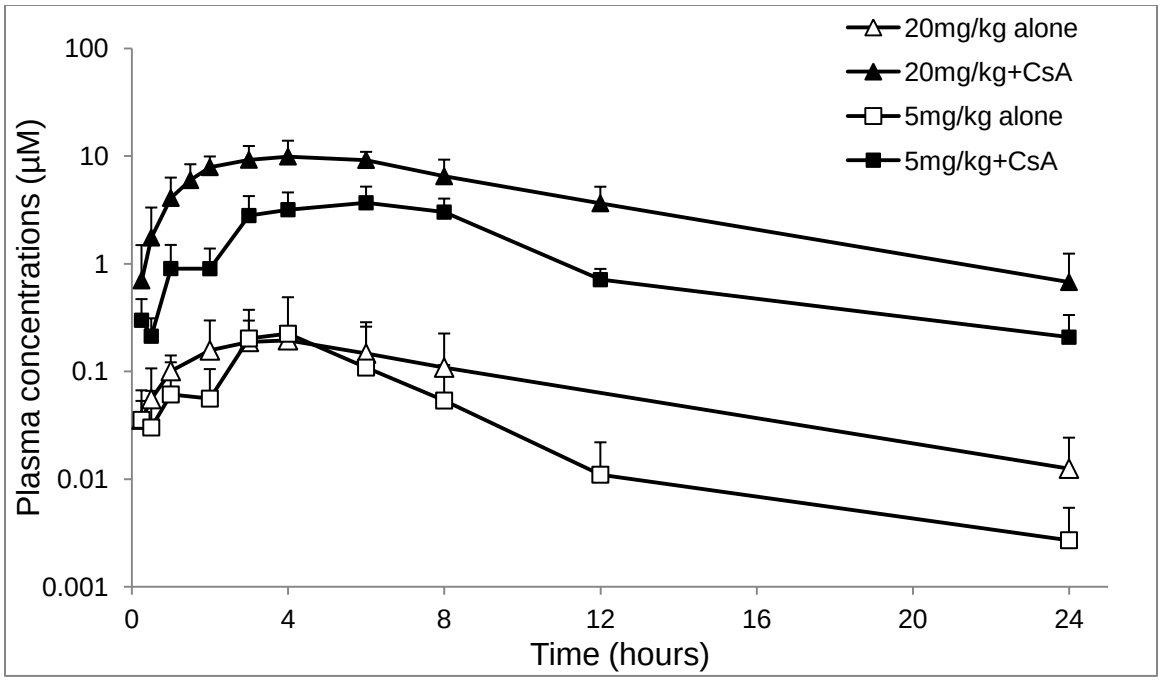

Figure 9. The plasma concentrations of Rh2s alone or with 50 mg/kg cyclosporine A (CsA) treatment after oral administrations at 5 and 20 mg/kg in A/J mice. Data are presented as mean ± S.D.; n=5.

Table 4. The pharmacokinetic parameters of Rh2s in A/J, FVB and MDR1a/b -/- mice at different doses following different routes of administration. Data are presented as mean ± S.D; n=5.

Animal Strain	Route/Dose	Inhibitor (CsA)	T_{max} (hr)	C_{max} (μM)	k_e (hr^{-1})	$t_{1/2}$ (hr)	V_{ss} (L/Kg)	CL (L/hr/Kg)	AUC $_{0-\infty}$ (hr*μM)	F (%)
A/J	i.v. 5mg/kg	-	-	-	0.40± 0.09	1.77± 0.37	0.36± 0.22	0.13± 0.06	98.52± 45.58	-
	p.o. 5mg/kg	-	2.80± 0.84	0.31± 0.30	0.48± 0.25	1.78± 0.90	0.26± 0.24	0.07± 0.01	0.92± 0.90	0.94± 0.92
	p.o. 5mg/kg	50mg/kg	6.50± 1.91*	4.46± 1.20***	0.17± 0.04*	4.41± 1.05**	0.49± 0.10*	0.08± 0	32.69± 4.92***	33.18± 4.99***
	p.o. 20mg/kg	-	4.17± 1.60	0.28± 0.10	0.32± 0.30	3.37± 1.78	0.38± 0.20	0.08± 0	2.04± 1.50	0.52± 0.38
	p.o. 20mg/kg	50mg/kg	4.60± 1.34	10.66± 1.35***	0.16± 0.03	4.60± 1.32	0.51± 0.12	0.08± 0	106.97± 26.02***	27.14± 6.60***
Wild type FVB	p.o. 20mg/kg	-	3.04± 2.70	0.35± 0.36	0.50± 0.25	1.85± 1.27	-	-	2.17± 3.42	-
MDR1a/b $^{-/-}$ FVB	p.o. 20mg/kg	-	4.25± 2.50*	6.01± 1.89**	0.15± 0.02*	4.60± 0.71*	-	-	49.90± 3.20***	-

Pharmacokinetic parameters of Rh2s in cyclosporine A (CsA) co-administration group were compared to Rh2s alone group at the same dose; and pharmacokinetic parameters of Rh2s in MDR1a/b $^{-/-}$mice group were compared to wild-type FVB mice group

* indicated $p<0.05$; ** indicated $p<0.01$; *** indicated $p<0.001$.

Note: V_{ss} and CL are not available in wt FVB and MDR1 knockout mice due to unknown oral bioavailability of Rh2s after oral administration.

5.4.5. In situ intestinal perfusion study of Rh2s

An intestinal perfusion study was performed to investigate intestinal absorption of Rh2s in A/J mice and MDR1 knockout FVB mice. Stability studies showed that Rh2s was stable in the intestinal perfusate for up to 8 hours (Figure 4). Since the UPLC-MS/MS assay has approximate 10% standard deviation based on our validation data, accurate determination of %absorption was difficult if the absorption was poor (i.e., less than 10%). Percent absorption of Rh2s was higher in MDR1a/b $^{-/-}$ mice (64% and 14%) compared to WT FVB mice (<10%) in upper small intestine and colon, respectively. Similarly, percent absorption of Rh2s increased from <10% to 49.4% ($p<0.05$) in upper small intestine and from <10% to 19.8% in colon in the presence of 10 µM cyclosporine A in A/J mice (Fig. 10). Consistently, the steady-state plasma concentration of Rh2s was significantly higher (0.80 µM) in MDR1a/b $^{-/-}$ mice than in WT FVB mice (0.13 µM) at the end of a 2.5 hour intestinal perfusion study. The steady-state plasma concentration of Rh2s was significantly increased by ~9 fold (from 0.12 µM to 1.07 µM, $p<0.05$) in the presence of 10 µM cyclosporine A in A/J mice (Figure 10).

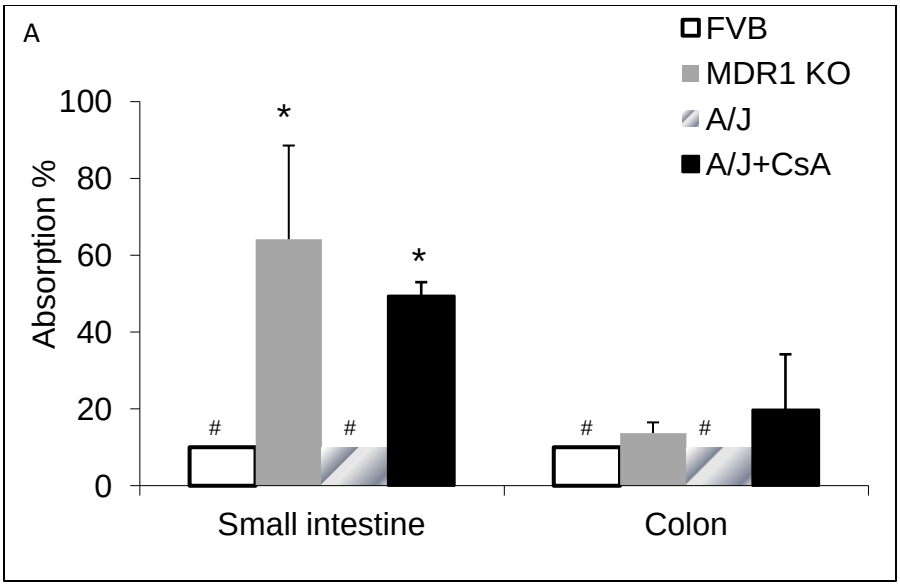

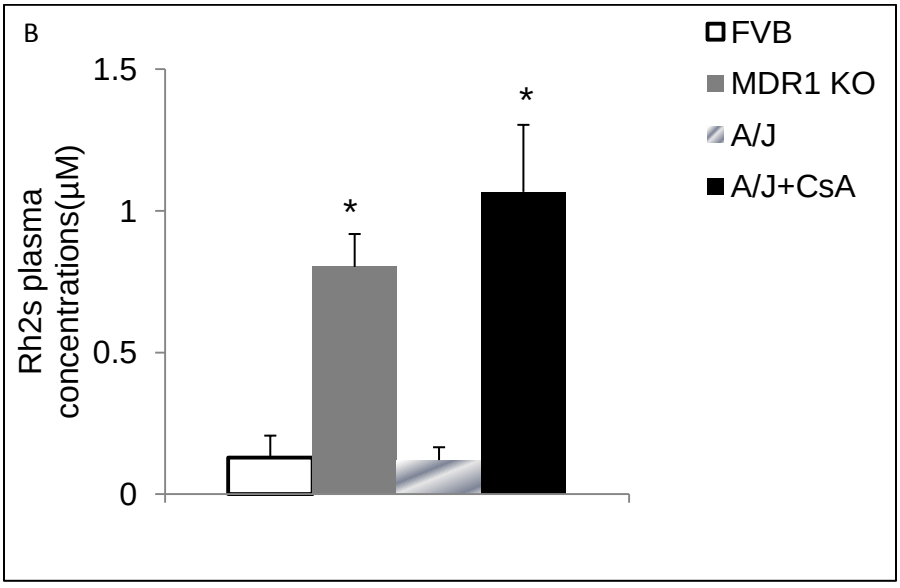

Figure 10. (A) The absorption percentages of Rh2s (2 μM) in intestinal perfusion in WT, MDR1a/b -/- FVB and A/J mice. (B) The plasma concentrations of Rh2s after intestinal perfusion in WT, MDR1a/b -/- FVB and A/J mice. 10 μM CsA were added in perfusate t to inhibit P-gp function in A/J mice. Data are presented as mean ± S.D.; n=4.

*** indicated p<0.05.**
 # indicated the absorption percentages of Rh2s were less than 10%.

5.5. Discussion

This is the first comprehensive study that demonstrates unequivocally that Rh2s is a good substrate of P-gp, and P-gp mediates the efflux of Rh2s in vitro and in vivo. Although poor oral absorption of ginsenosides have been extensively reported, the results were mostly observational [141]. One paper reported that Rh2s is not a substrate of P-gp because 10 μM verapamil did not decrease the efflux of Rh2s in the Caco-2 cell model [171], which is contradictory to our conclusion. The discrepancy may be due to different P-gp expression level in Caco-2 cells among labs or the low concentration of inhibitor they used. Taken together, this means each model has its own limitation and we cannot rely on one single method to ascertain the transport mechanism of a substrate. Therefore, a series of studies ranging from *in vitro, in situ* and *in vivo* models were designed and conducted to support our conclusion that P-gp is the predominant efflux transporter responsible for Rh2s's poor bioavailability.

Our results showed that the other two apically located efflux transporters, MRP2 and BCRP, played a minimal role in the efflux of Rh2s. This conclusion was based on a lack of inhibition of Rh2s efflux or an absence of increase in intracellular accumulations of Rh2s in the presence of 20 μM MK571 or 5 μM Ko143 in Caco-2 cells. Previously, we reported that 10 μM MK571 significantly inhibited (by 61%) apical efflux of apigenin sulfate, which is a substrate of MRP2 in Caco-2 cells [152].

The results of this study clearly demonstrated that inhibition of P-gp by cyclosporine A and deletion of P-gp can substantially increase oral bioavailability of Rh2s. Consistent

results in pharmacokinetic studies of Rh2s were observed in two strains of mice, FVB and A/J mice. FVB mice were used since the P-gp knockout mice were derived from this strain of mice. A/J mice were chosen in this paper because it was the strain used for lung cancer carcinogenesis and chemoprevention [172]. The dominant role of P-gp in limiting the oral bioavailability of Rh2s was demonstrated by the facts that oral bioavailability of Rh2s was substantially increased (from 1% to above 30%) in A/J mice following cyclosporine A co-administration (Table 2), and that there were substantial increases in plasma C_{max} (17.2 fold) and $AUC_{0-\infty}$ (23.0 fold) in MDR1a/b $^{-/-}$ mice compared to WT FVB mice. The improved bioavailability of Rh2s in the presence of a P-gp inhibitor was mainly attributed to enhanced intestinal absorption in mice based on the intestinal perfusion study (Fig. 4). Mechanisms responsible for increased absorption were likely to be increased permeability and elevated intracellular accumulations, as shown in both Caco-2 and MDR1-MDCKII cell models (Table 1). The improved bioavailability could also be contributed by decreased elimination, as indicated by a slower elimination rate constant (k_e) and a prolonged terminal half-life.

The extremely poor oral bioavailability of Rh2s (<1%) was consistent with its low solubility and low permeability observed in this study, suggesting that Rh2s belongs to the class iv compounds in the BCS classification system [173]. However, the apparent low permeability of Rh2s is due to efflux by P-gp, since its intrinsic permeability (passive diffusion) is promising with the highest P_{a-b} exceeding $3x10^{-6}$ cm/sec (obtained in the presence of P-gp inhibitors) (Table 1). The substantial increase in oral bioavailability of

Rh2s in the presence of cyclosporine A to a level above 30% suggests that this compound holds great promise for oral administration (necessary for cancer chemoprevention) if it is properly formulated. Therefore, we have shown that it is possible to derive good oral bioavailability for Rh2s in animals as long as we can inhibit the function of P-gp during absorption.

We have shown that inhibition or deletion of P-gp was the main reason for improved Rh2s bioavailability in mice. In demonstrating the large changes in oral bioavailability of Rh2s, we have seen some minor inconsistency. For example, the AUC value of Rh2s (20 mg/kg) in cyclosporine A treatment group in A/J mice was higher than that in the MDR1a/b $^{-/-}$ FVB mice. It was likely due to strain differences in absorption and/or clearance of this compound. Additional factors such as difference in CYP metabolism of Rh2s were also possible. We believed that a major contribution from CYP was less likely since CYP metabolites of Rh2s were never reported except its hydrolysis product (aglycone) in vivo [43]. In addition, the large differences in C_{max} and AUC values existed between FVB control and MDR1a/b $^{-/-}$ FVB mice were comparable to those achieved with P-gp inhibition by cyclosporine A in A/J mice. However, the contribution from CYP cannot be excluded since other ginsenosides with similar structures were reported as substrates of CYP enzyme [17], and cyclosporine A is also a potent inhibitor of CYP.

We did not observe an increase in oral bioavailabilty of Rh2s at the higher dose (in absence of P-gp inhibitor) as expected since efflux ratios were smaller at higher concentrations (Table 1). We hypothesized that poor solubility was the reason that this enhancment did not occur. This is because ginsenosides with less sugar moiety (e.g., protopanaxadiol, protopanaxtriol, Rh2, and Rg3) usually have poor aqueous solubilities [164]. Our solubility study showed the low aqueous solubility of Rh2s (~3 µg/ml at pH 7.4) in HBSS buffer, (~5 µg/ml at pH 7.4) in water and (~7 µg/ml at pH 6.8) in SIF. The poor aqueous solubility of Rh2s further substantiates the important role of P-gp efflux in vivo since Rh2s cannot fully saturate/inhibit P-gp efflux in lumen due to limited and low solubility. This result did not contradict the results reported by Zhang et al, who showed that Rh2s suspended in sodium CMC could act as an P-gp inhibitor at 25 mg/kg in rats [171], but it did signify that unformulated Rh2s is probably not a very useful P-gp inhibitor in vivo due to solubility limit. Further studies are planned to determine how solubilization of Rh2s could be used to further increase its bioavailability when used together with a P-gp inhibitor.

This proof of principle study demonstrated that oral bioavailability of Rh2s can be enhanced to a clinically acceptable level (30%) if P-gp function is completely inhibited. Since many potent ginsenosides were also showed to be substrates of P-gp in Caco-2 and MDR1-MDCKII cells (unpublished data), P-gp efflux appeared to be an important mechanism responsible for their low bioavailabilities. These results may therefore redefine our understanding on absorption of potent ginsenosides, and point to a strategy to increase their oral bioavailability so their clinical potentials can be fully

evaluated. However, cyclosporine A is not an ideal P-gp inhibitor for continuous clinical usage in healthy humans due to its known therapeutic and adverse effects. Further studies are ongoing to screen other less pharmacologically active compound that may serve as potent P-gp inhibitors to enhance oral bioavailability of Rh2s.

In summary, we demonstrated clearly that Rh2s is a good substrate of P-gp both in vitro and in vivo, and that effective and efficient inhibition of P-gp by cyclosporine A led to an increased oral bioavailability of Rh2s in A/J mice. The conclusion is supported by the facts that (1) deletion of P-gp functionality (as in MDR1a/b$^{-/-}$ FVB mice) significantly increases the oral absorption and bioavailability of Rh2s; and (2) inhibition of efflux transporter P-gp substantially increases cellular uptake and transcellular transport of Rh2s in Caco-2 and MDR1-MDCKII cells. Additional studies are currently ongoing to search for P-gp inhibitors that are effective and clinically applicable for long-term use.

Inhibition of P-glycoprotein leads to improved oral bioavailability of Compound K, an anti-cancer metabolite of ginseng produced by gut microflora

6.1. Abstract

Compound K (C-K) is a known secondary metabolite of ginsenosides after oral administration and it is active in vitro and in vivo against cancers. In this study, we determined the sources of C-K in vivo, its activities against a lung cancer cells, and its pharmacokinetic behaviors in vivo and the mechanisms responsible for the observed pharmacokinetic behaviors. The results showed that the formation of C-K was rapid when primary ginsenosides (e.g. Rb_1 and R_c) were hydrolyzed by microflora glycosidases. The results also show that C-K is active against cancer cell growth with an IC_{50} value of 18.5 μM in LM1 cells, which are much more active than ginseng extract and secondary ginsenosides such as F2. Pharmacokinetic studies in normal mice showed that C-K had low oral bioavailability. To define the mechanisms responsible, two P-gp inhibitors verapamil and cyclosporine A were used to demonstrate they substantially decreased C-K's efflux ratio in Caco-2 cells from 26.6 to less than 3, and significantly increased its intracellular concentrations (as much as 40 fold). Similar results were obtained when transcellular transport of C-K were determined using MDR1-overexpressing MDCKII cells. In MDR1a/b $^{-/-}$ FVB mice, its plasma C_{max} and $AUC_{0\text{-}24h}$ were substantially increased by 4.0 and 11.7 folds, respectively. In the same study, the elimination rate was also significantly decreased in MDR1a/b $^{-/-}$ mice. In

conclusion, C-K is the major active metabolite of ginsenosides after microflora hydrolysis of primary ginsenosides, and inhibition/deficiency of P-gp can significantly enhance its absorption and bioavailability.

Keywords: Ginsenoside Compound K, P-glycoprotein, gut microflora, metabolite, anticancer, bioavailability.

6.2. Introduction

Ginseng, the root of *Panax ginseng* C. A. Meyer, has been used as an herbal supplement to improve life and physical condition in the Orient for thousands of years [1] and American ginseng gained great interest in the last two decades for its various beneficial pharmacological effects on central nervous system disorders, cardiovascular activity and antidiabetics [148, 174, 175]. Ginsenosides, the dammarane-type triterpene saponins, have been found to be the major components responsible for its biological activity, especially on chemoprevention and inhibition of lung cancer. So far, more than 150 ginsenosides with different types/numbers of sugar moieties have been identified, although the diversity in the aglycone moiety was far less with protopanaxadiol and protopanaxatriol representing the two major backbones [5-7].

The biggest barrier to extend ginseng or ginsenosides' clinical use on lung cancer chemoprevention is their low oral bioavailability, usually less than 5% in rodents [13, 47, 48]. Low oral bioavailability may cause large variations in clinical studies, which may lead to ambiguous results in the clinical trial unless an extraordinary number of patients are enrolled in the clinical trials. The latter is often too expensive to conduct. The low oral bioavailability was mainly attributed to their poor oral absorption caused by large molecular weight and bulky sugar moieties [18]. In addition to the poor absorption in GI tract, primary ginsenosides may go through extensive hydrolysis by gut bacteria in GI tract and transform into deglycosylated ginsenosides [176, 177]. However, the metabolism pathways of many abundant ginsenosides by gut microflora and the

bioactivities of the resulting secondary ginsenosides against lung cancers remain to be revealed.

Compound K (C-K) is one of the extensively investigated ginsenosides which showed potent chemoprevention and anticancer activity in various cancer cell lines, and the mechanism includes induction of apoptosis [178, 179], suppression of NF-kB pathway activation [180], and inhibition of mutagenicity [181]. Although C-K has low abundance in the raw ginseng or ginseng extract, previous studies indicated that it could be the major metabolite of ginsenoside after oral administration [177].

C-K was reported to have low oral bioavailability (~5%) in rats [45, 46], which may affect its in vivo efficacy. The absorption mechanism of C-K was generally considered as passive diffusion as one study showed that there was no difference between bidirectional transports in Caco-2 cells [18]. However, there was evidence showed that C-K could reverse multi-drug resistance in tumor cells [182] and our previous study on ginsenoside Rh2s (glucose attached in C3 position instead of C21 position), which has the same molecular weight and log P value as Compound K, showed strong P-gp efflux both in vitro and in vivo [183].

P-gp is one of the most prevalent efflux transporters expressed not only in multidrug resistance cancer cells but also in many organs such as intestine, liver, kidney and the blood-brain barrier [78]. P-gp plays an important role in limiting the intestinal absorption of its substrates [79] and inhibition of P-gp leads to the improvement of oral

bioavailability of several anticancer drugs [80-82]. Profound understanding of P-gp involved transport and its related drug-drug interaction is important for drug development as recommended by FDA in a recently published white paper [68].

In this study, we will first investigate the metabolism pathway of ginseng in gut microflora and identify the active component after biotransformation in GI tract. We will continue our efforts to reveal the absorption mechanism of its major metabolite, C-K to better understand the underlying mechanism responsible for its low oral bioavailability. Therefore, the aims of this study were 1) to delineate metabolism pathway of ginseng in gut bacteria and their efficacy to lung cancer; 2) to systemically investigate mechanisms responsible for poor absorption of active component, C-K, by elucidate which efflux transporter was mainly involved in the transport of C-K using a complementary set of *in vitro* and *in vivo* models.

6.3. Materials and Methods

6.3.1. Chemicals and reagents

Ginsenosides Rb_1, (purity > 98%) was purchased from National Institute for the Control of Pharmaceutical and Biological Products (Beijing, China); Rb_2, R_c, R_d, 20(*S*)-Rg_3, 20(*R*)-Rg_3, 20(*S*)-Rh_2, 20(*R*)-Rh_2 (Each purity > 98%) were purchased from Scholarbio-Tech (Chengdu, China). Compound K and F_2 (Each purity > 98%) were purchased from Must Bio-technology Co. Ltd. (Chengdu, China). Rk_1/Rg_5 mixture (Total purity > 90%) was prepared in Dr.Zhi-Hong Jiang's lab and identified by high-resolution mass. Red ginseng water extract was prepared in Dr. Zhi-Hong Jiang's lab. All chemicals were of analytical grade purity.

Cloned Caco-2 cells (TC7) cells were kept in house. Lung carcinoma LM1 cell line was provided by Dr. Ming You's lab at Medical College of Wisconsin. Parental MDCKII and MDR1-MDCKII cells were provided by the Netherland Cancer Institute (Amsterdam, Netherland). MTT, Digoxin, cyclosporine A, verapamil and Hanks' balanced salt solution (powder form) were purchased from Sigma-Aldrich (St. Louis, MO). Oral suspension vehicle was obtained from Professional Compounding Centers of America (Houston, TX). BCA protein assay kit was purchased from Thermo Scientific (Rockford, IL). All other materials (typically analytical grade or better) were used as received.

6.3.2. Animals

Male FVB and A/J mice (6-10 weeks) were purchased from Harlan Laboratory (Indianapolis, IN). Male MDR1a/b knockout mice (6-10 weeks) were purchased from Taconic Farms (Germantown, NY). They were acclimated in an environmentally controlled room (temperature: 25 ± 2°C, humidity: 50 ± 5%, 12 h dark-light cycle) for at least 1 week prior to experiments. The mice were fed with rodent diet (Labdiet® 5001), and fasted overnight before pharmacokinetic studies.

6.3.3. Cell culture

LM1 is a metastatic cell line derived from A/J mice [184], which is the strain used for lung cancer carcinogenesis and chemoprevention [172]. LM1 cells were grown in Dulbecco's modified Eagle's medium supplemented with 10% fetal bovine serum, 2 mM glutamine, 50 units/ml penicillin, 50 pg/ml streptomycin and 1% nonessential amino acids. LM1 cells were seeded at 5×10^3 per well. LM1 cells were fed every day and cells were ready for use after 2-3 days post-seeding.

The Caco-2 cell culture is routinely maintained in this laboratory for the last 2 decades. The culture conditions for growing Caco-2 cells were the same as those described previously [147]. Porous polycarbonate cell culture inserts (3 μm) were used to seed the cells at a seeding density of 60,000 cells/cm^2. The TEER value >100 Ω/cm^2 was used as quality control to test the tightness of tight junction in Caco-2 cells. Caco-2 TC7 cells were fed every other day, and cell monolayers were ready for experiments from 19 to 22 days post-seeding.

Parental MDCKII and MDR1-MDCKII cells were cultured in Dulbecco's modified Eagle's medium supplemented with 10% fetal bovine serum, 1% nonessential amino acids, 100U/ml penicillin and gentamicin. Cell culture was maintained at 5% CO_2 and 90% relative humidity at 37°C. They were seeded at 2.0×10^6 cells/well into the same cell culture inserts as those used for Caco-2 cells, and fed every day. The parental MDCKII and MDR1-MDCKII cell monolayers were ready for experiments from 4-5 days post-seeding. The expression levels of MDR1 in MDR1-MDCKII were monitored by western blotting analysis.

6.3.4. Hydrolysis of ginsenosides by glycosidases prepared from gut microflora

Fresh feces were collected from A/J mice. One part of feces was mixed with ten parts (volumes) of 0.1 mM ice-cold potassium phosphate buffer. They were vortexed for 30 seconds and sonicated in iced water for 30 min. The suspension was subjected to centrifugation at 1,000 rpm and 4°C for 30 min. The final supernatant of fecal homogenate was stored in aliquots at -80 °C until use. Protein concentrations were determined by the BCA protein assay kit using bovine serum albumin as protein standard.

Frozen fecal homogenate was thawed and 200 µl was taken to disposable glass vials from VWR (Houston, TX). The homogenate was diluted with ice-cold potassium phosphate buffer to 2 ml. Then red ginseng extract was added to make the final concentration 1 mg/ml and the study was performed in triplicate. The mixture was incubated at 37 °C and shaken at 120 rpm for 24 hrs. 100 µl samples were taken at 0, 4

and 24 hr, and the reaction was stopped with addition of 500 µl 2.5 µM testosterone (internal standard) in 100% acetonitrile. The samples were vortexed for 15 seconds and centrifuged at 15, 000 rpm for 15 minutes. 540 µl supernatant was taken, air dried and reconstituted with 100 µl 30% acetonitrile. After centrifugation, 10 µl of the final solution was injected into Q-TOF/MS for analysis.

6.3.5. Cytotoxicity of ginsenosides in LM1 cell line

The cell growth inhibitory effect of ginseng powder and various metabolites generated in gut bacteria was determined using MTT assay in LM1 cell line. Cells were suspended in fresh medium at a concentration of 5×10^3 cells/ml and seeded in a 96-well flat bottomed plate in a volume of 100 µl/well. Cells were stabilized by incubation for 24 hrs at 37ºC and 100 µl aliquots of each drug with different concentrations (0.5% DMSO) ranging from 0.41 to 100 µM were added to wells. The plate was incubated at 37ºC for 48 hrs. For assay, 50 µl of MTT were added to each well and the plate was incubated for 4 hrs at 37ºC. The optical density was measured at 570 nm on a microplate reader (Bio-Rad, California). Each experiment was performed in triplicate and repeated at least twice. Antitumor activity was evaluated using IC_{50} determined by non-linear regression analysis using the GraphPad PRISM 5 (San Diego, CA).

6.3.6. Transcellular transport study

The transcellular transport study was performed as described previously [183]. Briefly, 2.5 ml of C-K solution was loaded onto one side of the cell monolayer, and 2.5 ml of

blank HBSS onto the other side. Five sequential samples (0.5 ml) were taken at different times (0, 1, 2, 3 and 4 hrs) from both sides of the cell monolayer. The same volume of C-K solution and receiver medium (fresh HBSS) was added immediately to replace the volume lost because of sampling. The pH values of HBSS in both apical and basolateral side were 7.4.

Both permeability from apical to basolateral side (P_{a-b}) and basolateral to apical side (P_{b-a}) were calculated according to the equation 1. The efflux ratio was calculated as P_{b-a}/P_{a-b}, which represented the degrees of efflux transporter involvement. Digoxin, a substrate of P-gp, was used as the positive control for the transport study in Caco-2 and MDR1-MDCKII cell monolayers. In the present study, inhibitors of efflux transporters were only added to the apical side of cell monolayers, regardless of where C-K was loaded.

Intracellular concentrations of C-K were determined at the end of a transport study. The protocol for determining C-K's intracellular amounts in cells was the same as those described previously [183]. Briefly, after 4 hours of a transcellular transport study, the cell membranes were rinsed three times with ice-cold HBSS buffer, and cells attached to the polycarbonate membranes were cut off from the inserts with a sharp blade. The latter was immersed into 1 ml HBSS, and sonicated for half an hour at 4°C to break up the cells. The mixture was centrifuged at 15,000 rpm for 15 minutes and 500 µl of the supernatant were taken and air-dried. The residue were reconstituted with 200 µl methanol and analyzed by UPLC-MS/MS. The protein concentration of cell lysate was

measured to normalize the accumulation of Compound K inside the cells using the BCA protein assay kit.

6.3.7. Pharmacokinetic studies of Compound K in WT and MDR1a/b $^{-/-}$ FVB Mice

Pharmacokinetic studies of C-K were performed in wild-type and MDR1a/b $^{-/-}$ FVB mice to investigate the role of MDR1/P-gp in determining bioavailability of C-K. C-K dispersed in the oral suspending vehicle was given by gavage to each group at 10 mg/kg. The ingredients of oral suspending vehicle are shown in Table S1. Each pharmacokinetic study was performed on five mice and 10 timed blood samples (20-25 µl) were taken by snipping its tail, after mice were anesthetized with isoflurane gas. The blood samples were collected in heparinized tubes and stored at -20°C until analysis.

6.3.8. Pharmacokinetic studies of red ginseng extract in A/J mice

Pharmacokinetic study of red ginseng extract was performed in A/J mice to confirm the in vivo hydrolysis of ginsenosides by gut microflora. Red ginseng extract was dissolved in distilled water and was orally gavaged to A/J mice at 200 mg/kg (n=5). The blood sample collection and processing procedures used for A/J mouse samples were the same as those described for the FVB mouse pharmacokinetic study.

6.3.9. Qualitative Determination of Microflora Generated Secondary Ginsenosides

A Waters ACQUITY UPLC^{TM} system (Waters Corp., MA, USA) coupled to Bruker MicroTOF mass spectrometer with an ESI source was used to qualitatively identify

metabolites of ginsenosides in gut microflora. The chromatography was performed on an Acquity BEH C_{18} column (2.1 × 100 mm, 1.7 um). The mobile phase consisted of 0.1% formic acid in distilled water (A) and acetonitrile containing 0.1% formic acid (B), starting with linear gradient from 20 to 40% B within 20 min, then from 40 to 100% B at 20 - 29 min, and maintained at 100% B for 3 min at flow rate of 0.35 mL/min. The data were acquired in negative mode and conditions of MS analysis were as follows: end plate offset, -500 V; capillary voltage, 4500V; nebulizing gas (N_2) pressure, 1.5 bar; drying gas (N_2) flow rate, 8.0L/min; drying gas temperature, 200 ℃; Mass range, *m/z* 300 - 1500. For accurate mass measurement, the TOF mass spectrometer was calibrated routinely using sodium formate solution infused at a flow rate of 2.5 mL/h. Sodium formate solution was prepared by mixing 0.05 mmol NaOH solution with 0.05% formic acid in 90:10 proportion of 2-propanol/distilled water.

The extracted ions for relative comparison of each ginsenosides were as follows: Rb_1, *m/z* 1107.5 ($[M-H]^-$); Rc, *m/z* 1077.5 ($[M-H]^-$); Rb_2, *m/z* 1077.5 ($[M-H]^-$); Rd, *m/z* 991.5 ($[M-HCOO]^-$); Rg_1, *m/z* 845.5 ($[M-HCOO]^-$); Re, *m/z* 991.5 ($[M-HCOO]^-$); Rg_2, Rg_3 and F_2, *m/z* 783.5 ($[M-H]^-$); Rh_1 *m/z* 667.4 ($[M-HCOO]^-$); Rk_1 and Rg_5, *m/z* 765.5 ($[M-H]^-$); Rh_2 and C-K, *m/z* 683.5 ($[M-HCOO]^-$); . Identification of ginsenosides and its metabolites was achieved by comparing retention time with authentic compounds in combination with accurate mass. Data were collected and analyzed by Bruker Daltonics software (version 4.0, Bruker, USA).

6.3.10. Quantitative Determination of Compound K and F2

An API 3200 Qtrap® triple quadrupole mass spectrometer (Applied Biosystems/MDS SCIEX, Foster City, CA, USA) equipped with a TurboIonspray™ source, operated in a positive ion mode, was used to quantitatively measure Compound K in various matrices.

The flow dependent parameters for introduction of the samples to the mass spectrometers ionization source were set as follows: ion spray voltage, 5.5 kV; ion source temperature, 650°C; the nebulizer gas (gas1), nitrogen, 50 psi; turbo gas (gas2), nitrogen, 50 psi; curtain gas, nitrogen, 10 psi. The quantification was performed using multiple reactions monitoring mode (MRM) with ion pair transitions to monitor C-K and formononetin (Internal standard). The fragments for each compound detected were 645.0/203.0 (m/z) for C-K and 269.2/197.1 (m/z) for formononetin. Data were collected and analyzed by Analyst 1.4.2 software (AB SCIEX, USA).

UPLC conditions for C-K analysis were: system, Waters Acquity™ (Milford, MA, USA) with DAD detector; column, Acquity UPLC BEH C18 column (50×2.1mm I.D., 1.7μm, Waters); mobile phase A, 0.1% formic acid; mobile phase B, 100%, acetonitrile; gradient, 0-0.5 min, 0% B, 0.5-1 min, 0-40% B, 1-1.9 min, 40-90% B, 1.9-2.3 min, 90-95% B, 2.3-2.5 min, 95% B, 2.5-32.8 min, 95-0% B. Flow rate, 0.55 ml/min, column temperature, 45 degree; injection volume, 10 μl. The chromatograph of C-K and I.S. is shown in Supplemental Figure 1.

The standard curves of C-K were linear in the concentration range of 19.5 nM-10 μM and the LLOQ was 9.8 nM in blood. The intra-day and inter-day precision were within 15% for all QC samples at three concentration levels (2.5, 0.3125 and 0.039 μM). The stability of C-K in mouse blood were evaluated by analyzing three replicates of quality control samples after short-term (25°C, 4h) and post processing (20°C, 8h). All the samples displayed 85-115% recoveries after various stability tests.

Before samples could be introduced into the UPLC, they were processed by protein precipitation. A volume of 200 μl methanol (containing 1 μM formononetin) was added into 20 μl aliquot of mouse blood sample. The sample mixtures were vortexed for about 30 seconds and precipitates were removed by centrifugation at 15,000 rpm for 15 min. The supernatant was evaporated to dryness at 40°C under air. The dry residue was reconstituted in 100 μl of 100% methanol (v/v), and a 10 μl aliquot of the resulting solution was injected into the UPLC-MS/MS system for analysis.

6.3.11. Pharmacokinetic analysis

WinNonlin 3.3 (Pharsight Corporation, Mountain View, California) was used for C-K and F2 pharmacokinetic analysis. The non-compartmental model was applied for pharmacokinetic analysis of Rh2s profiles. Pharmacokinetic parameters, including Cmax, Tmax, ke, half-life, MRT and AUC were directly derived from WinNonlin.

6.3.12. Statistical analysis

The data in this paper were presented as means ± S.D., if not specified otherwise. Significance differences were assessed by using Student's t-test or one-way ANOVA. A p value of less than 0.05 was considered as statistically significant.

6.4. Results and Discussion

6.4.1. Hydrolysis of ginsenoside by glycosidases derived from gut microflora

After incubation with glycosidases prepared from gut microflora, the concentration of Rb1, Rb2 and Rc in red ginseng extract decreased with time (Figure 11). Rc was completely hydrolyzed while Rb1 and Rb2 was hydrolyzed by >80% (estimated from peak area) at 24 hr (Figure 11A & C). As a result, they were transformed into serial deglycosylated products, Rd, F2 and C-K. Both F2 and C-K kept increasing at 4 and 24 hr compared to 0 hr while Rd did not show obvious change in term of peak area (Figure 11 A-C), probably because it is the key intermediate of hydrolysis. Blank fecal extraction did not interfere with ginsenoside analytes in chromatography (Figure 11D). In order to better visualize metabolites change with time, UPLC-TOF-MS chromatograms were overlaid from different time points (Figure 11E) and F2 and C-K kept increasing while both Rg3 and Rh2 slightly decreased with time (the peak of Rh2 was not shown). These results also suggested the tendency of stepwise de-glycosylation was terminal sugar > inner sugar (C-3) > inner sugar (C-20).

Human gut microflora could similarly hydrolyze various glycosides rapidly and its deglycosylated metabolites were usually considered as the active components in vivo [185]. After incubated in gut microflora, the primary PPD-type ginsenosides (Rb1, Rb2 and Rc) in red ginseng extract were transformed into more hydrophobic ginsenosides F2 and Compound K. However, PPT-type ginsenosides (Re, Rg1 and Rg2) were not metabolized during the 24-hr incubation (Figure 11).

Plasma profile of C-K after oral administration of red ginseng extract at 200 mg/kg in A/J mice further confirmed that conversion of ginsenosides by gut microflora in vivo (Figure 12) considering C-K was not absent in red ginseng extract at 0 hr (Figure 11A). The plasma C_{max} of C-K was 1.1 μM and it kept relatively high concentration up to 24 hr, possibly due to sustained biotransformation in vivo. F2 was also detectable in plasma after oral administration of red ginseng extract. Its plasma level (C_{max} =0.58 μM) was lower than C-K and showed variable concentrations with time, which can be explained as the intermediate product of hydrolysis. Therefore, a clear understanding of metabolic pathway of ginseng in gut microflora may hold the key to understand the biotransformation of primary ginsenosides in vivo, which can impact their in vivo efficacies.

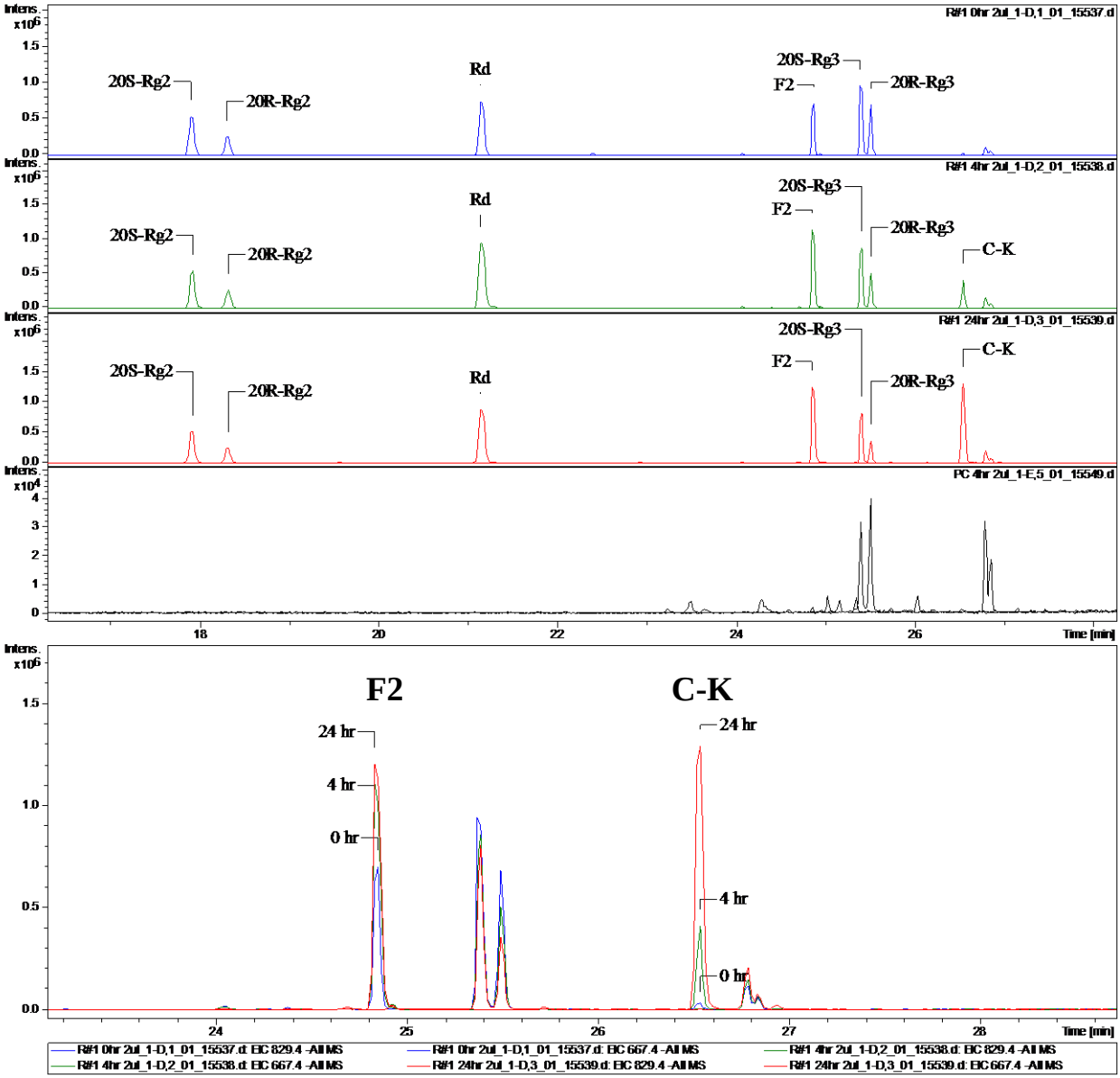

Figure 11. UPLC-TOF-MS chromatograms of red ginseng extract incubated in gut bacteria at 0 hr (A), 4 hr (B) and 24 hr (C), blank fecal extraction without ginsenosides (4 hr, D), and overlaid chromatograms of F2 and Compound K at different time points where 0 hr was marked as blue, 4 hr was marked as green and 24 hr was marked as red (E). n=3.

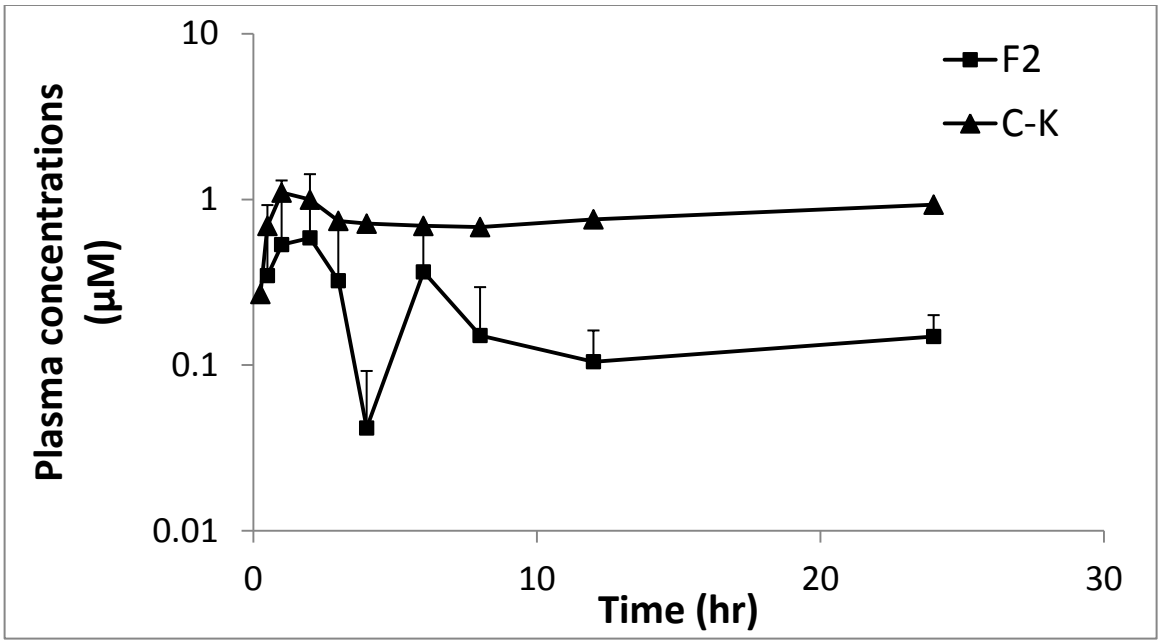

Figure 12. The plasma concentrations of C-K and F2 in A/J mice after oral administration of red ginseng extract at 200 mg/kg. Data are presented as mean ± S.D.; n=5.

6.4.2. Antiproliferative effects of ginsenosides in lung cancer LM1 cell line

The extensive hydrolysis of ginsenoside in gut bacteria indicated that these metabolites (especially F2 and C-K) may represent major active components after oral administration of ginseng. The inhibitory effects of red ginseng and its two major bacteria metabolites, F2 and C-K against cell growth were tested in LM1 cell line. 5-Fluorouracil was used as positive control and it showed potent inhibitory effect against cell growth with IC_{50}= 1.20 μM. Red ginseng extract did not show any antiproliferation effect in LM1 cell line even the concentration reached 100 μM. F2 showed concentration dependent inhibitory effect but IC_{50} is more than 100 μM. C-K showed significant antitumor activity with IC_{50}= 18.45 μM (Figure 13). Lee et al also showed that the mean IC_{50} values of C-K against four other cancer cell lines was 32.9 μM, and they also showed that primary ginsenoside Rb1 and Rd (ginsenosides present in abundance in nature), the precursor of C-K, showed no cytotoxic effect on any of the four cancer cell lines shown above [148]. The results were consistent with several structure-activity relationship studies showed that anticancer activity of ginsenoside is inversely correlated to the number of sugars, which means the hydrolysis products have stronger anticancer activities than the precursor ginsenoisdes [186, 187] .

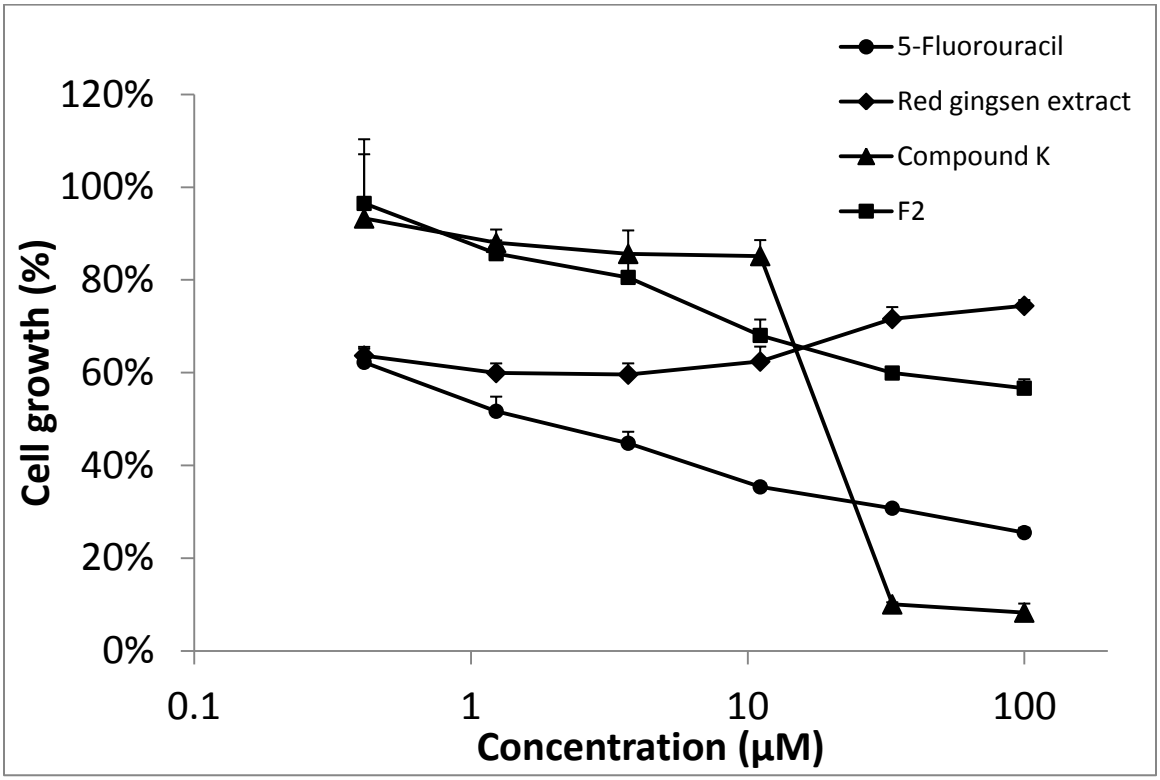

Figure 13. Antiproliferation activity of red ginseng extract, F2 and Compound K against lung cancer LM1 cell line. Each points represents the mean and standard error of three experiments. 5-Fluorouracil was used as a positive control. n=3.

6.4.3. Transcellular transport of Compound K across Caco-2 cell monolayers

Since C-K was the major active metabolite after hydrolysis of primary ginsenosides by gut microflora and it had inhibitory effects to lung cancer LM1 cells, its absorption mechanisms were further investigated to aim for better understanding of its low oral bioavailability. The transcellular transport of digoxin was measured as the positive control before the transport study of C-K was performed using Caco-2 cell monolayers. The results showed that transcellular transport of digoxin displayed significant efflux ratio (21.0) and P_{a-b} was 1.48×10^{-6} cm/s, which was similar to the our previous results [183]. In the presence of 20 μM cyclosporine A, the efflux ratio of digoxin was decreased from 21 to 1.2.

As expected, transcellular transport of C-K (2 μM) across the Caco-2 monolayers from basolateral (B) to apical (A) side (as measured by P_{b-a}) was significantly higher than the transport from A to B side (Figure 14 A), and the efflux ratios (P_{b-a} /P_{a-b}) were 26.. Two P-gp inhibitors, 50 μM verapamil or 20 μM cyclosporine A added at the apical side, were able to greatly inhibit the efflux transport of C-K (Figure 14B&C), and the efflux ratio was decreased to 2.9 (for verapamil) and 1.1 (for cyclosporine A), respectively. In the presence of inhibitors, the P_{a-b} was significantly increased by 2.9 and 2.8 fold; and the P_{b-a} was significantly decreased by 3.1 and 8.5 fold after verapamil and cyclosporine A treatment, respectively (Table 5). Consistent with the permeability results, two p-glycoprotein inhibitors also significantly increased the intracellular accumulation of Compound K following treatment with 50 μM verapamil (from 0.01 to 0.50 nmol/mg) or 20 μM cyclosporine A (from 0.01 to 0.15 nmol/mg).

6.4.4. Transcellular transport of Compound K in MDR1- MDCKII cells

Human MDR1/P-gp over-expressing MDCKII cells were used to confirm the predominant role of P-gp in the transport of C-K. Prior to the transport studies of C-K, 2 μM digoxin was used as a positive control in MDR1-MDCKII cell transport study. The efflux ratio of digoxin was 64.0 in MDR1-MDCKII cell and the P_{a-b} is 2.98×10^{-7} cm/s showing the normal expression of P-gp in MDR1-MDCKII cells.

The transport of C-K in parental MDCKII cells was used as a negative control since it has low expression of human P-gp. As expected, the efflux ratio of Compound K was much lower in parental MDCKII cells (Figure 15A) compared to MDR1-MDCKII cells (Figure 15B) at 2 μM (18.2 vs 1.8). However, the P_{a-b} of C-K was unexpectedly higher in MDR1-MDCKII cells (1.84×10^{-6} cm/s) than parental MDCKII cells (0.58×10^{-6} cm/s,Table 5), which may due to batch difference of MDCKII cells in term of tightness of tight junction.

The intracellular accumulations of C-K were also measured and the results showed that C-K accumulation was significantly higher (3.1 fold) in parental MDCKII cells (0.27 nmol/mg) than in MDR1-MDCKII cells (0.08 nmol/mg).

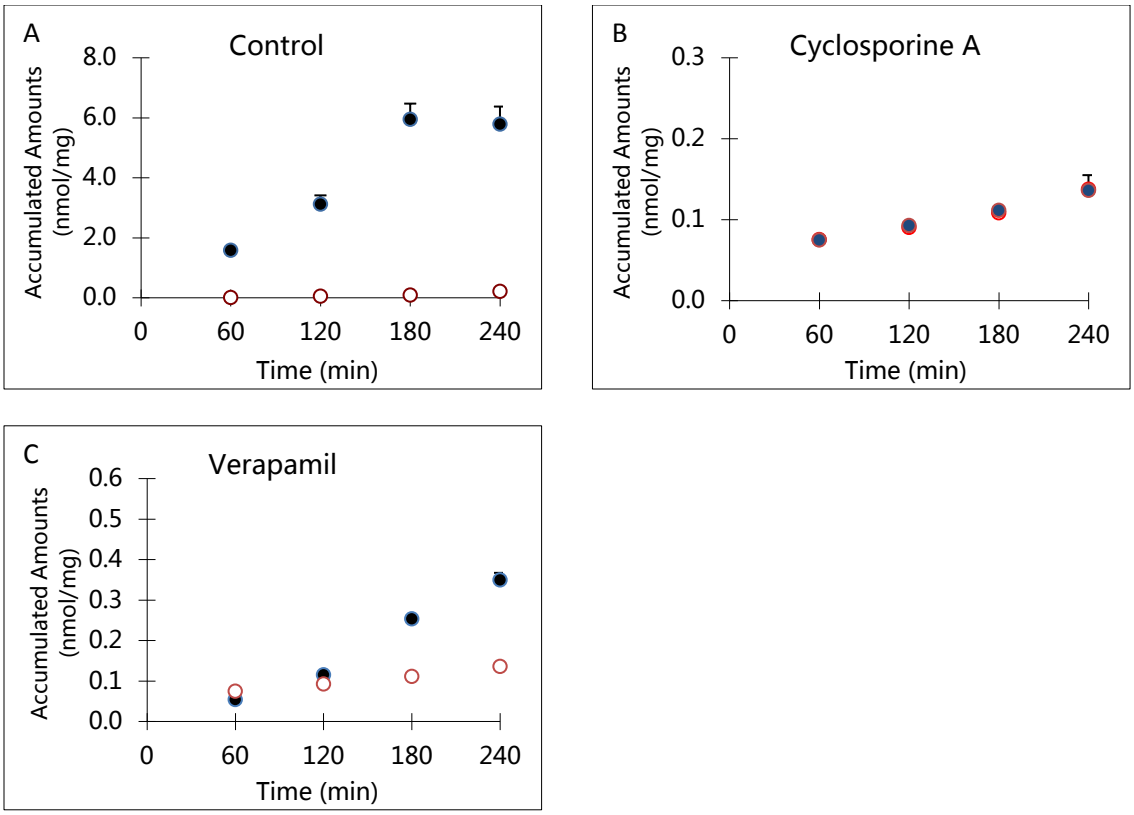

Figure 14. Transcellular transport of 2 μM Compound K across monolayers of Caco-2 cells with different inhibitors. (A) Compound K transport alone; (B) Compound K transport with 20 μM cyclosporine A; (C) Compound K transport with 50 μM verapamil. Transpor from A to B is represented by ○ and that from B to A is represented by ●. Data are presented as mean ± S.D; n=3.

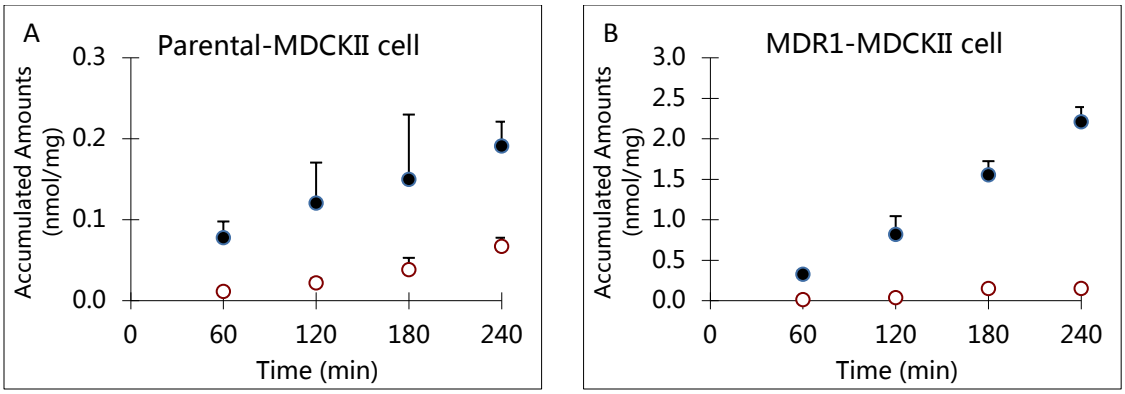

Figure 15. Transcellular transport of Compound K across monolayers of parental MDCKII and MDR1- MDCKII cells. (A) 2 μM Compound K transport in parental MDCKII cells; (B) 2 μM Compound K transport in MDR1- MDCKII cells. Transport from A to B is represente by ○ and that from B to A is represented by ●. Data are presented as mean ± S.D; n=3.

Table 5. Transcellular transport of C-K across monolayers of Caco-2, MDCKII, and MDR1-MDCKII cells in the absence or presence of P-gp inhibitors.

Cell model	Inhibitor	Inhibitor concentration (μM)	P_{a-b} ($\times 10^{-6}$ cm/s)	P_{b-a} ($\times 10^{-6}$ cm/s)	Efflux ratio (P_{b-a}/P_{a-b})	Intracellular amounts (nmol/mg)
Caco-2	-	-	1.16 ± 0.33	30.96 ± 4.31**	26.6	0.01 ± 0
	Verapamil	50	3.39 ± 0.41	9.89 ± 0.11*	2.9	0.50 ± 0.01***
	Cyclosporin A	20	3.30 ± 0.67	3.62 ± 0.22	1.1	0.15 ± 0.01***
MDCK II	-	-	0.58 ± 0.12	1.13 ± 0.11*	1.8	0.27 ± 0.03
MDR1- MDCK II	-	-	1.84 ± 0.70	33.64 ± 8.08**	18.2	0.08 ± 0.01**

Data were presented as mean ± S.D; n=3.

"P_{a-b}" refers to the permeability from apical to basolateral and "P_{b-a}" refers to the permeability from basolateral to apical side. The values of permeability were compared between different direction and intracellular amounts were compared to control group. Data are the means ± S.D. of three independent experiments.

– indicated no inhibitor; * indicated $p<0.05$; ** indicated $p<0.01$; *** indicated $p<0.001$.

6.5. Effects of MDR1 on the oral bioavailabilities of Compound K

In order to investigate whether MDR1/P-gp has major effects on oral bioavailability of C-K, plasma profiles of C-K were compared between MDR1a/b $^{-/-}$ and wild-type FVB mice after oral dosing of C-K (10 mg/kg). In MDR1a/b $^{-/-}$ mice, the T_{max} was significantly prolonged (from 2.8 ± 0.84 hr to 5.6 ± 2.19 hr, $p<0.05$) compared to wild-type FVB mice. More importantly, the plasma C_{max} was significantly increased by 4.0 fold ($p<0.05$), and AUC_{0-t} and $AUC_{0-\infty}$ was significantly increased ($p<0.001$) by 11.7 fold and 23.5 fold, respectively, when compared to wild-type FVB mice (Table 6).

In MDR1a/b $^{-/-}$ mice, K_e was significantly decreased by 73% (from 0.13 ± 0.07 to 0.04 ± 0.01 hr^{-1}, $p<0.05$) compared to wild-type FVB mice. As expected, the $t_{1/2}$ of Compound K was significantly increased by 3.2 fold (from 5.87 ± 3.04 to 18.68 ± 6.84 hr, $p<0.05$). Consistently, the MRT was also significantly increased from 7.8 hr (WT) to 30.8 hr (Knockout mice). Although in MDR1a/b $^{-/-}$ mice, our sample time was not long enough (<2 times of $t_{1/2}$) to accuratly estimate k_e and $t_{1/2}$, the trend of slow elimination was very obvious (Figure 16). The decreased k_e and increased $t_{1/2}$ could be attributed to the decreased elimination of C-K due to the knockout of the MDR1 gene (Table 6). Combined with Caco-2 transport study, both increased absorption as reflected by increased plasma C_{max} and decreased elimination of C-K (decreased k_e and prolonged $t_{1/2}$) contributed to the increased bioavailability of C-K after oral administration to MDR1-/- mice.

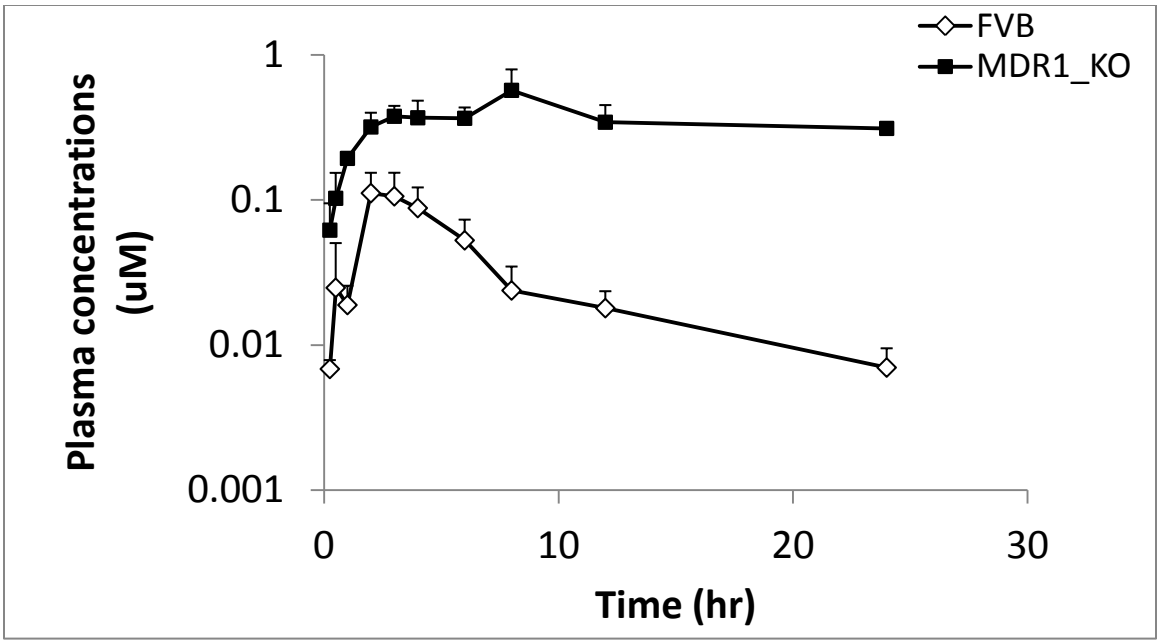

Figure 16. The plasma concentrations of Compound K in wild-type and MDR1a/b -/- FVB mice after oral administration at 10 mg/kg. Data are presented as mean ± S.D.; n=5.

Table 6. The pharmacokinetic parameters of C-K in FVB and MDR1a/b -/- FVB mice after oral administration of 10 mg/kg of C-K.

Animal Strain	T_{max} (hr)	C_{max} (μM)	k_e (hr^{-1})	$t_{1/2}$ (hr)	MRT_{inf} (hr)	AUC_{0-t}	$AUC_{0-\infty}$ (hr*μM)
Wild type FVB	2.8 ± 0.84	0.13 ± 0.03	0.13 ± 0.07	5.87 ± 3.04	7.82 ± 1.73	0.66 ± 0.19	0.75 ± 0.21
MDR1a/b $^{-/-}$ FVB	5.6 ± 2.19*	0.53 ± 0.23*	[a]0.04 ± 0.01*	[a]18.68 ± 6.84*	[a]30.72 ± 8.62*	7.70 ± 2.27***	[a] 17.58 ± 3.16***

Data were presented as mean ± S.D; n=5.

* indicated p<0.05; ** indicated p<0.01; *** indicated p<0.001.

"a" indicated that estimated pharmacokinetic parameters may not be very accurate due to limited sample time (24hr) in MDR1a/b $^{-/-}$mice.

This is the first comprehensive study that demonstrates unequivocally that C-K is a good substrate of P-gp, and P-gp mediates the efflux of C-K in vitro and in vivo. One paper reported that passive diffusion is the major absorption mechanism for C-K since its bidirectional permeability values were comparable in the Caco-2 cell model [18], which is contradictory to our conclusion. The discrepancy may due to different P-gp expression level in Caco-2 cells among laboratories and/or high substrate concentration (up to 50 μM) they used which may not be soluble or saturate efflux. Therefore, in our study, 2 μM of C-K were used in cell transport study to eliminate the possible saturation and inhibition of P-gp. Both studies using chemical inhibitors of P-gp and P-gp/MDR1 oeverexpressed cell line support our conclusion that P-gp is the predominant efflux transporter responsible for C-K's in vitro disposition.

Previous study showed that compound K has linear pharmacokinetics in term of AUC, clearance and volume of distribution from 3 to 30 mg/kg [45], the current dose (10 mg/kg) is appropriate to reveal the role of P-gp on pharmacokinetics of C-K. The in vivo pharmacokinetic study demonstrated that $AUC_{0\text{-}24h}$ of C-K was 12 fold higher in P-gp knockout mice than WT mice. Considering the oral bioavailability of C-K were reported around 5% in rodents [45, 46], the current study showed great promise to increase oral bioavailability of C-K as long as we can completely inhibit P-gp-mediated efflux. Our previous publication showed that Rh2s, another potent ginsenoside with similar structure, is a good substrate of P-gp, and coadministration of cyclosporine A can substantially increase its oral bioavailability from 1% to over 30% [183]. P-gp efflux

appeared to be an important mechanism responsible for ginsenoside's low bioavailabilities. These results greatly changed previous understanding that passive diffusion is the major absorption mechanism of active ginsenosides.

In summary, we demonstrated clearly that C-K is the major metabolite of primary ginsenosides after they are hydrolyzed by gut microflora. Its in vitro inhibitory effects against lung cancer demonstrated its potential efficacy after oral administration of red ginseng containing large quantities of primary ginsenosides. C-K is a good substrate of P-gp and its absorption was greatly impeded by P-gp efflux. Knockout of P-gp significantly increased bioavailability of C-K with both increased absorption and decreased elimination in vivo.

Structural basis of p-glycoprotein-mediated efflux of ginsenosides: impact of sugar moiety

7.1. Abstract

Major limitation for clinical use of ginsenosides is due to poor oral absorption. Previous studies showed that efflux transport, especially mediated by P-glycoprotein is the major mechanism for disposition of ginsenosides Rh2 and C-K. The purpose of this study is to investigate the absorption mechanism of ginsenosides family with different backbones and sugar moieties to reveal structure-absorption relationship. Twenty-two ginsenosides ranging from aglycone to four sugar glycosides were investigated in this study. In Caco-2 monolayer cells, ginsenosides with 3 or 4 sugars as well as aglycone showed efflux ratios close to 1 indicating the passive diffusion might be the major transport mechanism. In contrast, several ginsenosides with 1 or 2 sugar moieties, including Rh2s, compound K (C-K), F1, Rh1 and F2 showed high efflux ratios at 29, 27, 43, 39 and 131, respectively, while ginsenoside Rg3, Rg1, Rg5 and Rk1 showed weak efflux ratios ~ 2. Administration of cyclosporine A and verapamil showed significant inhibition on efflux of F1, Rh1 and F2 in Caco-2 cells indicating the involvement of P-gp. BCRP were also found to be involved for the transport of F1 and F2. WT and MDR1-MDCKII cells confirmed the role of P-gp on transport of ginsenoside F1, Rh1, Rg1 and F2 in term of efflux ratio and intracellular concentrations. Molecular docking studies provided possible binding sites for ginsenosides Rh2 and C-K. In conclusion, 1 or 2 glucose attached ginsensides were probably P-gp substrate while aglycone or ginsenosides with 3 or 4 sugar moieties are likely transported via passive diffusion.

Key words: ginsenosides, sugar moiety, efflux, P-glycoprotein, breast cancer resistance protein, molecular docking.

7.2. Introduction

Currently 42 clinical trials on ginseng are completed or ongoing all over the world and ginsenosides are the major active components in ginseng which are responsible for various pharmacological and therapeutical effects including anticancer, chemoprevention and cardiovascular activities. More than 150 ginsenosides had been identified from both Panax ginseng C.A. Meyer (Asian ginseng) and Panax quinquefolius L. (American ginseng) [7]. There are four major groups of ginsenosides, including series of protopanaxadiol, protopanaxatriol, type C and type D [188], with different types/numbers of sugar moieties have been identified [29]. It is known from previous reports that Rb1, Rb2 and Rc represented quantitatively the main components of the protopanaxadiol ginsenosides, whereas Rg1 and Re are the main components of the protopanaxatriol ginsenosides [189]. Rk1, Rg5, Rk2 and Rh3 are the major dehydration metabolites of Rg3 and Rh2, which are the active anticancer component among ginsenosides [19] .

The most challenge to utilize ginsenosides as effective therapeutics is limited by their poor oral bioavailability which may generate large variations among patients. The low oral bioavailability was generally attributed to their poor oral absorption caused by large molecular weight and bulky sugar moieties [18]. Previous studies showed different transport mechanism for ginsenosides, including passive diffusion for most of ginsenosides [18], SGLT1 mediated transport for Rg1 [190], and efflux transporter involved absorption for F1, F2 and Rh2 [3, 18]. However, our previous studies showed that ginsenoside Rh2 had strong P-gp-mediated efflux at in vitro and in vivo [183]. The

significantly variable and even contradictory results of transport mechanism caused ambiguous understanding of their ADME property, which may hold the key for development of ginsenosides as effective therapeutic agents.

In this study, the absorption mechanism of twenty-two ginsensodies including the abundant primary ginsenosides (i.e., Rb1, Rb2, Rc, Rg1, Re), secondary ginsenosides (i.e., Rg3, Rh2, Rg5, Rk1), deglycolated metabolites, (i.e., C-K, F1, F2) and aglycone (PPD, PPT) were investigated in Caco-2 cells. These 22 ginsenosides can represent the ginsenoside family by covering all four major categories (different backbones) with different types/numbers of sugar moieties.

ABC (ATP-binding cassette) transporters, which include P-glycoprotein, MRP family, BCRP, BSEP, Cholesterol transporter have a major impact on drug in vivo disposition. These transporters are not only expressed in multidrug resistance cancer cells but also in many organs such as intestine, liver, kidney and the blood-brain barrier under normal physiological conditions [78]. P-glycoprotein, the most prevalent efflux pump, has 1280 amino acids with molecular weight of 170 kDa. P-gp consists of 12 transmembrane domains and 2 nucleotide binding domain. A recently published mouse P-gp crystal structure revealed an inward facing conformation that is believed to be important for binding substrate along the inner leaflet of the membrane [77].

The penetration of many drugs into the intestine is extensively limited by ABC transporters, including ginsenosides (e.g., Rh2) [183]. A better understanding of

absorption mechanism involved in the transport of ginsenosides, and a more quantitative measurement with regards to if and how efflux transporters affects their bioavailability and potential for drug-drug interaction is important for the development of ginsenosides as chemopreventive agents [68].

In this study, we will continue our efforts to investigate the transport mechanism of various ginsenosides and reveal the possible structure-P-gp mediated transport relationship. Human Caco-2 cells was used to reveal the absorption pattern of ginsenosides and specific chemical inhibitors and P-gp engineered cell lines were used to confirm the role of P-gp in the transport of ginsenosides. In vitro physic-chemical property and molecular docking analysis were used to provide structure explanations for the biological results.

7.3. Materials and Methods

7.3.1. Chemicals and reagents

Ginsenosides Rb_1, (purity > 98%) was purchased from National Institute for the Control of Pharmaceutical and Biological Products (Beijing, China); Rb_2, Rb_3, R_c, R_e, R_d, 20(*S*)-Rg_3, 20(*S*)-Rh_2, (Each purity > 98%) were purchased from Scholarbio-Tech (Chengdu, China). Compound K, F_1, Rg_1, Rg_2, Rh_1, R_1, R_2 and F_2 (Each purity > 98%) were purchased from Must Bio-technology Co. Ltd. (Chengdu, China). Rk_1, Rg_5, Rk_2, Rh_3, PPD and PPT (Each purity > 95%) was prepared in Dr. Zhi-Hong Jiang's lab and identified by high-resolution mass. All chemicals were of analytical grade purity.

7.3.2. Cell culture

The Caco-2 cell culture is routinely maintained in this laboratory for the last 2 decades. Porous polycarbonate cell culture inserts (3 µm) from Corning (6 well plate) were used to seed the cells at a seeding density of 60,000 cells/cm^2. Other conditions such as growth media (Dulbecco's modified Eagle's medium supplemented with 10% fetal bovine serum), and quality control criteria were all implemented according to a previous published report [147] . Caco-2 TC7 cells were fed every other day, and cell monolayers were ready for experiments from 19 to 22 days post-seeding.

MDR1-MDCKII cells were cultured in Dulbecco's modified Eagle's medium supplemented with 10% fetal bovine serum, 1% nonessential amino acids, 100U/ml penicillin and gentamicin. Cell culture was maintained at 5% CO_2 and 90% relative

humidity at 37°C. They were seeded at 2.0×10^6 cells/well into the same cell culture inserts as those used for Caco-2 cells, and fed every day. The MDCKII or MDR1-MDCKII cell monolayers were ready for experiments from 4-5 days post-seeding. The expression levels of MDR1 in MDR1-MDCKII were monitored by western blotting analysis.

7.3.3. Transcellular transport study

The transcellular transport study was performed as described previously [147]. Briefly, 2.5 ml of different ginsenoside solution at 2 or 10 μM was loaded onto one side of the cell monolayer, and 2.5 ml of blank HBSS onto the other side. Five sequential samples (0.5 ml) were taken at different times (0, 1, 2, 3 and 4 hrs) from both sides of the cell monolayer. The same volume of donor solution and receiver medium (fresh HBSS) was added immediately to replace the volume lost because of sampling. The pH values of HBSS in both apical and basolateral side were 7.4.

Both permeability from apical to basolateral side (P_{a-b}) and basolateral to apical side (P_{b-a}) were calculated according to equation 1. Digoxin, a substrate of P-gp, was used as the positive control for the transport study in Caco-2 and MDR1-MDCKII cell monolayers. The efflux ratio was calculated as P_{b-a}/P_{a-b}, which represented the degrees of efflux transporter involvement. In the present study, inhibitors of efflux transporters were only added to the apical side of cell monolayers, regardless of where donor solution was loaded.

Intracellular concentrations of different ginsenosides were determined at the end of a transport study. The protocol for determining intracellular amounts of ginsenosides in cells was the same as those described previously [183]. Briefly, after 4 hours of a transcellular transport study, the cell membranes were rinsed three times with ice-cold HBSS buffer, and cells attached to the polycarbonate membranes were cut off from the inserts with a sharp blade. The latter was immersed into 1 ml HBSS, and sonicated for half an hour at 4°C to break up the cells. The mixture was centrifuged at 15,000 rpm for 15 minutes and 500 µl of the supernatant were recovered and air-dried. The residue were reconstituted with 200 µl methanol and analyzed by UPLC-MS/MS. The protein concentration of cell lysate was measured to normalize the accumulation of various ginsenosides inside the cells using the BCA protein assay kit.

7.3.4. Sample Processing and Quantitative Determination of various ginsenosides

An API 3200 Qtrap® triple quadrupole mass spectrometer (Applied Biosystems/MDS SCIEX, Foster City, CA, USA) equipped with a TurboIonspray™ source was used to perform the analysis of various ginsenosides after eluted from UPLC.

The flow dependent parameters for introduction of the samples to the mass spectrometer ionization source were optimized to stabilize and maximize ion intensity for each ginsenoside, respectively. The quantification was performed using multiple reactions monitoring mode (MRM) with ion pair transitions to monitor various ginsenosides and formononetin (Internal standard). The compound dependent parameters for each ginsenosides were shown in Table 7. UPLC conditions for most of

ginsenosides analysis in positive mode measurement were: system, Waters Acquity™ (Milford, MA, USA) with DAD detector; column, Acquity UPLC BEH C18 column (50×2.1mm I.D., 1.7μm, Waters); mobile phase A, 0.1% formic acid; mobile phase B, 100%, acetonitrile; gradient, 0-0.5 min, 0% B, 0.5-1 min, 0-80% B, 1-2.3 min, 80-95% B, 2.3-2.9 min, 95% B, 2.9-3.2 min, 95-0% B, 3.2-3.7 min, 0% B. UPLC conditions for ginsenosides analysis in negative mode measurement is similar to what was described in positive mode and mobile phase A was water and mobile phase B was methanol. Flow rate, 0.45 ml/min, column temperature, 60 degree; injection volume, 10 μl.

The standard curves of all ginsenosides (except Rb1, Rb2, Rb3 and Rc) were linear in the concentration range of 0.0195-10 μM. The standard curves of Rb1, Rb2, Rb3 and Rc were linear in the concentration range of 0.039-10 μM. The $1/x^2$ weighting was used for quantification. The intra-day and inter-day precision were within 15% for all QC samples at three concentration levels (2.5, 0.3125 and 0.039 μM).

500 μl of HBSS samples taken from transport study were added with 100 μl of internal standard (formononetin, 1 μM) and dried under air. The dry residue was reconstituted in 200 μl of 100% methanol (v/v), and a 10 μl aliquot of the resulting solution was injected into the UPLC-MS/MS system for analysis.

7.3.5. Molecular docking analysis

Molecular docking was employed to explain the effect of sugar moiety on determining whether the ginsenosides are the substrates of P-gp. To this end, we docked all

ginsenosides into the catalytic site of P-gp. These chemical structures were minimized with root mean square gradient of 0.000001 in MOE (Chemical Computing Group, Montreal, CA) based on MMFF94x forcefield and partial charges. The human homology model derived from crystal structure of mouse P-gp (PDB entry code: 3G61)[77] was provided by Dr. Gyorgy M Keseru [191] and used as a template for molecular docking performed by docking program GOLD (CCDC, Cambridge, UK). Hydrogen atoms were added in GOLD and default parameters were used unless otherwise stated. No structural water molecules were observed in the active site and hence all water molecules were deleted. Based on the co-crystal structure of P-gp and inhibitor QZ59, the central coordinates for substrate docking was set as x=18.934, y=55.701 and z=6.456 with searching distance at 20Å. The maximum search efficiency was applied during docking runs. For each ligand, up to 40 top poses were saved and scored with analysis.

7.3.6. Statistical analysis

The data in this paper were presented as means ± S.D., if not specified otherwise. Significance differences were assessed by using Student's t-test or one-way ANOVA. A p value of less than 0.05 was considered as statistically significant.

Table 7. Compound dependent parameters of twenty-two ginsenosides used in LC/MS/MS determination.

ESI(-)	Q1 (m/z)	Q3 (m/z)	Time (ms)	DP (v)	CEP (v)	CE (v)	CXP (v)
Rd	945.0	475.2	100	-93	-49	-72	-3
Rg3	783.6	621.5	100	-94	-37	-38	-4
Rb1	1107.4	783.2	100	-68	-53	-28	-3
Rh2	621.4	160.9	100	-68	-35	-28	-3
PPD	459.4	375.4	100	-81	-36	-36	-4
Rg5	765.0	161.0	100	-101	-35	-46	-1
RK1	765.0	161.0	100	-101	-35	-46	-1
R2	769.0	161.0	100	-115	-31	-53	-1
R1	932.0	638.7	100	-99	-43	-51	-5
Rk2	603.7	161.0	100	-56	-26	-29	-1
Rh3	603.7	161.0	100	-56	-26	-29	-1
Rg2	830.5	784.8	100	-42	-46	-34	-3

ESI(+)	Q1	Q3	Time (ms)	DP (v)	CEP (v)	CE (v)	CXP (v)
F2	807.6	627.5	100	125	50	53	5
CK	645.0	203.0	100	96	32	46	3
F1	661.8	203.0	100	78	32	43	2
Re	970.4	790.7	100	181	62	56	6
PPT	477.4	109.2	100	56	32	47	2
Rc	1078.0	325.1	100	38	45	28	3
Rb2	1102.2	335.2	100	185	54	82	5
Rh1	661.7	203.3	100	92	28	47	2
Rg1	823.8	203.3	100	95	37	55	2
Rb3	1102.2	335.2	100	109	54	78	4

7.4. Results

7.4.1. Transcellular transport of ginsenosides across Caco-2 cell monolayers

7.4.1.1. Impact of four sugar moieties on the absorption mechanism of ginsenosides

Ginsenoside Rb1, Rb2, Rb3 and Rc have four sugar moieties attached to their two hydroxyside groups (each group has two sugar moieties, Table 1). Bidirectional transport study showed that efflux ratio of Rb1, Rb2, Rb3 and Rc were 1.0, 1.1, 1.2 and 1.2, respectively (Table 8). According to FDA guideline for transporter medicated drug-drug interaction, efflux ratio close to 1 indicated that these ginsenosides were mainly transported via passive diffusion (FDA, 2006). The permeability of Rb1, Rb2, Rb3 and Rc were 1.2, 1.4, 2.0 and 3.8×10^{-7} cm/s, respectively at 10 μM and these results were consistent with previous reports that permeability of Rb1 and Rc were between $0.6\sim3\times10^{-7}$ cm/s [18, 192].

After 4 hours incubation in Caco-2 cells, the intracellular concentrations of Rb1, Rb2, Rb3 and Rc were 0.03, 0.03, 0.03 and 0.19 nmol/mg protein. The low intracellular concentration of these ginsenosides indicated they have poor uptake in Caco-2 cells .

7.4.1.2. Impact of three sugar moieties on the absorption mechanism of ginsenosides

Ginsenoside Rd, Re and R1 have three sugar moieties attached to their hydroxyside groups (Table 1). Transport study showed comparable bidirectional permeability and

efflux ratio of Rd, Re and R1 were 1.2, 1.3 and 1.0, respectively. These resutls indicated that they were mainly transported via passive diffusion. The permeability of Rd, Re and R1 were 5.5, 5.5 and 4.7×10^{-7} cm/s, significantly higher than the values of ginsenosides with four sugar moieties (Table 8).

After 4 hours incubation in Caco-2 cells, the intracellular concentrations of Rd, Re and R1 were 0.11, 0.17 and 0.12 nmol/mg protein, which were also significantly higher than Rb1, Rb2 and Rb3. Both increased permeability and intracellular concentration showed that sugar number may determine the absorption rate and extent.

7.4.1.3. Impact of two sugar moieties on the absorption mechanism of ginsenosides

Ginsenoside Rg3, F2, Rg1, R2, Rg5, Rk1 and Rg2 have two sugar moieties attached to their hydroxyside groups (Table 1). For F2 and Rg1, each –OH group is attached to one glucose while for the other five ginsenosides (Rg3, R2, Rg5, Rk1 and Rg2), only one –OH group is attached to two sugar moieties. Bidirectional transport study showed that efflux ratio of Rg3, F2, Rg1, R2, Rg5, Rk1 and Rg2 were very different at 2.0, 131, 1.7, 1.5, 2.1, 2.2 and 1.0, respectively. Accodring to FDA guideline, A net flux ratio over 2 is considered a positive result indicating the probe substrate has weak efflux whereas the net flux ratio over 5 is considered a strong efflux. These resutls showed that transport of Rg3, Rg1, Rg5, Rk1 and F2 may be mediated by efflux transporters and the efflux transport could signficantly affect the absorption of F2 as its efflux was more than 100. Although the efflux ratio of Rg1 was less than 2 (ER=1.7), its secretive permeability was

significantly higher than absorptive permeability, indicating the role of efflux transporter for absorption (Table 8). The permeability of Rg3, F2, Rg1, R2, Rg5, Rk1 and Rg2 were 10.0, 0.9, 2.3, 1.4, 1.9, 7.7 and 4.3×10^{-7} cm/s, respectively. The much lower permeability of F2 was possibly due to extensive efflux observed in Caco-2 cells.

After 4 hours incubation in Caco-2 cells, the intracellular concentrations of Rg3, F2, Rg1, R2, Rg5, Rk1 and Rg2 were very different at 0.29, 0.14, 0.03, 0.01, 0.04, 0.05 and 0.01 nmol/mg protein. The resutls showed the uptake varied greatly with similar sugar numbers.

7.4.1.4. Impact of one sugar moiety on the absorption mechanism of ginsenosides

Ginsenoside Rh2, C-K, F1, Rh1, Rh3 and Rk2 have only one sugar moiety attached to hydroxyside group (Table 1). Bidirectional transport study showed that efflux ratio of Rh2, C-K, F1 and Rh1 (protopanaxadiol and protopanaxatriol series) were much higher than 1 at 28.5, 26.6, 43.2 and 38.7, respectively whereas the efflux ratio of Rh3 and Rk2 (type C and D) were close to 1 at 1.0 and 1.5, respectively (Table 8). These resutls showed interesting trend that ginsenosides with one sugar moiety in protopanaxadiol and protopanaxatriol series was absorbed via transporter mediated mechanism. The permeability of Rh2, C-K, F1, Rh1, Rh3 and Rk2 were 0.37, 1.16, 0.29, 0.22, 0.35 and 0.29×10^{-6} cm/s, respectively. The much lower permeability of F2 was due to extensive efflux observed in Caco-2 cells.

After 4 hours incubation in Caco-2 cells, the intracellular concentrations of Rh2, C-K, F1, Rh1, Rh3 and Rk2 were very different at 0.14, 0.01, 0.03, 0.02, 0.12 and 0.05 nmol/mg protein. The resutls showed the uptake varied greatly with similar sugar numbers and we did not observe significantly increased uptake compared to ginsenosides with two sugar moieties.

7.4.1.5. The absorption mechanism of ginsenoside aglycone

Protopanaxadiol and protopanaxatriol are the ginsenoside aglycone (Table 1). Bidirectional transport study showed that efflux ratio of Protopanaxadiol and protopanaxatriol were 1.2 and 0.9, respectively. These results indicated absorption of ginsenoside aglycone may via passive diffusion. The permeability protopanaxadiol and protopanaxatriol were 1.94 and 3.06×10^{-6} cm/s, respectively (Table 8). They were significantly higher than the other ginsenosides as shown above.

After 4 hours incubation in Caco-2 cells, the intracellular concentrations of protopanaxadiol and protopanaxatriol were 1.06 and 0.40 nmol/mg protein, respectively. The resutls showed the uptake of ginsenoside aglycone were much higher than the other ginsenosides.

Table 8. Transcellular transport of twenty-two ginsenosides across monolayers of Caco-2 cells at 2 or 10 μM.

Ginsenosides	Sugar moieties	Concentrations (μM)	P_{a-b} ($\times 10^{-6}$ cm/s)	P_{b-a} ($\times 10^{-6}$ cm/s)	Efflux ratio (P_{b-a}/P_{a-b})	Intracellular amounts (nmol/mg)
Rb1	4 (2+2)	10	0.12 ± 0.03	0.12 ± 0.04	1.0	0.03 ± 0.01
Rb2	4 (2+2)	10	0.14 ± 0.08	0.15 ± 0.11	1.1	0.03 ± 0.01
Rb3	4 (2+2)	10	0.20 ± 0.04	0.24 ± 0.06	1.2	0.03 ± 0.01
Rc	4 (2+2)	10	0.38 ± 0.07	0.47 ± 0.42	1.2	0.19 ± 0.03
Rd	3 (2+1)	10	0.87 ± 0.14	1.05 ± 0.55	1.2	0.11 ± 0.04
Re	3 (2+1)	10	0.55 ± 0.08	0.70 ± 0.26	1.3	0.17 ± 0.02
R1	3 (2+1)	10	0.47 ± 0.26	0.46 ± 0.25	1.0	0.12 ± 0.01
Rg3	2 (2+0)	2	0.99 ± 0.09	2.01 ± 0.27*	2.0	0.29 ± 0.05
F2	2 (1+1)	2	0.09 ± 0.09	11.50 ± 1.23***	131	0.14 ± 0.04
Rg1	2 (1+1)	2	0.23 ± 0.05	0.39± 0.07*	1.7	0.03 ± 0
R2	2 (0+2)	2	0.14 ± 0.05	0.21 ± 0.04	1.5	0.01 ± 0
Rg5	2 (2+0)	2	0.19 ± 0.06	0.40 ± 0.08*	2.1	0.04 ± 0.01
Rk1	2 (2+0)	2	0.77 ± 0.33	1.66 ± 0.08*	2.2	0.09 ± 0.01
Rg2	2 (2+0)	2	0.43 ± 0.11	0.41 ± 0.26	1.0	0.04 ± 0.01
Rh2	1 (1+0)	2	0.37±0.01	10.66±1.74***	28.5	0.14 ± 0.02
CK	1 (0+1)	2	1.16 ± 0.33	30.96 ± 4.31***	26.6	0.01 ± 0
F1	1 (0+1)	2	0.29 ± 0.04	12.41 ± 0.58***	43.2	0.03 ± 0
Rh1	1 (1+0)	2	0.22 ± 0.05	8.33 ± 1.36***	38.7	0.02 ± 0
Rh3	1 (1+0)	2	0.35 ± 0.03	0.36 ± 0.20	1.0	0.12 ± 0.04
Rk2	1 (1+0)	2	0.29 ± 0.04	0.43± 0.17	1.5	0.05 ± 0.02
Protopanaxadiol	0	2	1.94 ± 0.06	2.26 ± 0.06	1.2	1.06 ± 0.27
Protopanaxatriol	0	2	3.06 ± 1.40	2.84 ± 1.40	0.9	0.40 ± 0.07

"P_{a-b}" refers to the permeability from apical to basolateral and "P_{b-a}" refers to the permeability from basolateral to apical side. "P_{a-b}" were compared to "P_{b-a}" to show the polarized transport. Data are the means ± S.D. of three independent experiments.

– indicated no inhibitor; * indicated $p<0.05$; ** indicated $p<0.01$; *** indicated $p<0.001$.

S configuration was used when ginsenosides have both S and R configurations due to better solubility and bioactivity.

7.4.2. Effect of chemical inhibitors on the transport of ginsenosides in Caco-2 cells

Rg1, Rh2, C-K, Rg3, Rg5, Rk1, F1, F2 and Rh1 showed significantly higher secretive permeability than absorptive permeability, which indicated that efflux transporter(s) were invovled. In order to investigate which transporter(s) were responsible for their dispositions, different chemical inhibitors were used in transport models.

7.4.2.1. Effect of inhibitors on the transport of F1

Transcellular transport of F1 (2 μM) across Caco-2 monolayer from basolateral (B) to apical (A) side was significantly higher than the transport from A to B side, and the efflux ratios (P_{b-a} /P_{a-b}) were 43.2. Use of two MDR1/P-gp inhibitors alone at the apical side, 50 μM verapamil or 20 μM cyclosporine A, was able to significantly inhibit the efflux transport of F1, and the efflux ratio was decreased to 8.3 and 1.3, respectively. Use of MRP inhibitor, MK571 did not change the efflux ratio of F1 while treatment of BCRP inhibitor, KO143 decreased the efflux ratio from 43.2 to 16.5 (Table 9) indicating BCRP may mediate its absorption. Stigmaterol and sitosterol were used as competitive inhibitors of ABCG5/G8, but they did not change the permeability or intracellular concentrations of F1. Similarly, treatment of troglitezone or rifamcie (inhibitor of BSEP) did not change the permeability or intracellular concentrations of F1 either, indicating BSEP may not be responsible for F1 transport.

7.4.2.2. Effect of inhibitors on the transport of F2

Transcellular transport of F2 (2 µM) across Caco-2 monolayer showed substantially polarized transport, and the efflux ratios (P_{b-a} /P_{a-b}) were 131. Use of two MDR1/P-gp inhibitors alone at the apical side, 50 µM verapamil or 20 µM cyclosporine A, was able to significantly inhibit the efflux transport of F2, and the efflux ratio was decreased to 37.8 and 1.5, respectively. Use of MK571 (MRP inhibitor) and KO143 (BCRP inhibitor) decreased the efflux ratio of F2 from 131 to 30.4 and 35.3 (Table 9) indicating MRP and BCRP may play a minor role for F2 transport. 20 µM of stigmaterol and sitosterol did not change the permeability or intracellular concentrations of F2. Similar to F1, treatment of 50 µM of troglitezone or rifamcie did not change the permeability or intracellular concentrations of F1 either, indicating BSEP may not be responsible for F2 transport.

Table 9. Transcellular transport of ginsenoside F1 and F2 at 2 μM across monolayers of Caco-2 cells in the absence or presence of different inhibitors.

Ginsenosides	Inhibitor	Inhibitor Concentrations (μM)	P_{a-b} ($\times 10^{-6}$ cm/s)	P_{b-a} ($\times 10^{-6}$ cm/s)	Efflux ratio (P_{b-a}/P_{a-b})	Intracellular amounts (nmol/mg)
F1	-	-	0.29 ± 0.04	12.41 ± 0.58***	43.2	0.03 ± 0
	Verapamil	50	0.10 ± 0.02	0.83 ± 0.08**	8.3	0.01 ± 0.01
	Cyclosporine A	20	1.01 ± 0.29*	1.32 ± 0.21	1.3	0.03 ± 0
	MK571	50	0.17 ± 0.07	6.99 ± 1.60	42.3	0.01 ± 0
	KO143	5	0.41 ± 0.52	6.70 ± 3.40	16.5	0.01 ± 0
	Stigmaterol+sitosterol	20+20	0.23 ± 0.01	-	NA	0.01 ± 0
	Troglitezon	50	0.23 ± 0.05	-	NA	0.01 ± 0
	Rifamcin	50	0.32 ± 0.07	-	NA	0.01 ± 0
F2	-	-	0.09 ± 0.09	11.50 ± 1.23	131	0.01 ± 0
	Verapamil	50	0.13 ± 0.03	4.75 ± 0.83**	37.8	0.02 ± 0.01
	Cyclosporine A	20	1.98 ± 0.47**	2.96 ± 0.27**	1.5	0.19 ± 0.03*
	MK571	50	0.71 ± 0.19*	22.0 ± 6.61	30.4	0.03 ± 0.01*
	KO143	5	1.30 ± 1.20	45.0 ± 21.1	35.3	0.03 ± 0.01*
	Stigmaterol+sitosterol	20+20	0.22 ± 0.04	-	NA	0.01 ± 0
	Troglitezon	50	0.22 ± 0.04	-	NA	0.01 ± 0
	Rifamcin	50	0.15 ± 0.05	-	NA	0.02 ± 0.01

"P_{a-b}" refers to the permeability from apical to basolateral and "P_{b-a}" refers to the permeability from basolateral to apical side. Permeability and intracellular amounts were compared to control group. Data are the means ± S.D. of three independent experiments.

* indicated $p<0.05$; ** indicated $p<0.01$; *** indicated $p<0.001$.

"-"means experiments were not performed. "NA" not available.

7.4.2.3. Effect of P-gp inhibitors on the transport of Rh1, Rg3, Rg5 and Rk1

Transcellular transport of Rh1 (2 µM) across Caco-2 monolayer from basolateral (B) to apical (A) side was significantly higher than the transport from A to B side, and the efflux ratios (P_{b-a} /P_{a-b}) were 38.7. Use of MDR1/P-gp inhibitor, 20 µM cyclosporine A, was able to completely inhibit the efflux transport of Rg3 by decreasing the efflux ratio to 1.3 (Table 10).

Similarly, the efflux ratios of Rg3 (2 µM) were 2.0 and use of MDR1/P-gp inhibitor, 50 µM verapamil, was able to completely inhibit the efflux transport of Rg3 by decreasing efflux ratio to 1 (Table 10). As expected, we found the consistent results for Rg5 and Rk1 that 50 µM verapamil was able to completely inhibit their efflux in Caco-2 cells by decreasing efflux ratios from 2.1 to 1.1 and 2.2 to 0.9, respectively (Table 10), indicating the role of P-gp for their in vitro disposition.

7.4.2.4. Effect of cyclosporine A on the transport of non-substrate of P-gp

Transcellular transport of Rb1 and Rd in the presence of cyclosporine A was investigated to see whether cyclosporine A, which we used as P-gp inhibitor, had any additional effect on non-substrate of P-gp to cause false positive inhibition results. The results showed that 20 µM of cyclosporine A did not change permeability, efflux ratio and intracellular concentration of Rb1 and Rd (Table 10) indicating that 20 µM of cyclosporine A had no effect on passive diffusion.

Table 10. Transcellular transport of ginsenoside Rh1, Rg3, Rg5, Rk1, Rb1 and Rd across monolayers of Caco-2 cells in the absence or presence of cyclosporine A or verapamil.

Ginsenosides	Ginsenosides Concentrations (μM)	Sugar moieties	Inhibitor	Inhibitor Concentrations (μM)	P_{a-b} ($\times 10^{-6}$ cm/s)	P_{b-a} ($\times 10^{-6}$ cm/s)	Efflux ratio (P_{b-a}/P_{a-b})	Intracellular amounts (nmol/mg)
Rh1	2	1 (1+0)	-	-	0.22 ± 0.05	8.33 ± 1.36	38.7	0.02 ± 0
			Cyclosporine A	20	1.02 ± 0.31**	1.38 ± 0.12**	1.3	0.06 ± 0.01*
Rg3	2	2 (2+0)	-	-	0.99 ± 0.09	2.01 ± 0.27	2	0.28 ± 0.05
			Verapamil	50	1.90 ± 0.47*	1.75 ± 0.54	0.9	0.30 ± 0.05
Rg5	2	2 (2+0)	-	-	0.19 ± 0.06	0.40 ± 0.08	2.1	0.04 ± 0.01
			Verapamil	50	0.20 ± 0.09	0.21 ± 0.08*	1.1	0.12 ± 0.09
Rk1	2	2 (2+0)	-	-	0.77 ± 0.33	1.66 ± 0.08*	2.2	0.09 ± 0.01
			Verapamil	50	0.93 ± 0.33	0.86 ± 0.44	0.9	0.13 ± 0.07
Rb1	10	4 (2+2)	-	-	0.12 ± 0.03	0.12 ± 0.04	1.0	0.03 ± 0.01
			Cyclosporine A	20	0.14 ± 0.06	0.13 ± 0.01	0.9	0.04 ± 0.01
Rd	10	3 (2+1)	-	-	0.87 ± 0.14	1.05 ± 0.55	1.2	0.11 ± 0.04
			Cyclosporine A	20	0.67 ± 0.13	0.83 ± 0.01	1.2	0.07 ± 0.01

"P_{a-b}" refers to the permeability from apical to basolateral and "P_{b-a}" refers to the permeability from basolateral to apical side. Permeability and intracellular amounts were compared to control group. Data are the means ± S.D. of three independent experiments.

* indicated $p<0.05$; ** indicated $p<0.01$; *** indicated $p<0.001$.

7.4.3. Transcellular transport of Rh2, C-K, F1, Rh1, F2 and Rg1 in WT and MDR1-MDCKII cells

Human MDR1/P-gp over-expressing MDCKII cells were used to confirm the predominant role of P-gp in the transport of F1, Rh1, F2 and Rg1. The permeability from basolateral (B) to apical (A) side was significantly higher than the transport from A to B side in MDR1-MDCKII cells. The efflux ratios of F1, Rh1, F2 and Rg1 at 2 μM were 6.4, 4.8, 2.6 and 2.5, respectively. The transport study were also performed in parental MDCKII cells and showed similar but lesser extent efflux with the efflux ratios of F1, Rh1, F2 and Rg1 at 3.0, 2.8, 2.0 and 1.6, respectively (Table 11). Consistently, the intracellular accumulations of F1, Rh1, F2 and Rg1 were significantly higher (4.0, 3.9, 2.0 and 4.1 fold) in parental MDCKII cells than in MDR1-MDCKII cells, which confirmed the role of P-gp in the uptake of F1, Rh1, F2 and Rg1 in MDCKII cells.

Table 11. Transcellular transport of ginsenosides Rh2, C-K, F1, Rh1 and F2 across monolayers of MDR1-MDCKII cells.

Cell models	Ginsenosides	Sugar moieties	Concentrations (μM)	P_{a-b} ($\times 10^{-6}$ cm/s)	P_{b-a} ($\times 10^{-6}$ cm/s)	Efflux ratio (P_{b-a}/P_{a-b})	Intracellular amounts (nmol/mg)
WT- MDCKII	[a]Rh2	1 (1+0)	2	4.97 ± 0.69	11.97 ± 2.40	2.4	0.25 ± 0.09
MDR1- MDCKII				0.68 ± 0.21*	19.16 ± 4.92	28.0	0.03 ± 0.02*
WT- MDCKII	[a]C-K	1 (0+1)	2	0.58 ± 0.12	1.13 ± 0.11	1.8	0.27 ± 0.03
MDR1- MDCKII				1.84 ± 0.70	33.64 ± 8.08**	18.2	0.08 ± 0.01*
WT- MDCKII	F1	1 (0+1)	2	0.30 ± 0.07	0.90 ± 0.04	3.0	0.08 ± 0.03
MDR1- MDCKII				0.14 ± 0.04*	0.89 ± 0.15	6.4	0.02 ± 0.01*
WT- MDCKII	Rh1	1 (1+0)	2	0.28 ± 0.07	0.77 ± 0.13	2.8	0.08 ± 0.01
MDR1- MDCKII				0.25 ± 0.07	1.17 ± 0.16	4.8	0.02 ± 0.01*
WT- MDCKII	F2	2 (1+1)	2	0.27 ± 0.10	0.54 ± 0.23	2.0	0.41 ± 0.08
MDR1- MDCKII				1.94 ± 0.79	5.07 ± 0.75	2.6	0.21 ± 0.08*
WT- MDCKII	Rg1	2 (1+1)	2	1.39 ± 0.38	2.28 ± 1.12	1.6	0.19 ± 0.08
MDR1- MDCKII				0.92 ± 0.30	2.33 ± 0.37	2.5	0.05 ± 0.02*

"P_{a-b}" refers to the permeability from apical to basolateral and "P_{b-a}" refers to the permeability from basolateral to apical side. Permeability and intracellular amounts were compared to control group. Data are the means ± S.D. of three independent experiments.

* indicated $p<0.05$; ** indicated $p<0.01$; *** indicated $p<0.001$.

[a] indicated that these results has been presented in previous chapter.

7.4.4. Molecular Docking Analysis

We used molecular docking to assess the possible binding sites for ginsenosides Rh2 and C-K, which were shown as good substrate of P-gp. Literature reports showed hydrophobic interaction is important for ligand binding due to hydrophobic and aromatic residues found in P-gp binding pocket [191, 193, 194]. Based on the pose which had best score (lowest binding energy), both ginsenosides Rh2 and C-K (pink) showed possible binding residues on Phe 303, Phe 336, Phe 343, Phe 728 and Phe 994 (yellow) and these residues showed less than 4Å interacting distance for hydrophobic interaction . Considering the hydrophilic end of sugar moieties, hydrogen bond interaction was also found in the binding pocket. Asn 72, Glu 725 and Glu 990 (yellow) showed ~3.2 Å distance (typical hydrogen bond interaction distance) with the glucose of ginsenosides Rh2 and C-K (pink) and these residues indicated the possible hydrogen bond interaction (Figure 17).

A

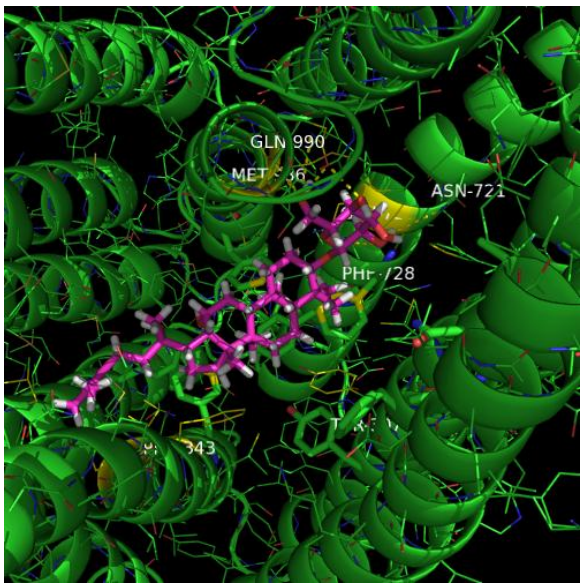

B

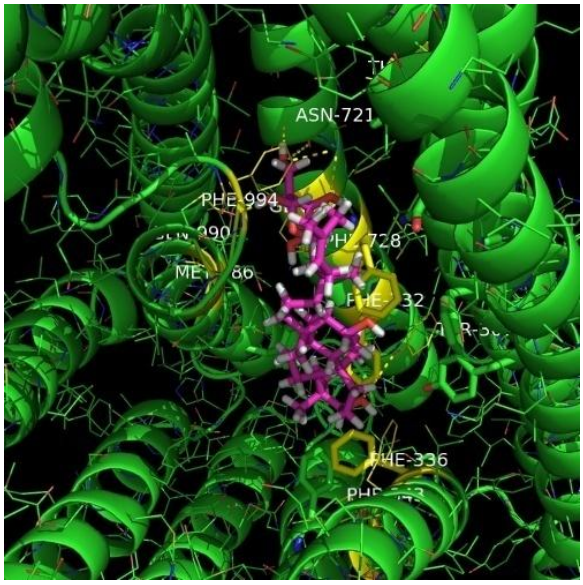

Figure 17. The best docking pose of Rh2 (A) and C-K (B) with human P-gp homology model derived from mouse P-gp (3G61).

7.5. Discussion

We have investigated the absorption mechanism of twenty-two ginsenosides using human Caco-2 cells. The results showed that the absorption mechanism was structure-dependent, and sugar moieties had significant role on determining the permeability and efflux mechanism of ginsenosides. Our results showed that all the ginsenosides with 3 or 4 sugar moieties as well as aglycones (PPD and PPT) exhibited comparable bidirectional permeability in Caco-2 cells, similar to those observed by Liu and co-workers [18], indicating passive diffusion was major transport mechanism for these ginsenosides. However, our results have shown significantly polarized transport for nine ginsenosides with 1 or 2 sugar moieties including Rh2, C-K, Rg3, Rg5, Rk1, F1, F2, Rg1 and Rh1, which were different from their report, who showed no significant efflux except F1 and F2 [18]. The discrepancy may due to different expression level of transporters in Caco-2 cells among laboratories and/or high substrate concentration (up to 50 μM) they used which may not be soluble or saturate efflux. Therefore, in our study, 2 μM of ginsenosides (maximum 10 μM) were used in cell transport study to eliminate the possible saturation and inhibition for potential transporters.

Nine ginsenosides showed polarized transport in Caco-2 cells indicating the possible roles of efflux transporters on their in vivo disposition. Considering much higher efflux ratio of Rh2, C-K, F1, Rh1 and F2 (ER>20) in Caco-2 cells, the efflux transporter may severely affect their in vivo pharmacokinetics including absorption, disposition and eliminations.

All these ginsenosides had promising clinical usage due to their potent pharmacological effects. Ginsenoside Rh2 has already been used as anticancer drugs in china (SHENYI® capsule) and C-K displayed potent chemoprevention and anticancer activities in various cancer cell lines [178, 179]. Rh1 is a bioreductive agent showed potent anticancer activity via induction of apoptosis [195, 196] and is currently in clinical trials [197]. F1 was the major metabolites of Rg1, which is the abundant component in ginseng showed potent antitumor activity [198]. F2 was the main hydrolysis product of Rb1 after oral administration [176, 177].

Efflux ratio of ginsenosides in MDR1-MDCKII cells showed different substrate affinity to P-gp, which may indicate the important structure requirement for binding with P-gp. In protopanaxadiol series, Rh2 showed the highest efflux ratio (28.0) with one glucose attached to C-3 position, followed by C-K (ER=18.2) with one glucose attached to C-20 position. When both C-3 and C-20 positions were occupied by one glucose (F2), the efflux ratio was decreased to 2.6. If two glucoses attached in C-3 position, the efflux ratio was also decreased to 2.0, indicating large size may impede its binding to P-gp. PPD (aglycone), Rd (three glucose) and Rb1, Rb2, Rb3 and Rc (four sugars) were non substrates of P-gp based on efflux ratio obtained in Caco-2 cells. These results suggested the rank order of binding affinity with P-gp in PPD series was one glucose (C-3) > one-glucose (C-20) > one-glucose (at both C-3 and C-20)$\geqslant$ two-glucose (C-3) >no glucose= three glucoses= four sugars .

Similarly, in protopanaxatriol series, F1 showed the highest efflux ratio (6.4) with one glucose attached to C-20 position, followed by Rh1 (ER=4.8) with one glucose attached to C-6 position. When both C-6 and C-20 positions were occupied by one glucose (Rg1), the efflux ratio was decreased to 2.5. PPT (aglycone), R2 (two sugars), Rg2 (two sugars) R1 (three sugars) and Re (three sugars) were non substrates of P-gp based on efflux ratio obtained in Caco-2 cells. Therefore, these results suggested the binding affinity with P-gp in PPT series was one-glucose (C-20) > one-glucose (C-6) > one-glucose (at both C-6 and C-20)> no glucose= two sugars=three sugars. It is noted that the substrate affinities of PPT series were lower than PPD series.

Based on the results obtained in both PPD and PPT series, one or two sugar moieties, especially glucose appear to hold the key structure as recognized by P-gp. In order to test our hypothesis, ginsenosides Rk1, Rg5, Rk2 and Rh3 with one or two glucose in type C and type D were chosen for this purpose. They are the major active dehydration metabolites of Rg3 and Rh2, and have similar structure with PPD series with double bond formed in side chain. However, we found different rank order for P-gp binding that Rg5 and Rk1 (two-glucose in C-3) > Rh3 and Rk2 (one-glucose in C-3). The discrepancy may be explained by high lipophilicity of Rh3 and Rk2 (Log P=5). Partition coefficient (Log P values) has good correlation with the substrates of P-gp. Nine ginsenosides which showed to be substrates of P-gp have Log P values ranging from 2.2 to 4.0, except Rg1 (Log P=1.1). The best ginsenosides Rh2 and Ck showed very similar Log P values at 3.9 and 4.0, respectively. The other thirteen ginsenosides which were non P-gp substrates showed Log P values either less than 2.2 or higher than 4.6

(Table 12). Too lipophilic or hydrophilic compounds cannot get into the binding site of P-gp based on many experimental results and computational modeling [199].

The current docking analysis of Rh2 and C-K provided possible binding residues for ginsenosides. Hydrophobic interaction was still the major interaction for P-gp substrates while sugar moieties provide a good balance between molecular size and decent octanol-water partition coefficient. It is noted that due to large and multiple binding sites for different substrates and relatively poor resolution of the crystal structure of mouse P-gp (4.3 Å), the current molecular docking model cannot accurately differentiate substrate or non-substrate among ginsenosides and expert knowledge is required to analyze the docking results of each compound and interpreted the modeling data (substrate or non-substrate) case by case.

Although Rg1 did not show high efflux ratio in Caco-2 cells (ER=1.7), secretive permeability (B to A) was significantly higher than its absorptive permeability (A to B). MDR1-MDCKII cells confirmed the role of P-gp by showing significantly polarized transport (ER>2), and higher intracellular concentration in WT compared to MDR1-MDCKII cells. F1, Rh1 and F2 showed much higher efflux ratio in Caco-2 than MDR1-MDCKII cells indicating that P-gp may not be the only transporter involved. In order to identify the possible involved transporters, we used chemical inhibitors of MRP (MK571), BCRP (KO143), ABCG5/G8 (sterols) and BSEP (Troglitezon and Rifamcin). These five apically expressed ABC transporters was the major efflux transporters expressed in Caco-2 TC7 cells we used and have significant pharmacokinetic effects based on our best knowledge [83, 200]. The results showed that BCRP may be involved for the

transport of F1 and F2, and further studies are needed to identify the other possible transporters. Therefore, multiple transporters may control the disposition of these ginsenosides in vivo.

We found that 20 μM cyclosporine A can completely inhibit the efflux of F1, F2 and Rh1 by decreasing the efflux ratio to ~1. It may due to its broad inhibitory effects on BCRP and ATPase [117, 201, 202]. We further tested the effects of cyclosporine A on non-substrates of P-gp, Rb1 and Rd. The results showed their permeability and the efflux ratio was not changed indicating no addition effect on Caco-2 cells (i.e., integrity of cell membrane) in the presence of cyclosporine A. These results further demonstrated that inhibition of efflux transporter can significantly inhibit its in vitro efflux. Our previous study demonstrated that inhibition of P-gp by cyclosporine A can significantly increase oral bioavailability of Rh2 [183].

In summary, ginsenosides showed structure-dependent P-glycoprotein-mediated efflux mechanism. Ginsenosides with one or two glucose are most likely substrates of P-gp due to suitable binding interaction and favorable lipophilicity, while aglycone, three or four sugars were majorly transported via passive diffusion. These studies greatly improved the previous understanding on absorption and disposition of ginsenosides and revealed structure-P-gp efflux relationship among ginsenosides which may provide valueable information on drug-drug interaction for rapidly growing researches on ginsenosides' clinical trial.

Table 12. Octanol-water partition coefficient of various ginsenosides.

Ginsenosides	Sugar numbers	Efflux ratio	Log P
Rb1	4	1.0	-1.198
Rb2	4	1.1	-0.688
Rb3	4	1.2	-0.438
Rc	4	1.2	-0.688
Rd	3	1.2	-0.621
Re	3	1.3	0.267
R1	3	1.0	1.092
Rg3s	2	2.0*	2.295
F2	2	131*	2.222
Rg1	2	1.7*	1.126
R2	2	1.5	1.637
Rg5	2	2.1*	3.307
Rk1	2	2.2*	3.315
Rg2	2	1.0	2.264
Rh2s	1	28.5*	4.042
CK	1	26.6*	3.969
F1	1	43.2*	2.94
Rh1	1	38.7*	2.873
Rh3	1	1.0	5.008
Rk2	1	1.5	5.062
PPD	0	1.2	5.789
PPT	0	0.9	4.62

The Log P values were predicted by Discovery Studio.
"*" indicated that efflux ratios were significantly higher than 1 (absorptive permeability were significantly lower than secretive permeability).

Enhancement of Oral Bioavailability of Ginsenosides Rh2 and Compound K via P-Glycoprotein Inhibition by a Combination of Biochanin A, Piperine and Wogonin

8.1. Abstract

The purpose of this study is to improve oral bioavailability of ginsenosides Rh2 and Compound K (C-K) via inhibition of P-glycoprotein (or P-gp) by using natural products previously shown to be active against P-gp. The effects of combinational natural products on the functions of P-glycoprotein were investigated based on P-gp mediated transport of affected ginsenosides across Caco-2 cell monolayers. Among eight groups of natural compound mixture, the combination of biochanine A, wogonin and piperine (BWP) at 50 μM showed the highest P-gp inhibitory effect. BWP decreased the efflux ratio of Rh2 from 28.5 to 4.5. Consistently, the permeability and intracellular accumulation of Rh2s increased 8.0 and 8.1 fold after the same treatment, respectively. However, individual compounds (i.e., biochanin A, wogonin and piperine) did not significantly improve the absorptive transport of Rh2 across the Caco-2 cell monolayers. This combination showed similar inhibitory effect on ginsenoside C-K, another P-gp substrate, by decreasing its efflux ratio from 26.6 to 8.9 and increasing its intracellular accumulation and permeability by 70.5 and 2.9 fold, respectively. In vivo pharmacokinetic studies in A/J mice showed that the plasma $AUC_{0-\infty}$ of Rh2s and C-K were substantially increased by 6.0 and 4.2 fold, respectively, after coadministration of BWP at 50 mg/kg. In addition, the elimination rate constant of Rh2s and C-K was substantially decreased, by 71% and 80%, respectively. In conclusion, concomitant

administration of biochanine A, wogonin and piperine significantly increased oral bioavailability of ginsenoside Rh2s and C-K via increased volume of distribution of ginsenosides, likely via the inhibition of P-glycoprotein.

Key words: ginsenosides Rh2, ginsenosides C-K, efflux, P-glycoprotein, natural product, pharmacokinetics, oral bioavailability.

8.2. Introduction

Ginsenosides are the active components responsible for various pharmacological and therapeutical effects in both Asian ginseng and American ginseng. Ginsenosides Rh2s and C-K are the most studied ginsenosides for cancer treatment and/or prevention since they displayed potent anticancer activities in various cancer cell lines and in preclinical animal models [1, 33, 163] . Coadministration of Rh2 with other anticancer drugs (i.e., doxetaxel and palicataxel) could significantly increase their therapeutical effect [203, 204]. Although C-K has low abundance in the raw ginseng or ginseng extract, it is the major metabolite of protopanaxadiol ginsenosides after oral administration and represents the active component in vivo [177, 205]. The chemoprevention and anticancer mechanism of ginsenoside Rh2s and C-K include antioxidant chemoprevention [206], antimetastatic effect [207] induction of apoptosis via G1 phase arrest [33, 178], suppression of NF-kB pathway activation [180], and inhibition of mutagenicity [181] as well as positive or stimulative immunomodulation [12].

Our previous study showed that ginsenosides Rh2 and C-K are the substrates of P-glycoprotein (or P-gp), and P-gp-mediated efflux is the major reason causing their low oral bioavailability (<5%) [45, 46, 183]. Low oral bioavailability greatly limited in vivo efficacy of ginsenosides, especially on chemoprevention activity. Inhibition of P-gp leads to the improvement of oral bioavailability and CNS penetration of anticancer drugs [208].

A literature search for possible P-gp inhibitors to block its activity had led to three generations of promising candidates. The first-generation of P-gp inhibitors including

verapamil and cyclosporine A, showed significant toxicity and low potency [136, 137], which lead to chemical synthesis of the second-generation of P-gp inhibitors (i.e., PSC-833) with improved potency but not negligible toxicity [209]. The third-generation of P-gp inhibitors (i.e., GF120918 and LY335979), were developed to overcome these limitations with high potency and specificity as well as minimal pharmacokinetic interactions [210]. Unfortunately, none of these inhibitors had been approved for clinical use due to insignificant improvement in the survival time of cancer patients when coadministrated with anticancer drugs. A recently published mouse P-gp crystal structure revealed that P-gp has poly-specific drug-binding sites [77], which may help developing SAR for effective P-gp inhibitors.

In the last ten years, the searching for potent P-gp inhibitors among natural compounds and its derivatives has been very productive [211], and the hits generated were considered as the fourth generation of P-gp reversing agents [138]. However, the potency of P-gp inhibition by natural compounds are generally low (i.e., high micromolar) and therefore individual compounds is unlikely to be developed as clinical modulators for P-gp activity [212]. Derived from the success examples of several drug combination medications (i.e., combivir), the combinations of natural compounds were proposed to have additive or synergistic effect to achieve desirable inhibitory effect [213]. Our previous study using first generation inhibitor, cyclosporine A, successfully increased the oral bioavailability of ginsenoside Rh2 [183] and we will continue our efforts to enhance oral bioavailability of ginsenosides with less pharmacologically active compound suitable for long-term clinical use. Therefore, the aims of this study were to

identify the most potent combination of natural compounds for P-gp inhibition and utilize this approach to increase the oral bioavailability of ginsenosides Rh2s and C-K.

8.3. Materials and Methods

8.3.1. Chemicals and reagents

Ginsenoside 20(*S*)-Rh_2, (purity > 98%) was purchased from Scholarbio-Tech (Chengdu, China). Compound K (purity > 98%) were purchased from Must Bio-technology Co. Ltd. (Chengdu, China). Quercetin, resveratrol, kaempferol, biochanin A, wogonin, piperine, baicalein, 7,8 benzoflavone, hesperidin, acacetin, glycyrrhetinic acid, galangin, EGCG, ursonic acid, chrysin, formononetin, phloretin, auraptene, nobiletin, morin, hesperitin, silymarin, silibin, curcumin and capsanthin were purchased from Indofine.Inc (Hillsborough, NJ) or LC Laboratory (Woburn, MA). Digoxin, cyclosporine A, verapamil and Hanks' balanced salt solution (powder form) were purchased from Sigma-Aldrich (St. Louis, MO). Oral suspension vehicle was obtained from Professional Compounding Centers of America (Houston, TX). All other chemicals used were of analytical grade or better.

8.3.2. Cell culture

The Caco-2 cell culture is routinely maintained in this laboratory for the last 2 decades. The culture conditions for growing Caco-2 cells were the same as those described previously [147]. Porous polycarbonate cell culture inserts (3 µm) from Corning (Catalog No: 3414) were used to seed the cells at a seeding density of 60,000 cells/cm^2. Other

conditions such as growth media (Dulbecco's modified Eagle's medium supplemented with 10% fetal bovine serum), and quality control criteria were all implemented according to a previous published report [147] . Caco-2 TC7 cells were fed every other day, and cell monolayers were ready for experiments from 19 to 22 days post-seeding.

8.3.3. Transcellular transport study

The transcellular transport study was performed as described previously [147]. Briefly, 2.5 ml of Rh2s/C-K solution was loaded onto one side of the cell monolayer, and 2.5 ml of blank HBSS onto the other side. 25 compounds were randomly divided into 8 groups and used as P-gp inhibitors. In the present study, inhibitors of efflux transporters were only added to the apical side of cell monolayers, regardless of where Rh2s/C-K was loaded. Five sequential samples (0.5 ml) were taken at different times (0, 1, 2, 3 and 4 hrs) from both sides of the Caco-2 cell monolayer. The same volume of Rh2s/C-K solution and receiver medium (fresh HBSS) was added immediately to replace the volume lost as the result of sampling. The pH values of HBSS in both apical and basolateral side were 7.4.

Both permeability from apical to basolateral side (P_{a-b}) and basolateral to apical side (P_{b-a}) were calculated according to the above equation. Digoxin, a substrate of P-gp, showed efflux ratio at 21.0 and P_{a-b} was 1.48×10^{-6} cm/s in Caco-2 cells indicating the normal expression level of P-gp. The efflux ratio was calculated as P_{b-a}/P_{a-b}, which represented the degrees of efflux transporter involvement.

Intracellular concentrations of Rh2s or CK were determined at the end of a transport study. The protocol for determining Rh2s intracellular amounts in cells was the same as those described previously [151]. Briefly, after 4 hours of a transcellular transport study, the cell membranes were rinsed three times with ice-cold HBSS buffer, and cells attached to the polycarbonate membranes were cut off from the inserts with a sharp blade. The latter was immersed into 1 ml HBSS, and sonicated for half an hour at 4°C to break up the cells. The mixture was centrifuged at 15,000 rpm for 15 minutes and 500 µl of the supernatant were recovered and air-dried. The residue were reconstituted with 200 µl methanol and analyzed by UPLC-MS/MS. The protein concentration of cell lysate was measured to normalize the accumulation of Rh2s inside the cells using the BCA protein assay kit.

8.3.4. Sample Processing and Quantitative Determination of ginsenoside Rh2s and C-K

A UPLC-MS/MS assay for analysis of ginsenosides Rh2s and C-K in various matrices was developed and validated in our previous publication [183]. For UPLC-MS/MS analysis, an API 3200-Qtrap triple quadrupole mass spectrometer (AB SCIEX) coupled with a UPLC (Waters) was used to analyze the samples. The quantification was performed using multiple reactions monitoring mode (MRM) with ion pair transitions to monitor Rh2s and C-K. The fragments for each compound detected were 645.0/203.0 (m/z) for C-K and 621.4/160.9 (m/z) for Rh2s. Data were collected and analyzed by Analyst 1.4.2 software (AB SCIEX, USA).

8.3.5. Pharmacokinetic studies of ginsenosides Rh2s and C-K in A/J Mice

The animal protocols used in this study were approved by the University of Houston's Institutional Animal Care and Uses Committee. Pharmacokinetic studies of ginsenosides Rh2s and C-K in the presence of natural compounds were performed in A/J mice to investigate the effect of biochanin A, wogonin and piperine combination on the bioavailability of Rh2s and C-K. Rh2s and C-K dispersed in the oral suspending vehicle was given by gavage to each group at 5 and 20 mg/kg, respectively. 50 mg/kg of biochanin A, wogonin, piperine (each) dispersed in the same oral suspending vehicle was orally administrated to A/J mice 30 minutes prior to Rh2s/C-K administration while the same volume of blank vehicle was given to the control group. Each pharmacokinetic study was performed on five mice and 10 timed blood samples (20-25 µl) were taken by snipping its tail, after the mice were anesthetized with isoflurane gas. The blood samples were collected in heparinized tubes and stored at -20°C until analysis.

8.3.6. Statistical analysis

The data in this paper were presented as means ± S.D., if not specified otherwise. Significance differences were assessed by using Student's t-test or one-way ANOVA. A p value of less than 0.05 was considered as statistically significant.

8.4. Results

8.4.1. Effect of natural compounds on the efflux ratio of Rh2s in Caco-2 cells

Among eight combinations comprised of different natural compounds, five of them showed decreased efflux ratio of ginsenoside Rh2s compared to the control group (Table 13). The efflux ratio of Rh2s was decreased from 28.5 to 4.5, 16.0, 23.7, 5.0 and 11.9 after treatment of “biochanin A+wogonin+piperine”, “baicalein+7,8 benzoflavone+hesperidin”, “acacetin+glycyrrhetinic acid+galangin”, “auraptene+nobiletin” and “silymarin+silibin+curcumin+capsanthin” in Caco-2 cells, respectively. The results indicated these five combinations inhibited P-gp mediated efflux of Rh2s, and the combination of “biochanin A+Wogonin+piperine” showed the best inhibitory effect by decreasing efflux ratio by 84%. In contrast, the combination of “quercetin+resveratrol+kaempferol”, “EGCG+ursonic acid+chrysin+formononetin+phloretin” and “morin+hesperitin” showed higher efflux ratio at 33.6, 82.3 and 62.4 compared to control group (ER=28.5), respectively. It indicated that these three combinations may not have inhibitory effect on P-gp. Both verapamil and cyclosporine A abolished efflux ratio to 1 in positive control experiments.

8.4.2. Effect of natural compounds on the absorptive permeability of Rh2s in Caco-2 cells

Although the efflux ratio was the overall indicator of inhibitory effect, the absorptive permeability is the direct measurement for in vitro absorption. Among treatment of eight combinations comprised of different natural compounds, seven of them showed

increased absorptive permeability of ginsenoside Rh2s compared to the control group (Table 13). Consistent to decreased efflux ratio of five groups as shown above, their absorptive permeability incresed 8.1, 4.0, 2.2, 3.4 and 5.5 fold compared to the control group, respectively. Treatment of “quercetin+resveratrol+kaempferol” and “morin+hesperitin” also increased permeability of Rh2, but the difference is less than 1.7 fold, indicating weak inhibitory effects. The combination of “EGCG+Ursonic acid+chrysin+formononetin+phloretin” decreased permeabiity of Rh2, which was consistent with efflux ratio change, confirming the combination did not inhibit P-gp. Again, the group of “biochanin A+wogonin+piperine” showed the highest improvement in absorptive permeability of Rh2s. Both verapamil and cyclosporine A showed increased permeability by 17.1 and 7.6 fold in positive control, respectively.

8.4.3. Effect of natural compounds on the intracellular concentration of Rh2s in Caco-2 cells

Intracellular concentration is another important parameter to show the inhibitory effect of natural compounds. Among the eight treatment groups, made of different combinations of natural compounds, six increased the intracellular concentration of ginsenoside Rh2s, when compared to the control group (Table 13). Consistent to decreased efflux ratio of five groups as mentioned above, their absorptive permeability incresed 3.8, 2.7, 1.9, 3.4 and 4.8 fold, respectively, when compared to the control group. Treatment of “quercetin+resveratrol+kaempferol” also increased intracellular concentration of Rh2 by 2.1 fold. Addition of “EGCG+ursonic acid+chrysin+formononetin+phloretin” decreased

intracellular concentration of Rh2, which was consistent with efflux ratio and permeability change, confirming the combination did not inhibit P-gp. Once again, the group with “biochanin A+wogonin+piperine” combination resulted in the highest improvement in the intracellular concentration of Rh2s. Both verapamil and cyclosporine A increased the intracellular concentration by 2.3 and 4.0 fold, respectively, in positive control experiments.

8.4.4. Effect of individual compounds on the transport of Rh2s in Caco-2 cells

The combination of “biochanin A+wogonin+piperine” showed the highest inhibitory effect on P-gp in term of three parameters, efflux ratio, permeability and intracellular concentration. In order to investigate the additive and syngistic effects of compound combination, the individual effect of each compound was conducted. 50 μM of biochanin A, wogonin or piperine (each) did not show significant inhibitory effects on P-gp. Wogonin showed a slight inhibitory effect on P-gp and it decreased the efflux ratio by 28% (from 28.5 to 20) in Caco-2 cells, but it did not increase intracellular concentration or permeability of Rh2s. Similarly, biochanin A resulted in higher intracellular concentration and permeability than the control group, but the efflux ratio did not decrease. Similarly, piperine increased intracellular concentration of Rh2s, but did not show consistent results in term of efflux ratio and permeability. All these results indicated that one single compound at 50 μM may not be potent enough to significantly inhibit P-gp activity.

Table 13. Transcellular transport of ginsenoside Rh2 across monolayers of Caco-2 cells in the presence of different natural compounds.

Inhibitor	Each Inhibitor Concentrations (μM)	P_{a-b} ($\times 10^{-6}$ cm/s)	P_{b-a} ($\times 10^{-6}$ cm/s)	Efflux ratio (P_{b-a}/P_{a-b})	Intracellular amounts (nmol/mg)
-	-	0.37 ± 0.01	10.66±1.74	28.5	0.14 ± 0.02
#1 combo	50	0.65 ± 0.18	22.04 ± 3.01	33.6	0.29 ± 0.04
#2 combo	50	3.01 ± 0.75*	13.60 ± 1.06	4.5	0.52 ± 0.18**
#3 combo	50	1.48 ± 0.21*	23.71 ± 4.34	16.0	0.38 ± 0.03*
#4 combo	50	0.81 ± 0.19	19.32 ± 2.61	23.7	0.25 ± 0.02
#5 combo	40	0.25 ± 0.06	20.64 ± 4.15	82.3	0.06 ± 0.01
#6 combo	50	1.27 ± 0.08*	6.32 ± 0.97*	5.0	0.47 ± 0.27*
#7 combo	50	0.62 ± 0.02	38.70 ± 2.91	62.4	0.12 ± 0.03
#8 combo	50	2.06 ± 0.38*	24.60 ± 5.38	11.9	0.65 ± 0.06*
Piperine	50	0.35 ± 0.03	19.50 ± 1.21	56.1	0.23 ± 0.02
Wogonin	50	0.26 ± 0.05	5.37 ± 2.68	20.6	0.12 ± 0.02
Biochanin A	50	0.71 ± 0.38	31.22 ± 2.45	44.4	0.47 ± 0.27*
Verapamil	50	3.21 ± 0.35*	3.25 ± 0.46*	1.0	0.31±0.04**
Cyclosporine A	20	1.42 ± 0.18*	1.71 ± 0.23*	1.2	0.54±0.08**

Combo #1 is the combination of quercetin, resveratrol and kaempferol; #2 is the combination of biochanin A, Wogonin and piperine, #3 is the combination of baicalein, 7,8 benzoflavone and hesperidin, #4 is the combination of acacetin, glycyrrhetinic acid and galangin, #5 is the combination of EGCG, Ursonic acid, chrysin, formononetin and phloretin, #6 is the combination of auraptene and nobiletin, #7 is the combination of morin and hesperitin, #8 is the combination of silymarin, silibin, curcumin and capsanthin.

"P_{a-b}" refers to the permeability from apical to basolateral and "P_{b-a}" refers to the permeability from basolateral to apical side. Permeability and intracellular amounts were compared to control group. Data are the means ± S.D. of three independent experiments.

"–" indicated no inhibitor; "N/A" indicated no experiment performed; "NI" indicated no inhibition; * indicated $p<0.05$; ** indicated $p<0.01$; *** indicated $p<0.001$.

8.4.5. Effect of “biochanin A+wogonin+piperine” combo on the transport of C-K in Caco-2 cells

In our previous study, ginsenoside C-K showed potent anticancer effect in lung cancer cell line LM1 and was found to be a good substrate of P-gp (Chapter 6). In order to test whether the combination of “Biochanin A+Wogonin+Piperine” also worked for other ginsenosides that are substrates of P-gp, the bidirectional transport of C-K was measured in the presence of 50 μM of “Biochanin A+Wogonin+Piperine” . The results showed a 66.7% inhibition in the efflux ratio of C-K (from 26.6 to 8.9). Consistently, the permeability of C-K significantly increased (3.2 fold) and the intracellular concentration also substantially increased (70 fold), when compared to the control (Table 4). The result indicated that the combination of “Biochanin A+Wogonin+Piperine” can significantly increase absorption of C-K in Caco-2 cells by inhibition of P-gp.

Table 14. Transcellular transport of ginsenoside C-K across monolayers of Caco-2 cells in the presence of biochanin A, wogonin and piperine.

Inhibitor	Each Inhibitor Concentrations (μM)	P_{a-b} ($\times 10^{-6}$ cm/s)	P_{b-a} ($\times 10^{-6}$ cm/s)	Efflux ratio (P_{b-a}/P_{a-b})	Intracellular amounts (nmol/mg)
-	-	1.16 ± 0.33	30.96 ± 4.31**	26.6	0.01 ± 0
Biochanin A, Wogonin and Piperine	50	3.31 ± 0.27*	29.38 ± 2.94	8.9	0.86 ± 0.21

"P_{a-b}" refers to the permeability from apical to basolateral and "P_{b-a}" refers to the permeability from basolateral to apical side. Permeability and intracellular amounts were compared to control group. Data are the means ± S.D. of three independent experiments.
"–" indicated no inhibitor; * indicated $p<0.05$; ** indicated $p<0.01$; *** indicated $p<0.001$.

8.4.6. Effect of "biochanin A+wogonin+piperine" combo on the pharmacokinetics of Rh2s in A/J mice

Coadministration of biochanin A, wogonin and piperine (50 mg/kg for each compound) significantly increased the AUC_{0-t} of Rh2s by 4.5 fold (from 0.90 to 4.05 hr×μM, $p<0.01$) and $AUC_{0-\infty}$ by 6.0 fold (from 0.92 to 5.51 hr×μM, $p<0.01$), which resulted in increased bioavailability from ~1% to 6% based on previous AUC after intravenous administration [183]. The plasma C_{max} was slightly increased from 0.31 to 0.47 μM, but the difference was not statistically significant. In addition, the time to reach maximum plasma concentration (T_{max}) was significantly prolonged from 2.80 to 5.75 hr. The concomitant administration of biochanin A, wogonin and piperine substantially decreased elimination rate constant (K_e) of Rh2s by 3.7 fold (from 0.48 to 0.13 hr^{-1}, $p=0.09$) while increased terminal half-life of Rh2s by 7.0 fold (from 1.8 to 12.6 hr, $p=0.09$). Co-administration of this combination of natural compounds also increased V_{ss} from 0.26 ± 0.24 to 1.41 ± 1.78 L/Kg ($p=0.10$), although clearance of Rh2s was not changed from 0.07 ± 0.01 to 0.08 ± 0.01 (Figure 18).

Figure 18. The plasma concentrations of Rh2s alone or with 50 mg/kg biochanin A, wogonin and piperine after oral administrations of 5 mg/kg Rh2s in A/J mice and its pharmacokinetic parameters. Data are presented as mean ± S.D.; n=5.

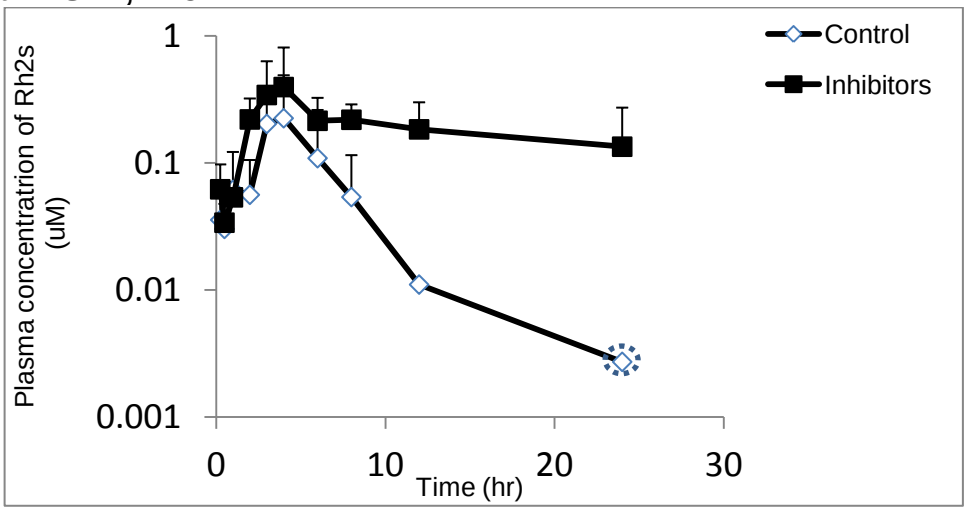

5mg/kg (n=4)	T_{max} (hr)	C_{max} (μM)	k_e (hr^{-1})	half-life (hr)	V_{ss} (L/Kg)	CL (L/hr/Kg)	AUC_{0-t} (hr*uM)	AUC_{inf} (hr*uM)	F%
Control	2.80 ± 0.84	0.31 ± 0.30	0.48 ± 0.25	1.78 ± 0.90	0.26 ± 0.24	0.07 ± 0.01	0.90 ± 0.90	0.92 ± 0.90	0.94 ± 0.92
Inhibitors	5.75 ± 2.63*	0.47 ± 0.36	0.13 ± 0.09 (P=0.09)	12.62 ± 15.04 (P=0.09)	1.41 ± 1.78 (P=0.10)	0.08 ± 0.01	4.05 ± 1.36**	5.51 ± 2.93**	5.60 ± 2.96**

* indicated p<0.05; ** indicated p<0.01; *** indicated p<0.001.

The circle means the concentration of several animals may below quantification limit.

8.4.7. Effect of "biochanin A+wogonin+piperine" combo on the pharmacokinetics of C-K in A/J mice

Coadministration of biochanin A, wogonin and piperine (50 mg/kg for each compound) significantly increased the AUC_{0-t} of C-K by 2.3 fold (from 22.7 to 53.1 hr×μM, $p<0.05$) and $AUC_{0-\infty}$ by 4.2 fold (from 23.2 to 97.0 hr×μM, $p<0.001$). The plasma C_{max} was not signifcantly changed from 2.98 (control) to 3.17 μM (treatment). Similarly, the time to reach maximum plasma concentration (T_{max}) was not changed from 5.2 to 5.0 hr. The concomitant administration of these three compounds significantly decreased K_e of Rh2s by 5.1 fold (from 0.16 to 0.03 hr^{-1}, $p<0.05$) while increased terminal half-life by 5.5 fold (from 4.15 to 22.74 hr, $p<0.001$) (Figure 19).

Figure 19. The plasma concentrations of C-K alone or with 50 mg/kg biochanin A, wogonin and piperine after oral administrations of 20 mg/kg C-K in A/J mice and its pharmacokinetic parameters. Data are presented as mean ± S.D.; n=5.

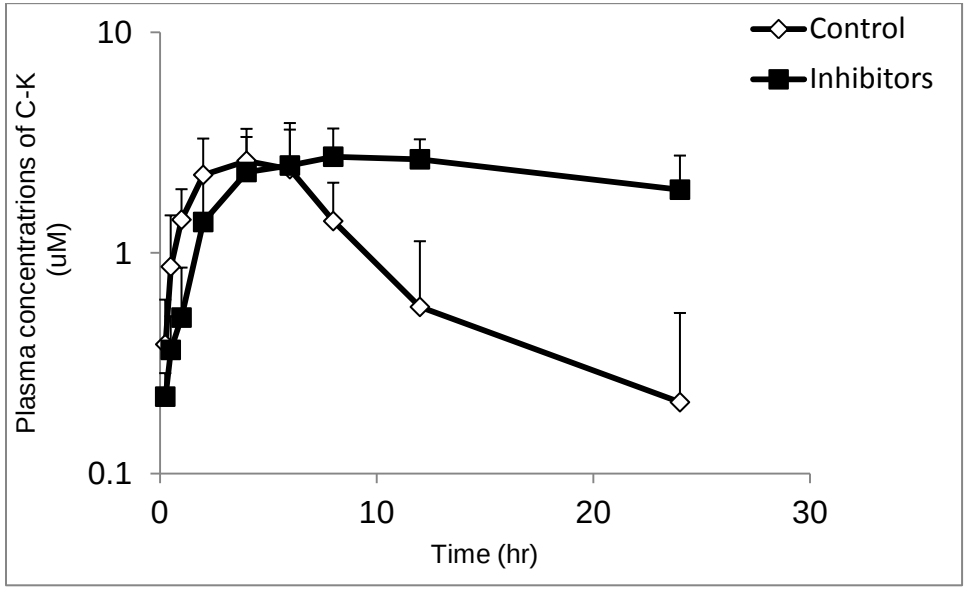

20 mg/kg (n=5)	T_{max} (hr)	C_{max} (μM)	k_e (hr^{-1})	half-life (hr)	AUC_{0-t} (hr*uM)	AUC_{inf} (hr*uM)
Control	5.20 ± 1.10	2.98 ± 1.21	0.16 ± 0.09	4.15 ± 1.62	22.74 ± 10.48	23.21 ± 10.58
Inhibitors	5.00 ± 2.58	3.17 ± 0.65	0.03 ± 0.01*	22.74 ± 4.90***	53.12 ± 14.45*	96.98 ± 15.50***

* indicated p<0.05; ** indicated p<0.01; *** indicated p<0.001.

8.5. Discussion

We have identified clinically useful combination of natural chemicals that can be used without consideration for significant toxicities since all of them have been consumed for a prolonged period of time by humans. In our previous study, cyclosporine A was found to increase oral bioavailability of ginsenoside Rh2s at 50 mg/kg in mice. Considering CsA is an immunosuppressing agent and ginsenosides can improve immune system as one of key mechanism for chemoprevention, CsA may not be suitable for concurrent use with ginsenosides in long-term. In patients, CsA was usually administrated at 300 mg/day [214]. Biochanin A is the major active component in red clover extract and used as estrogen supplement [215, 216] and four clinical trials on red clover were conducted (http://clinicaltrials.gov). Piperine is a major ingredient in pepper. It was tested for treatment of Oropharyngeal Dysphagia or coadministrated with curcumin and resveratrol to enhance their bioavailability in clinical trials. There are seven clinical trials are complete or ongoing (http://clinicaltrials.gov) .Wogonin is the active ingredient in a Chinese herb, scutellaria baicalensis radix, which can be used as an antioxidant and antiinflamatory ingredient in many formulations [217]. Together they have very attractive clinical profile and their repeated administration of 30-45 mg/kg/day in human had been demonstrated to be safe [218, 219].

We were able to identify this particular combination by using both in vitro Caco-2 cells and in vivo pharmacokinetic models. The resulting natural P-gp inhibitor combo were able to significantly improve the oral bioavailability of ginsenosides, C-K and Rh2s, which are good substrates of P-gp [183]. The three main rational for using the strategy

of identifying inhibitor combo instead of single inhibitor are as follows. First, solubility may limit the inhibitory effects, most of natural P-gp inhibitors are quite hydrophobic and have low aqueous solubility [220], usually much less than 100 μM [221, 222]. Low aqueous solubility greatly limited the effectiveness of a single compound to exert its inhibitory effect in vivo, since a large dose may not produce a higher concentration. Second, many of these natural inhibitors are also the substrates of P-gp or undergo extensive metabolism in vivo [223, 224]. A combination of natural compounds may have a better chance to survive in vivo. Third, P-gp is said to have multiple binding sites and there are more than one mechanism of inhibition, a combination of inhibitors therefore may have a synergistic effect [77].

The fact that our triple compound combo, made of biochanin A+wogonin+piperine, showed significant P-gp inhibitory effects, somewhat validate our approach. Biochanin A has an aqueous solubility of 6.73 μg/ml [225], and wogonin's solubility was less than 50 μM (data not shown). Piperine has very good solubility and was reported to inhibit UDP-glucuronosyltransferase (UGT) activity [226]. Because wogonin and biochanin A were good substrates of UGT, the presence of piperine could decrease their metabolism. Hence, concomitant administration of piperine with biochanin A and wogonin could increase the parent concentration of these flavonoids, which may result in stronger P-gp inhibitory effect in vivo.

All twenty-five compounds used in this study were chosen because they had shown positive P-gp inhibitory activity in various cell lines and animal models, based on

previous publications (Appendix). In this study, they were randomly mixed into eight groups as combination compounds to test their inhibitory effects. Only five groups, “biochanin A+wogonin+piperine”, “baicalein+7,8 benzoflavone+hesperidin”, “acacetin+glycyrrhetinic acid+galangin”, “auraptene+nobiletin” and “silymarin+silibin+curcumin+capsanthin” showed significant inhibition on P-gp, using the criteria of decreased efflux ratio, increased absorptive permeability, and enhanced intracellular accumulation in Caco-2 cells (Table 1). It was apparent that another two groups “quercetin+resveratrol+kaempferol” and “morin+hesperitin” showed less potent P-gp inhibitory effects, since changes in the efflux ratio, permeability and intracellular concentration of Rh2s were not always consistent with inhibition of P-gp. Surprisingly, the combination of “EGCG + ursonic acid + chrysin + formononetin + phloretin” unexpectedly induced P-gp activity in Caco-2 cells as reflected by higher efflux ratio as well as lower absorptive permeability and intracellular concentrations of Rh2s. These results indicated that a combination of natural P-gp inhibitors could result in antagonism effect, as suggested by Chou [227]. Due to the large binding cavity inside of P-gp and multiple binding residues for different substrates [77], it is rather difficult to predict the multiple drug interaction with P-gp and therefore should be studied further.

Although it was reported that biochanin A increased digoxin transport across Caco-2 Cell monolayers at 50 μM [228] and piperine inhibited digoxin and CsA transport in Caco-2 cells with IC_{50} values of 15.5 and 74.1 μM, respectively [226], while wogonin potentiated etoposide-induced apoptosis in HL-60 cells at 30 μM [229], 50 μM of biochanin A, wogonin or piperine alone did not show significant inhibitory effects on P-

gp when measured using the transport of Rh2s across Caco-2 cells. This may be due to substrate-dependent inhibition because of different substrate size and relative affinity [230]. In general, P-gp function can be inhibited through the following three major approaches: 1) blocking drug binding site via competitively, noncompetitively or allosterically modulation [231]; 2) interfering ATP hydrolysis process [232]; 3) altering integrity of cell membrane [233]. The mechanisms of inhibition of P-gp by these natural compounds were most likely via the first two, since there have been no reported evidence that any of these compounds could alter the membrane integrity.

In this study, ginsenoside Rh2s was chosen as the substrate because P-gp is the exclusive transporter involved in Rh2s transport at both in vitro and in vivo models [183]. Three transport parameters including efflux ratio, absorptive permeability (permeability from apical and basolateral side) and intracellular concentration were compared with those obtained using the control group to fully evaluate their P-gp inhibitory effects. Compared to significantly increased absorptive permeability, secretive permeability was not significantly decreased after treatment with various natural compounds combinations (Table 1). The discrepancy could be due to asymmetric inhibitory effect of P-gp inhibitor combos [234], and the real mechanism should be further studied.

In vivo pharmacokinetic study after coadministration of “biochanin A+wogonin+piperine” showed slightly increased C_{max} while substantially decreased apparent elimination rate constant (~70% decrease) of Rh2s. The PK change of Rh2s after coadministration of natural compounds was different with cyclosporine A coadministration, which showed

significantly increased C_{max} but minimal change on apparent elimination rate constant (Fig 9). Possible reasons are that CsA has stronger inhibitory effect on intestinal P-gp than combo as demonstrated in Caco-2 transport study, which resulted in significantly increased intestinal absorption (reflected as higher C_{max}) after CsA treatment than combo treatment. CsA has relatively low and variable oral absorption (~30%) due to large molecular weight and being substrate of P-gp [235, 236]. The low plasma level of CsA may explain the weak P-gp inhibitory effect during elimination phase of Rh2s. However, biochanin A, wogonin and piperine all have good oral absorption and this unique combination may increase their in vivo exposure and subsequently increase P-gp inhibition on liver or kidney, which may change the apparent elimination rate.

Similarly, coadministration of “biochanin A+wogonin+piperine” did not increase C_{max} of C-K, but significantly decreased apparent elimination rate constant by 80%, which resulted in prolonged half-life. It was consistent with previous reports that coadministration of piperine significantly reduced elimination of phenytoin, propranolol, theophylline and cucumin in humans and rats [237-239]. The altered pharmacokinetics of both ginsenosides indicated that biochanin A+wogonin+piperine could reduce apparent elimination rate of ginsenosides, which is the major contribution to enhanced oral bioavailability. It was consistent to our previous pharmacokinetic study using MDR1-knockout mice, which showed significantly prolonged half-life of C-K compared to wild-type mice (Yang et al, unpublished data).

In summary, natural compounds can decrease transport of ginsenosides Rh2s and C-K via P-gp inhibition in Caco-2 cells. The effective and efficient inhibition of P-gp by combination of biochanin A, wogonin and piperine led to an increased oral bioavailability of Rh2s and C-K in A/J mice, possibly due to decreased clearance. The findings of this study have demonstrated the proof of concept that combination of natural compounds can significantly increase oral bioavailability of ginsenosides and may represent another useful and practical approach to search for clinically useful P-gp inhibitors that will increase other anticancer drug's bioavailability.

SUMMARY

The purpose of these studies was to determine the biopharmaceutical characteristics of ginsenosides, in order to reveal the major factors limiting their oral bioavailability and then utilize the knowledge gained to increase their oral bioavailability via a mechanism-based approach. We first determined major reasons causing low oral bioavailability of ginsenosides using various ADME assays including presystemic stability, solubility, permeability and metabolism. We found that poor solubility and low permeability are the major reasons for low oral bioavailability of ginsenosides, with possible small contribution by CYP metabolism in vivo.

Systematic transport mechanism study of ginsenosides Rh2 and C-K, the most two potent ginsenosides for anticancer and chemoprevention activity, undoubtedly demonstrated that they are good substrates of P-gp. Inhibition/knockout of P-gp can significantly enhance their oral bioavailability via increased intestinal absorption and/or decreased elimination.

We then determined the absorption mechanism of twenty-two ginsenosides in Caco-2 and engineered MDCK II cells and we found that ginsenosides showed structure-dependent P-glycoprotein-mediated efflux. Ginsenosides with one or two glucose were most likely substrates of P-gp while ginsenosides with three or four sugars as well as aglycones were majorly transported via passive diffusion. BCRP were also involved for the transport of several ginsenosides.

We continued on with the efforts to improve oral bioavailability of ginsenosides by identifying the potent combination of natural compounds that could inhibit the functions of P-gp. Natural compound combo was able to decrease the efflux and/or increase the absorptive transport of ginsenosides Rh2s and C-K across Caco-2 cells via P-gp inhibition. The effective and efficient inhibition of P-gp by combination of biochanin A, wogonin and piperine led to significantly increased oral bioavailability of Rh2s and C-K in A/J mice, possibly due to increased distribution in vivo.

Taken together, we have shown the importance of P-gp in the disposition of ginsenosides Rh2 and C-K. Moreover, ginsenosides showed structure-dependent p-glycoprotein-mediated efflux. Ginsenosides with one or two glucose were most likely substrates of P-gp while ginsenosides with three or four sugars as well as aglycones were mainly transported via passive diffusion. Furthermore, natural compounds can decrease efflux of ginsenosides Rh2s and C-K via P-gp inhibition. The effective and efficient inhibition of P-gp by a combination of biochanin A, wogonin and piperine significantly increased oral bioavailability of Rh2s and C-K in A/J mice. Improved understanding of transport mechanism for ginsenosides and good progress made on overcome P-gp resistance provided both theoretically and practically approach for future development of ginsenosides into chemotherapeutic and chemopreventive agents.

REFERENCES

1. Yun, T.K., *Experimental and epidemiological evidence on non-organ specific cancer preventive effect of Korean ginseng and identification of active compounds.* Mutat Res, 2003. **523-524**: p. 63-74.
2. Hasegawa, H., *Proof of the mysterious efficacy of ginseng: basic and clinical trials: metabolic activation of ginsenoside: deglycosylation by intestinal bacteria and esterification with fatty acid.* J Pharmacol Sci, 2004. **95**(2): p. 153-7.
3. Gu, Y., et al., *Pharmacokinetic characterization of ginsenoside Rh2, an anticancer nutrient from ginseng, in rats and dogs.* Food Chem Toxicol, 2009. **47**(9): p. 2257-68.
4. Yoon, S.R., et al., *Ginsenoside composition and antiproliferative activities of explosively puffed ginseng (Panax ginseng C.A. Meyer).* J Food Sci. **75**(4): p. C378-82.
5. Li, L., et al., *Liquid chromatographic method for determination of four active saponins from Panax notoginseng in rat urine using solid-phase extraction.* J Chromatogr B Analyt Technol Biomed Life Sci, 2004. **808**(2): p. 177-83.
6. Kim, M.K., et al., *Microbial conversion of major ginsenoside rb(1) to pharmaceutically active minor ginsenoside rd.* J Microbiol, 2005. **43**(5): p. 456-62.
7. Christensen, L.P., *Ginsenosides chemistry, biosynthesis, analysis, and potential health effects.* Adv Food Nutr Res, 2009. **55**: p. 1-99.
8. Bae, E.A., et al., *Metabolism of 20(S)- and 20(R)-ginsenoside Rg3 by human intestinal bacteria and its relation to in vitro biological activities.* Biol Pharm Bull, 2002. **25**(1): p. 58-63.
9. Popovich, D.G. and D.D. Kitts, *Mechanistic studies on protopanaxadiol, Rh2, and ginseng (Panax quinquefolius) extract induced cytotoxicity in intestinal Caco-2 cells.* J Biochem Mol Toxicol, 2004. **18**(3): p. 143-9.
10. Kwon, H.Y., et al., *Selective toxicity of ginsenoside Rg3 on multidrug resistant cells by membrane fluidity modulation.* Arch Pharm Res, 2008. **31**(2): p. 171-7.
11. Zhang, X., et al., *Determination of 25-OH-PPD in rat plasma by high-performance liquid chromatography-mass spectrometry and its application in rat pharmacokinetic studies.* J Chromatogr B Analyt Technol Biomed Life Sci, 2007. **858**(1-2): p. 65-70.
12. Helms, S., *Cancer prevention and therapeutics: Panax ginseng.* Altern Med Rev, 2004. **9**(3): p. 259-74.
13. Qian, T., et al., *In vivo rat metabolism and pharmacokinetic studies of ginsenoside Rg3.* J Chromatogr B Analyt Technol Biomed Life Sci, 2005. **816**(1-2): p. 223-32.
14. Li, K., et al., *Liquid chromatography/tandem mass spectrometry for pharmacokinetic studies of 20(R)-ginsenoside Rg3 in dog.* Rapid Commun Mass Spectrom, 2005. **19**(6): p. 813-7.
15. Li, H., et al., *Biotransformation of 20(S)-protopanaxadiol by Mucor spinosus.* Phytochemistry, 2009. **70**(11-12): p. 1416-20.
16. Li, L., et al., *Identification of 20(S)-protopanaxadiol metabolites in human liver microsomes and human hepatocytes.* Drug Metab Dispos, 2011. **39**(3): p. 472-83.
17. Hao, H., et al., *Microsomal cytochrome p450-mediated metabolism of protopanaxatriol ginsenosides: metabolite profile, reaction phenotyping, and structure-metabolism relationship.* Drug Metab Dispos, 2010. **38**(10): p. 1731-9.
18. Liu, H., et al., *Absorption and disposition of ginsenosides after oral administration of Panax notoginseng extract to rats.* Drug Metab Dispos, 2009. **37**(12): p. 2290-8.

19. Qi, L.W., C.Z. Wang, and C.S. Yuan, *American ginseng: potential structure-function relationship in cancer chemoprevention.* Biochem Pharmacol, 2010. **80**(7): p. 947-54.
20. Huang, J.Y., et al., *[Efficacy of Shenyi Capsule combined with gemcitabine plus cisplatin in treatment of advanced esophageal cancer: a randomized controlled trial]*. Zhong Xi Yi Jie He Xue Bao, 2009. **7**(11): p. 1047-51.
21. Lu, P., et al., *Effect and mechanism of ginsenoside Rg3 on postoperative life span of patients with non-small cell lung cancer.* Chin J Integr Med, 2008. **14**(1): p. 33-6.
22. Xia, C.H., et al., *Herb-drug interactions: in vivo and in vitro effect of Shenmai injection, a herbal preparation, on the metabolic activities of hepatic cytochrome P450 3A1/2, 2C6, 1A2, and 2E1 in rats.* Planta Med, 2010. **76**(3): p. 245-50.
23. Yang, L., et al., *Determination of ginsenoside-Rg(1) in human plasma and its application to pharmacokinetic studies following intravenous administration of 'Shenmai' injection.* Phytother Res, 2009. **23**(1): p. 65-71.
24. Xiaohui, F., W. Yi, and C. Yiyu, *LC/MS fingerprinting of Shenmai injection: a novel approach to quality control of herbal medicines.* J Pharm Biomed Anal, 2006. **40**(3): p. 591-7.
25. Vuksan, V., et al., *Konjac-Mannan and American ginsing: emerging alternative therapies for type 2 diabetes mellitus.* J Am Coll Nutr, 2001. **20**(5 Suppl): p. 370S-380S; discussion 381S-383S.
26. Zhou, W., et al., *Molecular mechanisms and clinical applications of ginseng root for cardiovascular disease.* Med Sci Monit, 2004. **10**(8): p. RA187-92.
27. Jia, L., Y. Zhao, and X.J. Liang, *Current evaluation of the millennium phytomedicine-ginseng (II): Collected chemical entities, modern pharmacology, and clinical applications emanated from traditional Chinese medicine.* Curr Med Chem, 2009. **16**(22): p. 2924-42.
28. Attele, A.S., J.A. Wu, and C.S. Yuan, *Ginseng pharmacology: multiple constituents and multiple actions.* Biochem Pharmacol, 1999. **58**(11): p. 1685-93.
29. Lu, J.M., Q. Yao, and C. Chen, *Ginseng compounds: an update on their molecular mechanisms and medical applications.* Curr Vasc Pharmacol, 2009. **7**(3): p. 293-302.
30. Kaneko, H. and K. Nakanishi, *Proof of the mysterious efficacy of ginseng: basic and clinical trials: clinical effects of medical ginseng, korean red ginseng: specifically, its anti-stress action for prevention of disease.* J Pharmacol Sci, 2004. **95**(2): p. 158-62.
31. Hofseth, L.J. and M.J. Wargovich, *Inflammation, cancer, and targets of ginseng.* J Nutr, 2007. **137**(1 Suppl): p. 183S-185S.
32. Li, B., et al., *Ginsenoside Rh2 induces apoptosis and paraptosis-like cell death in colorectal cancer cells through activation of p53.* Cancer Lett, 2011. **301**(2): p. 185-92.
33. Cheng, C.C., et al., *Molecular mechanisms of ginsenoside Rh2-mediated G1 growth arrest and apoptosis in human lung adenocarcinoma A549 cells.* Cancer Chemother Pharmacol, 2005. **55**(6): p. 531-40.
34. Kim, B.J., et al., *Transient Receptor Potential Melastatin 7 Channels are Involved in Ginsenoside Rg3-Induced Apoptosis in Gastric Cancer Cells.* Basic Clin Pharmacol Toxicol, 2011. **109**(4): p. 233-9.
35. Yuan, H.D., et al., *20(S)-Ginsenoside Rg3-induced apoptosis in HT-29 colon cancer cells is associated with AMPK signaling pathway.* Mol Med Report, 2010. **3**(5): p. 825-31.

36. Li, G., et al., *Ginsenoside 20(S)-protopanaxadiol inhibits the proliferation and invasion of human fibrosarcoma HT1080 cells.* Basic Clin Pharmacol Toxicol, 2006. **98**(6): p. 588-92.
37. Cai, B.X., et al., *Ginsenoside Rb1 suppresses ultraviolet radiation-induced apoptosis by inducing DNA repair.* Biol Pharm Bull, 2009. **32**(5): p. 837-41.
38. Zhang, Q.H., et al., *Protective effects of ginsenoside Rg(3) against cyclophosphamide-induced DNA damage and cell apoptosis in mice.* Arch Toxicol, 2008. **82**(2): p. 117-23.
39. Liu, X., et al., *Efficacy and safety of ginsenoside-Rd for acute ischaemic stroke: a randomized, double-blind, placebo-controlled, phase II multicenter trial.* Eur J Neurol, 2009. **16**(5): p. 569-75.
40. Reeds, D.N., et al., *Ginseng and ginsenoside Re do not improve beta-cell function or insulin sensitivity in overweight and obese subjects with impaired glucose tolerance or diabetes.* Diabetes Care, 2011. **34**(5): p. 1071-6.
41. Pang, H., et al., *[Pharmacokinetic studies of 20(R)-ginsenoside RG3 in human volunteers]*. Yao Xue Xue Bao, 2001. **36**(3): p. 170-3.
42. Wang, H., et al., *Determination of ginsenoside Rg3 in plasma by solid-phase extraction and high-performance liquid chromatography for pharmacokinetic study.* J Chromatogr B Biomed Sci Appl, 1999. **731**(2): p. 403-9.
43. Qian, T., et al., *Liquid chromatography/mass spectrometric analysis of rat samples for in vivo metabolism and pharmacokinetic studies of ginsenoside Rh2.* Rapid Commun Mass Spectrom, 2005. **19**(23): p. 3549-54.
44. Xie, H.T., et al., *High performance liquid chromatographic-mass spectrometric determination of ginsenoside Rg3 and its metabolites in rat plasma using solid-phase extraction for pharmacokinetic studies.* J Chromatogr B Analyt Technol Biomed Life Sci, 2005. **818**(2): p. 167-73.
45. Lee, P.S., et al., *Pharmacokinetic characteristics and hepatic distribution of IH-901, a novel intestinal metabolite of ginseng saponin, in rats.* Planta Med, 2006. **72**(3): p. 204-10.
46. Paek, I.B., et al., *Pharmacokinetics of a ginseng saponin metabolite compound K in rats.* Biopharm Drug Dispos, 2006. **27**(1): p. 39-45.
47. Joo, K.M., et al., *Pharmacokinetic study of ginsenoside Re with pure ginsenoside Re and ginseng berry extracts in mouse using ultra performance liquid chromatography/mass spectrometric method.* J Pharm Biomed Anal, 2010. **51**(1): p. 278-83.
48. Xu, Q.F., X.L. Fang, and D.F. Chen, *Pharmacokinetics and bioavailability of ginsenoside Rb1 and Rg1 from Panax notoginseng in rats.* J Ethnopharmacol, 2003. **84**(2-3): p. 187-92.
49. Li, X., et al., *Pharmacokinetic and absolute bioavailability study of total panax notoginsenoside, a typical multiple constituent traditional chinese medicine (TCM) in rats.* Biol Pharm Bull, 2007. **30**(5): p. 847-51.
50. Sun, J., et al., *Simultaneous rapid quantification of ginsenoside Rg1 and its secondary glycoside Rh1 and aglycone protopanaxatriol in rat plasma by liquid chromatography-mass spectrometry after solid-phase extraction.* J Pharm Biomed Anal, 2005. **38**(1): p. 126-32.
51. Ren, H.C., et al., *Sensitive determination of 20(S)-protopanaxadiol in rat plasma using HPLC-APCI-MS: application of pharmacokinetic study in rats.* J Pharm Biomed Anal, 2008. **48**(5): p. 1476-80.

52. Han, M., et al., *Development of a UPLC-ESI-MS/MS assay for 20(S)-protopanaxadiol and pharmacokinetic application of its two formulations in rats.* Anal Sci, 2010. **26**(7): p. 749-53.
53. Ming Hu, X.L., *Oral Bioavailability: Basic Principles, Advanced Concepts, and Applications*. 2011: Wiley.
54. Yang, Z., et al., *Simultaneous determination of genistein and its four phase II metabolites in blood by a sensitive and robust UPLC-MS/MS method: Application to an oral bioavailability study of genistein in mice.* J Pharm Biomed Anal, 2010. **53**(1): p. 81-9.
55. Andrade, J.E., et al., *Absolute bioavailability of isoflavones from soy protein isolate-containing food in female BALB/c mice.* J Agric Food Chem, 2010. **58**(7): p. 4529-36.
56. Setchell, K.D., et al., *Bioavailability of pure isoflavones in healthy humans and analysis of commercial soy isoflavone supplements.* J Nutr, 2001. **131**(4 Suppl): p. 1362S-75S.
57. Kano, M., et al., *Bioavailability of isoflavones after ingestion of soy beverages in healthy adults.* J Nutr, 2006. **136**(9): p. 2291-6.
58. Chiou, W.L., *The rate and extent of oral bioavailability versus the rate and extent of oral absorption: clarification and recommendation of terminology.* J Pharmacokinet Pharmacodyn, 2001. **28**(1): p. 3-6.
59. Amidon, G.L., et al., *A theoretical basis for a biopharmaceutic drug classification: the correlation of in vitro drug product dissolution and in vivo bioavailability.* Pharm Res, 1995. **12**(3): p. 413-20.
60. Tawab, M.A., et al., *Degradation of ginsenosides in humans after oral administration.* Drug Metab Dispos, 2003. **31**(8): p. 1065-71.
61. Benet, L.Z., F. Broccatelli, and T.I. Oprea, *BDDCS Applied to Over 900 Drugs.* AAPS J, 2011.
62. Thomas, V.H., et al., *The road map to oral bioavailability: an industrial perspective.* Expert Opin Drug Metab Toxicol, 2006. **2**(4): p. 591-608.
63. Karlsson, J., et al., *Paracellular drug transport across intestinal epithelia: influence of charge and induced water flux.* Eur J Pharm Sci, 1999. **9**(1): p. 47-56.
64. Ungell, A.L., et al., *Membrane transport of drugs in different regions of the intestinal tract of the rat.* J Pharm Sci, 1998. **87**(3): p. 360-6.
65. Lipinski, C.A., et al., *Experimental and computational approaches to estimate solubility and permeability in drug discovery and development settings.* Adv Drug Deliv Rev, 2001. **46**(1-3): p. 3-26.
66. Wojtal, K.A., et al., *Changes in mRNA expression levels of solute carrier transporters in inflammatory bowel disease patients.* Drug Metab Dispos, 2009. **37**(9): p. 1871-7.
67. Hediger, M.A., et al., *The ABCs of solute carriers: physiological, pathological and therapeutic implications of human membrane transport proteinsIntroduction.* Pflugers Arch, 2004. **447**(5): p. 465-8.
68. Giacomini, K.M., et al., *Membrane transporters in drug development.* Nat Rev Drug Discov, 2010. **9**(3): p. 215-36.
69. Choudhuri, S. and C.D. Klaassen, *Structure, function, expression, genomic organization, and single nucleotide polymorphisms of human ABCB1 (MDR1), ABCC (MRP), and ABCG2 (BCRP) efflux transporters.* Int J Toxicol, 2006. **25**(4): p. 231-59.
70. Adachi, Y., et al., *Role of breast cancer resistance protein (Bcrp1/Abcg2) in the extrusion of glucuronide and sulfate conjugates from enterocytes to intestinal lumen.* Mol Pharmacol, 2005. **67**(3): p. 923-8.

71. Ahmed, S., et al., *Involvement of Mrp2 (Abcc2) in biliary excretion of moxifloxacin and its metabolites in the isolated perfused rat liver.* J Pharm Pharmacol, 2008. **60**(1): p. 55-62.
72. Enokizono, J., H. Kusuhara, and Y. Sugiyama, *Involvement of breast cancer resistance protein (BCRP/ABCG2) in the biliary excretion and intestinal efflux of troglitazone sulfate, the major metabolite of troglitazone with a cholestatic effect.* Drug Metab Dispos, 2007. **35**(2): p. 209-14.
73. Kessel, D., V. Botterill, and I. Wodinsky, *Uptake and retention of daunomycin by mouse leukemic cells as factors in drug response.* Cancer Res, 1968. **28**(5): p. 938-41.
74. Gottesman, M.M. and V. Ling, *The molecular basis of multidrug resistance in cancer: the early years of P-glycoprotein research.* FEBS Lett, 2006. **580**(4): p. 998-1009.
75. Riordan, J.R. and V. Ling, *Purification of P-glycoprotein from plasma membrane vesicles of Chinese hamster ovary cell mutants with reduced colchicine permeability.* J Biol Chem, 1979. **254**(24): p. 12701-5.
76. Smith, A.J., et al., *MDR3 P-glycoprotein, a phosphatidylcholine translocase, transports several cytotoxic drugs and directly interacts with drugs as judged by interference with nucleotide trapping.* J Biol Chem, 2000. **275**(31): p. 23530-9.
77. Aller, S.G., et al., *Structure of P-glycoprotein reveals a molecular basis for poly-specific drug binding.* Science, 2009. **323**(5922): p. 1718-22.
78. Sharom, F.J., *ABC multidrug transporters: structure, function and role in chemoresistance.* Pharmacogenomics, 2008. **9**(1): p. 105-27.
79. Kusuhara, H. and Y. Sugiyama, *Role of transporters in the tissue-selective distribution and elimination of drugs: transporters in the liver, small intestine, brain and kidney.* J Control Release, 2002. **78**(1-3): p. 43-54.
80. van Waterschoot, R.A., et al., *Absence of both cytochrome P450 3A and P-glycoprotein dramatically increases docetaxel oral bioavailability and risk of intestinal toxicity.* Cancer Res, 2009. **69**(23): p. 8996-9002.
81. Kemper, E.M., et al., *The influence of the P-glycoprotein inhibitor zosuquidar trihydrochloride (LY335979) on the brain penetration of paclitaxel in mice.* Cancer Chemother Pharmacol, 2004. **53**(2): p. 173-8.
82. Meerum Terwogt, J.M., et al., *Co-administration of cyclosporin enables oral therapy with paclitaxel.* Lancet, 1998. **352**(9124): p. 285.
83. Maubon, N., et al., *Analysis of drug transporter expression in human intestinal Caco-2 cells by real-time PCR.* Fundam Clin Pharmacol, 2007. **21**(6): p. 659-63.
84. Bonin, S., et al., *Gene expression of ABC proteins in hepatocellular carcinoma, perineoplastic tissue, and liver diseases.* Mol Med, 2002. **8**(6): p. 318-25.
85. Burger, H., et al., *RNA expression of breast cancer resistance protein, lung resistance-related protein, multidrug resistance-associated proteins 1 and 2, and multidrug resistance gene 1 in breast cancer: correlation with chemotherapeutic response.* Clin Cancer Res, 2003. **9**(2): p. 827-36.
86. Bart, J., et al., *The distribution of drug-efflux pumps, P-gp, BCRP, MRP1 and MRP2, in the normal blood-testis barrier and in primary testicular tumours.* Eur J Cancer, 2004. **40**(14): p. 2064-70.
87. Berggren, S., et al., *Gene and protein expression of P-glycoprotein, MRP1, MRP2, and CYP3A4 in the small and large human intestine.* Mol Pharm, 2007. **4**(2): p. 252-7.

88. Lohner, K., et al., *Flavonoids alter P-gp expression in intestinal epithelial cells in vitro and in vivo.* Mol Nutr Food Res, 2007. **51**(3): p. 293-300.
89. Watanabe, T., et al., *Kinetic analysis of hepatobiliary transport of vincristine in perfused rat liver. Possible roles of P-glycoprotein in biliary excretion of vincristine.* J Hepatol, 1992. **16**(1-2): p. 77-88.
90. Ballet, F., et al., *Hepatic extraction, metabolism and biliary excretion of doxorubicin in the isolated perfused rat liver.* Cancer Chemother Pharmacol, 1987. **19**(3): p. 240-5.
91. Lin, J.H. and M. Yamazaki, *Role of P-glycoprotein in pharmacokinetics: clinical implications.* Clin Pharmacokinet, 2003. **42**(1): p. 59-98.
92. Seelig, A., *Unraveling membrane-mediated substrate-transporter interactions.* Biophys J, 2006. **90**(11): p. 3825-6.
93. Didziapetris, R., et al., *Classification analysis of P-glycoprotein substrate specificity.* J Drug Target, 2003. **11**(7): p. 391-406.
94. Ecker, G., et al., *The importance of a nitrogen atom in modulators of multidrug resistance.* Mol Pharmacol, 1999. **56**(4): p. 791-6.
95. Hirohashi, T., et al., *ATP-dependent transport of bile salts by rat multidrug resistance-associated protein 3 (Mrp3).* J Biol Chem, 2000. **275**(4): p. 2905-10.
96. St-Pierre, M.V., et al., *Expression of members of the multidrug resistance protein family in human term placenta.* Am J Physiol Regul Integr Comp Physiol, 2000. **279**(4): p. R1495-503.
97. Schaub, T.P., et al., *Expression of the conjugate export pump encoded by the mrp2 gene in the apical membrane of kidney proximal tubules.* J Am Soc Nephrol, 1997. **8**(8): p. 1213-21.
98. Kool, M., et al., *Analysis of expression of cMOAT (MRP2), MRP3, MRP4, and MRP5, homologues of the multidrug resistance-associated protein gene (MRP1), in human cancer cell lines.* Cancer Res, 1997. **57**(16): p. 3537-47.
99. Wang, Q., et al., *Application and limitation of inhibitors in drug-transporter interactions studies.* Int J Pharm, 2008. **356**(1-2): p. 12-8.
100. Chen, C., et al., *Impact of Mrp2 on the biliary excretion and intestinal absorption of furosemide, probenecid, and methotrexate using Eisai hyperbilirubinemic rats.* Pharm Res, 2003. **20**(1): p. 31-7.
101. Sasabe, H., A. Tsuji, and Y. Sugiyama, *Carrier-mediated mechanism for the biliary excretion of the quinolone antibiotic grepafloxacin and its glucuronide in rats.* J Pharmacol Exp Ther, 1998. **284**(3): p. 1033-9.
102. Sasabe, H., et al., *Stereoselective hepatobiliary transport of the quinolone antibiotic grepafloxacin and its glucuronide in the rat.* J Pharmacol Exp Ther, 1998. **284**(2): p. 661-8.
103. Kusuhara, H., et al., *Reduced folate derivatives are endogenous substrates for cMOAT in rats.* Am J Physiol, 1998. **275**(4 Pt 1): p. G789-96.
104. Kawabe, T., et al., *Enhanced transport of anticancer agents and leukotriene C4 by the human canalicular multispecific organic anion transporter (cMOAT/MRP2).* FEBS Lett, 1999. **456**(2): p. 327-31.
105. Chen, J., H. Lin, and M. Hu, *Absorption and metabolism of genistein and its five isoflavone analogs in the human intestinal Caco-2 model.* Cancer Chemother Pharmacol, 2005. **55**(2): p. 159-69.

106. Zhu, W., et al., *Breast cancer resistance protein (BCRP) and sulfotransferases contribute significantly to the disposition of genistein in mouse intestine.* AAPS J, 2010. **12**(4): p. 525-36.
107. Zelcer, N., et al., *Mice lacking multidrug resistance protein 3 show altered morphine pharmacokinetics and morphine-6-glucuronide antinociception.* Proc Natl Acad Sci U S A, 2005. **102**(20): p. 7274-9.
108. Zamek-Gliszczynski, M.J., et al., *Evaluation of the role of multidrug resistance-associated protein (Mrp) 3 and Mrp4 in hepatic basolateral excretion of sulfate and glucuronide metabolites of acetaminophen, 4-methylumbelliferone, and harmol in Abcc3-/- and Abcc4-/- mice.* J Pharmacol Exp Ther, 2006. **319**(3): p. 1485-91.
109. Ishikawa, T., et al., *Expression and functional characterization of human ABC transporter ABCG2 variants in insect cells.* Drug Metab Pharmacokinet, 2003. **18**(3): p. 194-202.
110. Doyle, L.A., et al., *A multidrug resistance transporter from human MCF-7 breast cancer cells.* Proc Natl Acad Sci U S A, 1998. **95**(26): p. 15665-70.
111. Young, A.M., C.E. Allen, and K.L. Audus, *Efflux transporters of the human placenta.* Adv Drug Deliv Rev, 2003. **55**(1): p. 125-32.
112. Maliepaard, M., et al., *Circumvention of breast cancer resistance protein (BCRP)-mediated resistance to camptothecins in vitro using non-substrate drugs or the BCRP inhibitor GF120918.* Clin Cancer Res, 2001. **7**(4): p. 935-41.
113. Kawabata, S., et al., *Expression and functional analyses of breast cancer resistance protein in lung cancer.* Clin Cancer Res, 2003. **9**(8): p. 3052-7.
114. Kawabata, S., et al., *Breast cancer resistance protein directly confers SN-38 resistance of lung cancer cells.* Biochem Biophys Res Commun, 2001. **280**(5): p. 1216-23.
115. Zhang, Y., et al., *BCRP transports dipyridamole and is inhibited by calcium channel blockers.* Pharm Res, 2005. **22**(12): p. 2023-34.
116. Zhu, W., et al., *Breast Cancer Resistance Protein (BCRP) and Sulfotransferases Contribute Significantly to the Disposition of Genistein in Mouse Intestine.* AAPS J, 2010.
117. Xia, C.Q., et al., *Interactions of cyclosporin a with breast cancer resistance protein.* Drug Metab Dispos, 2007. **35**(4): p. 576-82.
118. Takahashi, K., et al., *ABC proteins: key molecules for lipid homeostasis.* Med Mol Morphol, 2005. **38**(1): p. 2-12.
119. Hazard, S.E. and S.B. Patel, *Sterolins ABCG5 and ABCG8: regulators of whole body dietary sterols.* Pflugers Arch, 2007. **453**(5): p. 745-52.
120. Berge, K.E., et al., *Accumulation of dietary cholesterol in sitosterolemia caused by mutations in adjacent ABC transporters.* Science, 2000. **290**(5497): p. 1771-5.
121. Yu, L., et al., *Disruption of Abcg5 and Abcg8 in mice reveals their crucial role in biliary cholesterol secretion.* Proc Natl Acad Sci U S A, 2002. **99**(25): p. 16237-42.
122. Tachibana, S., et al., *Cholesterol and plant sterol efflux from cultured intestinal epithelial cells is mediated by ATP-binding cassette transporters.* Biosci Biotechnol Biochem, 2007. **71**(8): p. 1886-95.
123. Hirano, M., et al., *Bile salt export pump (BSEP/ABCB11) can transport a nonbile acid substrate, pravastatin.* J Pharmacol Exp Ther, 2005. **314**(2): p. 876-82.
124. Ahlin, G., et al., *Endogenous gene and protein expression of drug-transporting proteins in cell lines routinely used in drug discovery programs.* Drug Metab Dispos, 2009. **37**(12): p. 2275-83.

125. Stieger, B., *Role of the bile salt export pump, BSEP, in acquired forms of cholestasis.* Drug Metab Rev, 2010. **42**(3): p. 437-45.
126. Sue Masters, B. and C.C. Marohnic, *Cytochromes P450--a family of proteins and scientists-understanding their relationships.* Drug Metab Rev, 2006. **38**(1-2): p. 209-25.
127. Fisher, M.B., et al., *In vitro glucuronidation using human liver microsomes and the pore-forming peptide alamethicin.* Drug Metab Dispos, 2000. **28**(5): p. 560-6.
128. Gopinathan, S., A. Nouraldeen, and A.G. Wilson, *Development and application of a high-throughput formulation screening strategy for oral administration in drug discovery.* Future Med Chem, 2010. **2**(9): p. 1391-8.
129. Strickley, R.G., *Solubilizing excipients in oral and injectable formulations.* Pharm Res, 2004. **21**(2): p. 201-30.
130. Gomez-Orellana, I., *Strategies to improve oral drug bioavailability.* Expert Opin Drug Deliv, 2005. **2**(3): p. 419-33.
131. Fasinu, P., et al., *Diverse approaches for the enhancement of oral drug bioavailability.* Biopharm Drug Dispos, 2011. **32**(4): p. 185-209.
132. Rautio, J., et al., *Prodrugs: design and clinical applications.* Nat Rev Drug Discov, 2008. **7**(3): p. 255-70.
133. Kinoshita, M., et al., *Improvement of solubility and oral bioavailability of a poorly water-soluble drug, TAS-301, by its melt-adsorption on a porous calcium silicate.* J Pharm Sci, 2002. **91**(2): p. 362-70.
134. Dietrich, C.G., A. Geier, and R.P. Oude Elferink, *ABC of oral bioavailability: transporters as gatekeepers in the gut.* Gut, 2003. **52**(12): p. 1788-95.
135. Fellner, S., et al., *Transport of paclitaxel (Taxol) across the blood-brain barrier in vitro and in vivo.* J Clin Invest, 2002. **110**(9): p. 1309-18.
136. Benson, A.B., 3rd, et al., *Phase I study of vinblastine and verapamil given by concurrent iv infusion.* Cancer Treat Rep, 1985. **69**(7-8): p. 795-9.
137. Tamai, I. and A.R. Safa, *Competitive interaction of cyclosporins with the Vinca alkaloid-binding site of P-glycoprotein in multidrug-resistant cells.* J Biol Chem, 1990. **265**(27): p. 16509-13.
138. Coley, H.M., *Overcoming multidrug resistance in cancer: clinical studies of p-glycoprotein inhibitors.* Methods Mol Biol, 2010. **596**: p. 341-58.
139. Baguley, B.C., *Novel strategies for overcoming multidrug resistance in cancer.* BioDrugs, 2002. **16**(2): p. 97-103.
140. Takara, K., T. Sakaeda, and K. Okumura, *An update on overcoming MDR1-mediated multidrug resistance in cancer chemotherapy.* Curr Pharm Des, 2006. **12**(3): p. 273-86.
141. Xie, H.T., et al., *Uptake and metabolism of ginsenoside Rh2 and its aglycon protopanaxadiol by Caco-2 cells.* Biol Pharm Bull, 2005. **28**(2): p. 383-6.
142. Zhang, J., et al., *20(S)-Ginsenoside Rh2 noncompetitively inhibits P-glycoprotein in vitro and in vivo: a case for herb-drug interactions.* Drug Metab Dispos, 2010. **38**: p. 2179-2187.
143. Dehring, K.A., et al., *Automated robotic liquid handling/laser-based nephelometry system for high throughput measurement of kinetic aqueous solubility.* J Pharm Biomed Anal, 2004. **36**(3): p. 447-56.
144. Shoghi, E., et al., *Kinetic and thermodynamic solubility values of some bioactive compounds.* Chem Biodivers, 2009. **6**(11): p. 1789-95.

145. Chen, J., H. Lin, and M. Hu, *Metabolism of flavonoids via enteric recycling: role of intestinal disposition.* J Pharmacol Exp Ther, 2003. **304**(3): p. 1228-35.
146. Hu, M., et al., *Identification of CYP1A2 as the main isoform for the phase I hydroxylated metabolism of genistein and a prodrug converting enzyme of methylated isoflavones.* Drug Metab Dispos, 2003. **31**(7): p. 924-31.
147. Yang, Z., et al., *Biopharmaceutical and pharmacokinetic characterization of matrine as determined by a sensitive and robust UPLC-MS/MS method.* J Pharm Biomed Anal, 2010. **51**(5): p. 1120-7.
148. Lee, S.J., et al., *Antitumor activity of a novel ginseng saponin metabolite in human pulmonary adenocarcinoma cells resistant to cisplatin.* Cancer Lett, 1999. **144**(1): p. 39-43.
149. Qi, L.W., C.Z. Wang, and C.S. Yuan, *Isolation and analysis of ginseng: advances and challenges.* Nat Prod Rep, 2011. **28**(3): p. 467-95.
150. Bae, E.A., et al., *Transformation of ginseng saponins to ginsenoside Rh2 by acids and human intestinal bacteria and biological activities of their transformants.* Arch Pharm Res, 2004. **27**(1): p. 61-7.
151. Jeong, E.J., X. Jia, and M. Hu, *Disposition of formononetin via enteric recycling: metabolism and excretion in mouse intestinal perfusion and Caco-2 cell models.* Mol Pharm, 2005. **2**(4): p. 319-28.
152. Hu, M., J. Chen, and H. Lin, *Metabolism of flavonoids via enteric recycling: mechanistic studies of disposition of apigenin in the Caco-2 cell culture model.* J Pharmacol Exp Ther, 2003. **307**(1): p. 314-21.
153. Jeong, E.J., H. Lin, and M. Hu, *Disposition mechanisms of raloxifene in the human intestinal Caco-2 model.* J Pharmacol Exp Ther, 2004. **310**(1): p. 376-85.
154. Rubash, H.E., et al., *Avoiding neurologic and vascular injuries with screw fixation of the tibial component in total knee arthroplasty.* Clin Orthop Relat Res, 1993(286): p. 56-63.
155. Han, B.H., et al., *Degradation of ginseng saponins under mild acidic conditions.* Planta Med, 1982. **44**(3): p. 146-9.
156. Hasegawa, H., et al., *Main ginseng saponin metabolites formed by intestinal bacteria.* Planta Med, 1996. **62**(5): p. 453-7.
157. Akao, T., et al., *Intestinal bacterial hydrolysis is required for the appearance of compound K in rat plasma after oral administration of ginsenoside Rb1 from Panax ginseng.* J Pharm Pharmacol, 1998. **50**(10): p. 1155-60.
158. Park, C.S., et al., *Biotransformation of ginsenosides by hydrolyzing the sugar moieties of ginsenosides using microbial glycosidases.* Appl Microbiol Biotechnol, 2010. **87**(1): p. 9-19.
159. Yun, T.K., *Experimental and epidemiological evidence of the cancer-preventive effects of Panax ginseng C.A. Meyer.* Nutr Rev, 1996. **54**(11 Pt 2): p. S71-81.
160. Varjas, T., et al., *Chemopreventive effect of Panax ginseng.* Phytother Res, 2009. **23**(10): p. 1399-403.
161. Buettner, C., et al., *Systematic review of the effects of ginseng on cardiovascular risk factors.* Ann Pharmacother, 2006. **40**(1): p. 83-95.
162. Coleman, C.I., J.H. Hebert, and P. Reddy, *The effects of Panax ginseng on quality of life.* J Clin Pharm Ther, 2003. **28**(1): p. 5-15.

163. Wang, Z., et al., *Ginsenoside Rh(2) enhances antitumour activity and decreases genotoxic effect of cyclophosphamide.* Basic Clin Pharmacol Toxicol, 2006. **98**(4): p. 411-5.
164. Gu, Y., et al., *Intestinal absorption mechanisms of ginsenoside Rh2: stereoselectivity and involvement of ABC transporters.* Xenobiotica, 2010. **40**(9): p. 602-12.
165. Zhang, J., et al., *20(S)-Ginsenoside Rh2 noncompetitively inhibits P-glycoprotein in vitro and in vivo: a case for herb-drug interactions.* Drug Metab Dispos.
166. Xu, J., M.L. Go, and L.Y. Lim, *Modulation of digoxin transport across Caco-2 cell monolayers by citrus fruit juices: lime, lemon, grapefruit, and pummelo.* Pharm Res, 2003. **20**(2): p. 169-76.
167. Walgren, R.A., et al., *Efflux of dietary flavonoid quercetin 4'-beta-glucoside across human intestinal Caco-2 cell monolayers by apical multidrug resistance-associated protein-2.* J Pharmacol Exp Ther, 2000. **294**(3): p. 830-6.
168. Brand, W., et al., *Metabolism and transport of the citrus flavonoid hesperetin in Caco-2 cell monolayers.* Drug Metab Dispos, 2008. **36**(9): p. 1794-802.
169. Taub, M.E., et al., *Functional assessment of multiple P-glycoprotein (P-gp) probe substrates: influence of cell line and modulator concentration on P-gp activity.* Drug Metab Dispos, 2005. **33**(11): p. 1679-87.
170. Shirasaka, Y., et al., *Expression levels of human P-glycoprotein in in vitro cell lines: correlation between mRNA and protein levels for P-glycoprotein expressed in cells.* Biopharm Drug Dispos, 2009. **30**(3): p. 149-52.
171. Zhang, J., et al., *20(S)-Ginsenoside Rh2 noncompetitively inhibits P-glycoprotein in vitro and in vivo: a case for herb-drug interactions.* Drug Metab Dispos, 2010. **12**: p. 2179-2187.
172. Yan, Y., et al., *Chemopreventive effect of aerosolized polyphenon E on lung tumorigenesis in A/J mice.* Neoplasia, 2007. **9**(5): p. 401-5.
173. Dahan, A., J.M. Miller, and G.L. Amidon, *Prediction of solubility and permeability class membership: provisional BCS classification of the world's top oral drugs.* AAPS J, 2009. **11**(4): p. 740-6.
174. Qi, L.W., C.Z. Wang, and C.S. Yuan, *Ginsenosides from American ginseng: chemical and pharmacological diversity.* Phytochemistry, 2011. **72**(8): p. 689-99.
175. Chae, S., et al., *Effect of compound K, a metabolite of ginseng saponin, combined with gamma-ray radiation in human lung cancer cells in vitro and in vivo.* J Agric Food Chem, 2009. **57**(13): p. 5777-82.
176. Bae, E.A., S.Y. Park, and D.H. Kim, *Constitutive beta-glucosidases hydrolyzing ginsenoside Rb1 and Rb2 from human intestinal bacteria.* Biol Pharm Bull, 2000. **23**(12): p. 1481-5.
177. Akao, T., M. Kanaoka, and K. Kobashi, *Appearance of compound K, a major metabolite of ginsenoside Rb1 by intestinal bacteria, in rat plasma after oral administration--measurement of compound K by enzyme immunoassay.* Biol Pharm Bull, 1998. **21**(3): p. 245-9.
178. Cho, S.H., et al., *Compound K, a metabolite of ginseng saponin, induces apoptosis via caspase-8-dependent pathway in HL-60 human leukemia cells.* BMC Cancer, 2009. **9**: p. 449.

179. Jeong, A., et al., *Compound K inhibits basic fibroblast growth factor-induced angiogenesis via regulation of p38 mitogen activated protein kinase and AKT in human umbilical vein endothelial cells.* Biol Pharm Bull, 2010. **33**(6): p. 945-50.
180. Ming, Y., et al., *Ginsenoside compound K attenuates metastatic growth of hepatocellular carcinoma, which is associated with the translocation of nuclear factor-kappaB p65 and reduction of matrix metalloproteinase-2/9.* Planta Med, 2010. **77**(5): p. 428-33.
181. Lee, B.H., et al., *In vitro antigenotoxic activity of novel ginseng saponin metabolites formed by intestinal bacteria.* Planta Med, 1998. **64**(6): p. 500-3.
182. Hasegawa, H., et al., *Interactions of ginseng extract, ginseng separated fractions, and some triterpenoid saponins with glucose transporters in sheep erythrocytes.* Planta Med, 1994. **60**(2): p. 153-7.
183. Yang, Z., et al., *Enhancement of oral bioavailability of 20(S)-ginsenoside Rh2 through improved understanding of its absorption and efflux mechanisms.* Drug Metab Dispos, 2011. **39**(10): p. 1866-72.
184. Zhang, Z., et al., *Positional cloning of the major quantitative trait locus underlying lung tumor susceptibility in mice.* Proc Natl Acad Sci U S A, 2003. **100**(22): p. 12642-7.
185. Manach, C., et al., *Polyphenols: food sources and bioavailability.* Am J Clin Nutr, 2004. **79**(5): p. 727-47.
186. Musende, A.G., et al., *Pre-clinical evaluation of Rh2 in PC-3 human xenograft model for prostate cancer in vivo: formulation, pharmacokinetics, biodistribution and efficacy.* Cancer Chemother Pharmacol, 2009. **64**(6): p. 1085-95.
187. Li, W., et al., *Anti-androgen-independent prostate cancer effects of ginsenoside metabolites in vitro: mechanism and possible structure-activity relationship investigation.* Arch Pharm Res, 2009. **32**(1): p. 49-57.
188. Haijiang, Z., W. Yongjiang, and C. Yiyu, *Analysis of 'SHENMAI' injection by HPLC/MS/MS.* J Pharm Biomed Anal, 2003. **31**(1): p. 175-83.
189. Chang, T.K., J. Chen, and S.A. Benetton, *In vitro effect of standardized ginseng extracts and individual ginsenosides on the catalytic activity of human CYP1A1, CYP1A2, and CYP1B1.* Drug Metab Dispos, 2002. **30**(4): p. 378-84.
190. Xiong, J., et al., *Active absorption of ginsenoside Rg1 in vitro and in vivo: the role of sodium-dependent glucose co-transporter 1.* J Pharm Pharmacol, 2009. **61**(3): p. 381-6.
191. Tarcsay, A. and G.M. Keseru, *Homology modeling and binding site assessment of the human P-glycoprotein.* Future Med Chem, 2011. **3**(3): p. 297-307.
192. Han, M., et al., *Oral absorption of ginsenoside Rb1 using in vitro and in vivo models.* Planta Med, 2006. **72**(5): p. 398-404.
193. Bikadi, Z., et al., *Predicting P-glycoprotein-mediated drug transport based on support vector machine and three-dimensional crystal structure of P-glycoprotein.* PLoS One, 2011. **6**(10): p. e25815.
194. Dolghih, E., et al., *Predicting binding to p-glycoprotein by flexible receptor docking.* PLoS Comput Biol, 2011. **7**(6): p. e1002083.
195. Park, M.T., et al., *The anti-tumour compound, RH1, causes mitochondria-mediated apoptosis by activating c-Jun N-terminal kinase.* Br J Pharmacol, 2011. **163**(3): p. 567-85.
196. Digby, T., et al., *Effect of NQO1 induction on the antitumor activity of RH1 in human tumors in vitro and in vivo.* Cancer Chemother Pharmacol, 2005. **56**(3): p. 307-16.

197. Yan, C., et al., *Dissecting the role of multiple reductases in bioactivation and cytotoxicity of the antitumor agent 2,5-diaziridinyl-3-(hydroxymethyl)-6-methyl-1,4-benzoquinone (RH1).* Mol Pharmacol, 2008. **74**(6): p. 1657-65.
198. Li, Q.F., et al., *Anticancer effects of ginsenoside Rg1, cinnamic acid, and tanshinone IIA in osteosarcoma MG-63 cells: nuclear matrix downregulation and cytoplasmic trafficking of nucleophosmin.* Int J Biochem Cell Biol, 2008. **40**(9): p. 1918-29.
199. Wang, Z., et al., *P-glycoprotein substrate models using support vector machines based on a comprehensive data set.* J Chem Inf Model, 2011. **51**(6): p. 1447-56.
200. Hilgendorf, C., et al., *Expression of thirty-six drug transporter genes in human intestine, liver, kidney, and organotypic cell lines.* Drug Metab Dispos, 2007. **35**(8): p. 1333-40.
201. Qadir, M., et al., *Cyclosporin A is a broad-spectrum multidrug resistance modulator.* Clin Cancer Res, 2005. **11**(6): p. 2320-6.
202. Tumlin, J.A. and J.M. Sands, *Nephron segment-specific inhibition of Na+/K(+)-ATPase activity by cyclosporin A.* Kidney Int, 1993. **43**(1): p. 246-51.
203. Musende, A.G., et al., *Rh2 or its aglycone aPPD in combination with docetaxel for treatment of prostate cancer.* Prostate, 2011. **70**(13): p. 1437-47.
204. Xie, X., et al., *Rh2 synergistically enhances paclitaxel or mitoxantrone in prostate cancer models.* J Urol, 2006. **175**(5): p. 1926-31.
205. Qi, L.W., et al., *Metabolism of Ginseng and its Interactions with Drugs.* Curr Drug Metab, 2011.
206. Liu, Z.Q., et al., *In vitro study of the relationship between the structure of ginsenoside and its antioxidative or prooxidative activity in free radical induced hemolysis of human erythrocytes.* J Agric Food Chem, 2003. **51**(9): p. 2555-8.
207. Hasegawa, H. and M. Uchiyama, *Antimetastatic efficacy of orally administered ginsenoside Rb1 in dependence on intestinal bacterial hydrolyzing potential and significance of treatment with an active bacterial metabolite.* Planta Med, 1998. **64**(8): p. 696-700.
208. Breedveld, P., J.H. Beijnen, and J.H. Schellens, *Use of P-glycoprotein and BCRP inhibitors to improve oral bioavailability and CNS penetration of anticancer drugs.* Trends Pharmacol Sci, 2006. **27**(1): p. 17-24.
209. Friedenberg, W.R., et al., *Phase III study of PSC-833 (valspodar) in combination with vincristine, doxorubicin, and dexamethasone (valspodar/VAD) versus VAD alone in patients with recurring or refractory multiple myeloma (E1A95): a trial of the Eastern Cooperative Oncology Group.* Cancer, 2006. **106**(4): p. 830-8.
210. Kuppens, I.E., et al., *A phase I, randomized, open-label, parallel-cohort, dose-finding study of elacridar (GF120918) and oral topotecan in cancer patients.* Clin Cancer Res, 2007. **13**(11): p. 3276-85.
211. Sterz, K., et al., *Activators of P-glycoprotein: Structure-activity relationships and investigation of their mode of action.* ChemMedChem, 2009. **4**(11): p. 1897-911.
212. Hayeshi, R., et al., *The potential inhibitory effect of antiparasitic drugs and natural products on P-glycoprotein mediated efflux.* Eur J Pharm Sci, 2006. **29**(1): p. 70-81.
213. Podolsky, S.H. and J.A. Greene, *Combination drugs--hype, harm, and hope.* N Engl J Med, 2011. **365**(6): p. 488-91.
214. Rasche, F.M., et al., *Single daily dose of cyclosporine in patients with primary glomerulonephritis and nephrotic syndrome.* Clin Nephrol, 2007. **67**(5): p. 285-92.

215. Beck, V., U. Rohr, and A. Jungbauer, *Phytoestrogens derived from red clover: an alternative to estrogen replacement therapy?* J Steroid Biochem Mol Biol, 2005. **94**(5): p. 499-518.
216. Slater, M., D. Brown, and A. Husband, *In the prostatic epithelium, dietary isoflavones from red clover significantly increase estrogen receptor beta and E-cadherin expression but decrease transforming growth factor beta1.* Prostate Cancer Prostatic Dis, 2002. **5**(1): p. 16-21.
217. Shieh, D.E., L.T. Liu, and C.C. Lin, *Antioxidant and free radical scavenging effects of baicalein, baicalin and wogonin.* Anticancer Res, 2000. **20**(5A): p. 2861-5.
218. Ishida, T., M. Ishizaki, and H. Yamada, *Piperine, a pepper ingredient, Improves the Hepatic Increases in Free Fatty Acids Caused by 2,3,7,8-Tetrachlorodibenzo-p-dioxin.*Journal of Health Science 2008. **54**(5): p. 551-558.
219. Hu, Z., et al., *Herb-drug interactions: a literature review.* Drugs, 2005. **65**(9): p. 1239-82.
220. Piskula, M.K., *Factors affecting flavonoids absorption.* Biofactors, 2000. **12**(1-4): p. 175-80.
221. Ng, S.P., et al., *Evaluation of the first-pass glucuronidation of selected flavones in gut by Caco-2 monolayer model.* J Pharm Pharm Sci, 2004. **8**(1): p. 1-9.
222. Kang, M.J., J.Y. Cho, and B.H. Shim, *Bioavailability enhancing activities of natural compounds from medicinal plants.* Journal of Medicinal Plants Research, 2009. **3**(13): p. 1204-11.
223. Pal, D. and A.K. Mitra, *MDR- and CYP3A4-mediated drug-herbal interactions.* Life Sci, 2006. **78**(18): p. 2131-45.
224. Zhou, S., L.Y. Lim, and B. Chowbay, *Herbal modulation of P-glycoprotein.* Drug Metab Rev, 2004. **36**(1): p. 57-104.
225. Han, H.K., B.J. Lee, and H.K. Lee, *Enhanced dissolution and bioavailability of biochanin A via the preparation of solid dispersion: in vitro and in vivo evaluation.* Int J Pharm, 2011. **415**(1-2): p. 89-94.
226. Bhardwaj, R.K., et al., *Piperine, a major constituent of black pepper, inhibits human P-glycoprotein and CYP3A4.* J Pharmacol Exp Ther, 2002. **302**(2): p. 645-50.
227. Chou, T.C., *Drug combination studies and their synergy quantification using the Chou-Talalay method.* Cancer Res, 2010. **70**(2): p. 440-6.
228. Zhang, S. and M.E. Morris, *Effect of the flavonoids biochanin A and silymarin on the P-glycoprotein-mediated transport of digoxin and vinblastine in human intestinal Caco-2 cells.* Pharm Res, 2003. **20**(8): p. 1184-91.
229. Lee, E., et al., *Inhibition of P-glycoprotein by wogonin is involved with the potentiation of etoposide-induced apoptosis in cancer cells.* Ann N Y Acad Sci, 2009. **1171**: p. 132-6.
230. Zolnerciks, J.K., et al., *Substrate- and species-dependent inhibition of P-glycoprotein-mediated transport: implications for predicting in vivo drug interactions.* J Pharm Sci, 2011. **100**(8): p. 3055-61.
231. Maki, N., P. Hafkemeyer, and S. Dey, *Allosteric modulation of human P-glycoprotein. Inhibition of transport by preventing substrate translocation and dissociation.* J Biol Chem, 2003. **278**(20): p. 18132-9.
232. Maki, N., et al., *Allosteric modulation bypasses the requirement for ATP hydrolysis in regenerating low affinity transition state conformation of human P-glycoprotein.* J Biol Chem, 2006. **281**(16): p. 10769-77.

233. Varma, M.V., et al., *P-glycoprotein inhibitors and their screening: a perspective from bioavailability enhancement.* Pharmacol Res, 2003. **48**(4): p. 347-59.
234. Troutman, M.D. and D.R. Thakker, *Efflux ratio cannot assess P-glycoprotein-mediated attenuation of absorptive transport: asymmetric effect of P-glycoprotein on absorptive and secretory transport across Caco-2 cell monolayers.* Pharm Res, 2003. **20**(8): p. 1200-9.
235. Drewe, J., et al., *Enhancement of the oral absorption of cyclosporin in man.* Br J Clin Pharmacol, 1992. **34**(1): p. 60-4.
236. Saeki, T., et al., *Human P-glycoprotein transports cyclosporin A and FK506.* J Biol Chem, 1993. **268**(9): p. 6077-80.
237. Bano, G., et al., *Effect of piperine on bioavailability and pharmacokinetics of propranolol and theophylline in healthy volunteers.* Eur J Clin Pharmacol, 1991. **41**(6): p. 615-7.
238. Bano, G., et al., *The effect of piperine on pharmacokinetics of phenytoin in healthy volunteers.* Planta Med, 1987. **53**(6): p. 568-9.
239. Shoba, G., et al., *Influence of piperine on the pharmacokinetics of curcumin in animals and human volunteers.* Planta Med, 1998. **64**(4): p. 353-6.
240. Limtrakul, P., O. Khantamat, and K. Pintha, *Inhibition of P-glycoprotein function and expression by kaempferol and quercetin.* J Chemother, 2005. **17**(1): p. 86-95.
241. Nabekura, T., S. Kamiyama, and S. Kitagawa, *Effects of dietary chemopreventive phytochemicals on P-glycoprotein function.* Biochem Biophys Res Commun, 2005. **327**(3): p. 866-70.
242. Zhang, S. and M.E. Morris, *Effects of the flavonoids biochanin A, morin, phloretin, and silymarin on P-glycoprotein-mediated transport.* J Pharmacol Exp Ther, 2003. **304**(3): p. 1258-67.
243. Peng, S.X., et al., *Altered oral bioavailability and pharmacokinetics of P-glycoprotein substrates by coadministration of biochanin A.* J Pharm Sci, 2006. **95**(9): p. 1984-93.
244. Lee, Y., et al., *Increased anti-P-glycoprotein activity of baicalein by alkylation on the A ring.* J Med Chem, 2004. **47**(22): p. 5555-66.
245. Zhang, S., et al., *Structure activity relationships and quantitative structure activity relationships for the flavonoid-mediated inhibition of breast cancer resistance protein.* Biochem Pharmacol, 2005. **70**(4): p. 627-39.
246. El-Readi, M.Z., et al., *Inhibition of P-glycoprotein activity by limonin and other secondary metabolites from Citrus species in human colon and leukaemia cell lines.* Eur J Pharmacol, 2010. **626**(2-3): p. 139-45.
247. Imai, Y., et al., *Phytoestrogens/flavonoids reverse breast cancer resistance protein/ABCG2-mediated multidrug resistance.* Cancer Res, 2004. **64**(12): p. 4346-52.
248. Nabekura, T., *Overcoming multidrug resistance in human cancer cells by natural compounds.* Toxins (Basel), 2010. **2**(6): p. 1207-24.
249. Jodoin, J., M. Demeule, and R. Beliveau, *Inhibition of the multidrug resistance P-glycoprotein activity by green tea polyphenols.* Biochim Biophys Acta, 2002. **1542**(1-3): p. 149-59.
250. Schrader, K.K., *Plant Natural Compounds with Antibacterial Activity towards Common Pathogens of Pond-Cultured Channel Catfish (Ictalurus punctatus).* Toxins (Basel), 2010. **2**(7): p. 1676-89.

251. Gyemant, N., et al., *In vitro search for synergy between flavonoids and epirubicin on multidrug-resistant cancer cells.* In Vivo, 2005. **19**(2): p. 367-74.
252. Nabekura, T., T. Yamaki, and S. Kitagawa, *Effects of chemopreventive citrus phytochemicals on human P-glycoprotein and multidrug resistance protein 1.* Eur J Pharmacol, 2008. **600**(1-3): p. 45-9.
253. Zhang, W. and L.Y. Lim, *Effects of spice constituents on P-glycoprotein-mediated transport and CYP3A4-mediated metabolism in vitro.* Drug Metab Dispos, 2008. **36**(7): p. 1283-90.
254. Kars, M.D., et al., *Reversal of multidrug resistance by synthetic and natural compounds in drug-resistant MCF-7 cell lines.* Chemotherapy, 2008. **54**(3): p. 194-200.

Appendix

Summary of inhibition results of natural compounds on P-gp in cell models

Compounds	Substrates	Models	References
Quercetin	Rhodamine 123 ,[3H]-vinblastine	KB-V1	[240]
Resveratrol	Daunorubicin	KB-C2	[241]
Kaempferol	Vinblastine and Paclitaxel	KB-V1	[240]
Biochanin A	[3H]-digoxin and [3H]-Vinblastine Doxorubicin Paclitaxel	Caco-2 MDA435/LCC6MDR1	[228] [242] [243]
Wogonin	Etoposide	HL-60	[229]
Piperine	Digoxin and Cyclosporine	Caco-2	[226]
Baicalein	Vinblastine	KB/MDR	[244]
7,8 benzoflavone	Mitoxantrone	MCF-7MX100	[245]
Hesperidin	Rhodamine 123	CEM/ADR5000	[246]
Acacetin	SN-38	K562/BCRP	[247]
Glycyrrhetinic acid	Daunorubicin	KB-C2	[248]
Galangin	Daunorubicin	KB-C2	[248]
EGCG	Vinblastine	CH(R) C5	[249]
Ursonic acid	Rhodamine 123	KB-C2	[248]
Chrysin	Topotecan	Caco-2	[250]
Formononetin	Rhodamine 123	MDA-MB-231	[251]
Phloretin	Doxorubicin	MDA435/LCC6	[242]
Auraptene	Daunorubicin	KB-C2	[252]
Nobiletin	Daunorubicin	KB-C2	[252]
Morin	Doxorubicin	MDA435/LCC6	[242]
Silymarin	Doxorubicin	MDA435/LCC6	[242]
Curcumin	[3H]-digoxin	L-MDR1 and Caco-2	[253]
Capsanthin	Rhodamine 123	MCF-7	[254]